

THE UNIVERSITY OF MICHIGAN
INDUSTRY PROGRAM OF THE COLLEGE OF ENGINEERING

LARGE SIGNAL ANALYSIS OF DISTRIBUTED AMPLIFIERS

Phil H. Rogers

This report was submitted in partial fulfillment of the requirements for the Degree of Doctor of Philosophy in the University of Michigan. It was originally distributed as Technical Report No. 52 by the Electronic Defense Group, the Department of Electrical Engineering, the University of Michigan, under Engineering Research Institute Project 2262, on Contract No. DA-36-039 sc-63203, Signal Corps, Department of the Army.

August, 1955

IP-125

ACKNOWLEDGEMENT

The Industry Program of the College of Engineering wishes to express its appreciation to Phil H. Rogers, Assistant Professor of Electrical Engineering, the University of Michigan, for making it possible to distribute this report under the Industry Program cover.

Errata Sheet

ELECTRONIC DEFENSE GROUP
Technical Report No. 52

Page ii - Add paragraph at beginning of Abstract, to read: "The primary importance of the distributed amplifier circuit is derived from its ability to operate in the frequency range above that covered by conventional amplifiers and below that covered by microwave amplifiers. The frequency range of conventional wide-band power amplifiers is generally limited to frequencies of the order of 10 mc. Microwave power amplifiers of the traveling-wave-tube type have been constructed to operate with lower frequency limits of the order of hundreds of megacycles. The distributed amplifier can be designed to operate from tens of megacycles to hundreds of megacycles, thus filling the gap between conventional techniques and microwave techniques."

Page 2, Paragraph 1, Line 3 - Add "line" after "transmission."

Page 2, Paragraph 2, Line 5 - Change "amplifier" to "amplifiers."

Page 3, Paragraph 1, Line 1 - Add hyphen between "high" and "frequency."

Page 8, Paragraph 3, Line 2 - Delete second "is independent."

Page 10, Paragraph 1, Line 9 - Change "are" to "is."

Page 10, Paragraph 2, Line 9 - Change "contribution" to "contributions."

Page 11, Paragraph 2, Line 3 - Change "impedances" to "impedance."

Page 19, Paragraph 2, Line 3 - Add hyphen between "low" and "frequency."

Page 23, Equation No. 3.7 - Change minus to plus.

Page 33, Paragraph 2, Line 4 - Change "logrithrim" to "logarithm."

Page 36, Title of Section 4.3 - Add asterisk after "line." Also add footnote at bottom of page, to read: "The small signal case is discussed in Ref. 2."

Page 51, Equation No. 5.4 - Delete superscript "2" on "n."

Page 56, Between 2nd and 3rd paragraphs - Add paragraph to read: "Figure 4.1 shows the plate load impedances for each tube of a six-tube distributed amplifier. The plate supply voltages on the first three tubes can be reduced without appreciably affecting the output power if the frequency of operation for this amplifier is limited to the range 60 to 270 mc. However, the dc power input could be reduced to 77 percent of the normal value. This increases the efficiency by a factor of 1.3."

Page 83, Paragraph 2, Line 3 - Change sentence beginning "It can be seen ... " to read: "It can be seen from these figures that the efficiency tends to increase with screen voltage; however, the peaks in the power output reach a maximum and decrease as the screen voltage is further increased."

Page 89, Paragraph 4, Line 1 - Add superscript "2" after "small-signal."

ENGINEERING RESEARCH INSTITUTE
UNIVERSITY OF MICHIGAN
ANN ARBOR

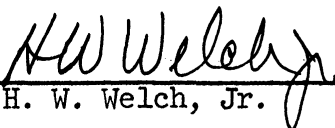
LARGE SIGNAL ANALYSIS OF DISTRIBUTED AMPLIFIERS

Technical Report No. 52
Electronic Defense Group
Department of Electrical Engineering

by

Phil H. Rogers

Approved by:


H. W. Welch, Jr.

Project 2262

TASK ORDER NO. EDG-1
CONTRACT NO. DA-36-039 sc-63203
SIGNAL CORPS, DEPARTMENT OF THE ARMY
DEPARTMENT OF ARMY PROJECT NO. 3-99-04-042
SIGNAL CORPS PROJECT NO. 194B

Submitted in partial fulfillment of the requirements for the
Degree of Doctor of Philosophy in the University of Michigan

July 1955

ABSTRACT

It is the purpose of this dissertation to extend the analysis of distributed amplifiers to account for large signal effects, to determine a graphical procedure for analyzing the non-linear operation of the tubes in a distributed amplifier, and to investigate the efficiency of distributed amplifiers.

General equations are derived describing the behavior of distributed amplifiers, including the operating load line for each tube in an n-tube distributed amplifier. The load lines for all but the last tube are ellipses and as a result graphical calculations are long and tedious. However, equations are derived whereby the output power can be calculated from the load line of the last tube at low frequencies, simplifying the graphical analysis considerably.

In addition the frequency response is examined under large-signal conditions and the modifications necessary in the small-signal design equations for a flat frequency response are indicated.

The frequency limitations in distributed amplifiers are determined on the basis of the realization of the constant-k artificial transmission line with finite grid and plate lead inductances. In practice the highest cut-off frequency is about 0.8 the series resonant frequency of the grid lead inductance and the input capacitance of the tube. An additional frequency limitation is present in large-signal distributed amplifiers in that clipping in the plate circuit of the last few tubes will cause the large-signal response to differ from the small-signal response.

The maximum theoretical efficiency of a distributed amplifier operating over its entire frequency range is 30 percent. This value occurs at a plate conduction angle of about 225 degrees. However, if the operating frequency range is limited to 0.2 to 0.9 of the design cut-off frequency, the efficiency can be increased by decreasing the plate supply voltage for the first few tubes.

A graphical procedure is presented for calculating the power output, the efficiency, the second harmonic power output, and the frequency above which clipping occurs.

ACKNOWLEDGMENT

The author wishes to express his appreciation to the members of his committee for their assistance, and especially to Professor Alan B. Macnee for his valuable criticisms and suggestions during the course of the work. Mr. Ward Getty assisted in the many graphical calculations.

The research on which this dissertation is based was supported by the U. S. Army Signal Corps under Contract No. DA-36-039 sc-63203.

TABLE OF CONTENTS

	Page
ABSTRACT	ii
ACKNOWLEDGMENT	iii
LIST OF TABLES	vi
LIST OF FIGURES	vii
CHAPTER I. INTRODUCTION	1
1.1 Statement of Problem	1
1.2 General Considerations of Distributed Amplifier	2
CHAPTER II. LARGE-SIGNAL ANALYSIS OF DISTRIBUTED AMPLIFIERS	4
2.1 Assumptions	7
2.2 Plate Load Impedance	9
2.3 Plate Load Impedance for Specific Cases	11
CHAPTER III. FREQUENCY LIMITATIONS IN DISTRIBUTED AMPLIFIERS	21
3.1 Cancellation of Lead Inductances	
3.2 Conductive Loading of the Grid Line Due to High Frequency Effects	24
3.3 Frequency Tolerance	28
3.4 Summary	31
CHAPTER IV. GRID LOSSES	
4.1 Attenuation Constant of Constant-k Filters with Losses	32
4.2 Determination of the Plate Load Impedance with Attenuation in the Grid Line	33
4.3 Modification of Gain Equation to Account for Losses in the Grid Line	36
CHAPTER V. EFFICIENCY	50
5.1 Calculation of Efficiency	50
5.2 Maximum Theoretical Efficiency of Distributed Amplifiers	52
5.3 Staggering the Plate Supply Voltages for Individual Tubes	56
CHAPTER VI. GRAPHICAL ANALYSIS	
6.1 Introduction	58
6.2 Graphical Determination of Power Output and Efficiency	58
6.3 Approximate Graphical Solution	60
6.4 Frequency Tolerance	61

TABLE OF CONTENTS (Cont.)

	Page
6.5 Second Harmonic Distortion	63
6.6 Sample Design of a Distributed Amplifier Using 4X150A Tubes	64
CHAPTER VII. CONCLUSIONS	89
7.1 Introduction	89
7.2 Summary of Results	89
7.3 Suggestions for Further Research	90
APPENDIX A. SERIES FOR PLATE-CATHODE VOLTAGE ON K^{TH} TUBE OF AN N-TUBE DISTRIBUTED AMPLIFIER	91
APPENDIX B. LOW-FREQUENCY DISTRIBUTED AMPLIFIER USING 807 TUBES	94
APPENDIX C. PLATE LOAD IMPEDANCE FOR PAIRED-PLATE	97
APPENDIX D. INPUT RESISTANCE OF A VACUUM TUBE DUE TO CATHODE LEAD INDUCTANCE	100
APPENDIX E. DETERMINATION OF PLATE LOAD IMPEDANCE WITH ATTENUATION IN THE GRID LINE	102
APPENDIX F. GRAPHICAL CALCULATION OF THE OPERATION OF A 9-TUBE DISTRIBUTED AMPLIFIER USING 4X150A TUBES	106
BIBLIOGRAPHY	142

LIST OF TABLES

		Page
6.1	Instantaneous Values of Plate Current and Grid Current $E_{bq} = 800v$; $E_{c2} = 400v$; $E_{c1} = -13.3$ volts; $E_{sig} = 33.3$ volts peak	74
6.2	Results and Computations $E_{bq} = 800v$, $E_{c2} = 400v$, $E_{c1} = -13.3$, $E_{sig} = 33.3$ volts peak	81
B.1	Measurements on Tube Number 1 of 15 KC Distributed Amplifier	96
F.1	Results and Computations $E_{bq} = 800v$, $E_{c2} = 400v$, $E_{c1} = -20$ v, $E_{sig} = 40$ v peak	107
F.2	Results and Computations $E_{bq} = 800v$, $E_{c2} = 400v$, $E_{c1} = -26.6v$, $E_{sig} = 46.6v$ peak	113
F.3	Results and Computations $E_{bq} = 800v$, $E_{c2} = 400v$, $E_{c1} = -40$ volts, $E_{sig} = 60$ v peak	119
F.4	Results and Computations $E_{bq} = 800v$, $E_{c2} = 400v$, $E_{c1} = -53.3v$, $E_{sig} = 73.3v$ peak	125
F.5	Results and Computations $E_{bq} = 800v$, $E_{c2} = 400v$, $E_{c1} = -66.6v$, $E_{sig} = 86.6$ v peak	131
F.6	Results and Computations $E_{bq} = 800v$, $E_{c2} = 400v$, $E_{c1} = -80v$, $E_{sig} = 100$ v peak	136

LIST OF FIGURES

		Page
Fig. 2.1	Block Diagram of an n-Tube Distributed Amplifier	5
Fig. 2.2	Z_p and θ as a Function of ϕ for Tube 1 of a 6-Tube Distributed Amplifier	12
Fig. 2.3	Z_p and θ as a Function of ϕ for Tube 2 of a 6-Tube Distributed Amplifier	13
Fig. 2.4	Z_p and θ as a Function of ϕ for Tube 3 of a 6-Tube Distributed Amplifier	14
Fig. 2.5	Z_p and θ as a Function of ϕ for Tube 4 of a 6-Tube Distributed Amplifier	15
Fig. 2.6	Z_p and θ as a Function of ϕ for Tube 5 of a 6-Tube Distributed Amplifier	16
Fig. 2.7	Z_p and θ as a Function of ϕ for Tube 6 of a 6-Tube Distributed Amplifier	17
Fig. 2.8	Plate Load Impedance for a 9-Tube Distributed Amplifier	18
Fig. 2.9	Plate Load Impedance for a 6-Tube Paired-Plate Distributed Amplifier	20
Fig. 3.1	Schematic Diagram for a Low-Pass, Pi-Section, Constant-k Filter	21
Fig. 3.2	Negative Mutual Transformer and Its Equivalent "T"	23
Fig. 3.3	Plot of Cut-off Frequency of Constant-k Filter as a Function of the Coefficient of Coupling of the Negative-Mutual Transformer Necessary to Cancel the Lead Inductance	25
Fig. 3.4	Equivalent Circuit for the Determination of Input Conductance Caused by the Feedback Resulting From Cathode Lead Inductance	26
Fig. 3.5	Variation of Mid-Shunt Image Impedance as a Function of Frequency	29
Fig. 3.6	Variation of the Plate Load Impedance of the Last Tube of a 6-Tube Distributed Amplifier as a Function of Frequency	30
Fig. 4.1	Plate Load Impedance as a Function of Frequency for a 6-Tube 4X150A Distributed Amplifier with a 90 Ω Plate Line	35

LIST OF FIGURES (Cont.)

	Page
Fig. 4.2 Plate Load Impedance as a Function of Frequency For Tube No. 1 and Tube No. 6 of a 6-Tube 4X150A Distributed Amplifier	37
Fig. 4.3 Normalized Voltage Amplification as a Function of Frequency for $\frac{n\alpha_0}{2} = 0.5$ and $\frac{\alpha_{odr}}{\alpha_0} = 0.05$	41
Fig. 4.4 Normalized Voltage Amplification as a Function of Frequency for $\frac{n\alpha_0}{2} = 0.5$ and $\frac{\alpha_{odr}}{\alpha_0} = 0.10$	42
Fig. 4.5 Normalized Voltage Amplification as a Function of Frequency for $\frac{n\alpha_0}{2} = 0.5$ and $\frac{\alpha_{odr}}{\alpha_0} = 0.15$	43
Fig. 4.6 Normalized Voltage Amplification as a Function of Frequency for $\frac{n\alpha_0}{2} = 0.45$ and $\frac{\alpha_{odr}}{\alpha_0} = 0.20$	44
Fig. 4.7 Normalized Voltage Amplification as a Function of Frequency for $\frac{n\alpha_0}{2} = 0.49$ and $\frac{\alpha_{odr}}{\alpha_0} = 0.20$	45
Fig. 4.8 Normalized Voltage Amplification as a Function of Frequency for $\frac{n\alpha_0}{2} = 0.5$ and $\frac{\alpha_{odr}}{\alpha_0} = 0.20$	46
Fig. 4.9 Normalized Voltage Amplification as a Function of Frequency for $\frac{n\alpha_0}{2} = 0.45$ and $\frac{\alpha_{odr}}{\alpha_0} = 0.25$	47
Fig. 4.10 Normalized Voltage Amplification as a Function of Frequency for $\frac{n\alpha_0}{2} = 0.48$ and $\frac{\alpha_{odr}}{\alpha_0} = 0.25$	48
Fig. 4.11 Normalized Voltage Amplification as a Function of Frequency for $\frac{n\alpha_0}{2} = 0.5$ and $\frac{\alpha_{odr}}{\alpha_0} = 0.25$	49
Fig. 5.1 Idealized Constant-Current Tube Plate Characteristics With Load Line Drawn for Class A Operation	53
Fig. 5.2 Idealized Constant-Current Tube Plate Characteristics With Load Line Drawn for Class B Operation	53
Fig. 5.3 Instantaneous Value of Plate Voltage and Plate Current	54
Fig. 5.4 Variation of Maximum Theoretical Efficiency of a Distributed Amplifier as a Function of the Conduction Angle of Plate Current	57
Fig. 6.1 Frequency Variation of the Plate Load Impedance of the 6th Tube in a Distributed Amplifier Using 6, 4X150A Tubes with a Nominal Grid Line Impedance of 50 Ohms and a Nominal Plate Line Impedance of 90 Ohms	62

LIST OF FIGURES (Cont.)

	Page	
Fig. 6.2	Second Harmonic Output Current Factor, $F_n\left(\frac{\omega}{\omega_c}\right)$, for $n = 6$ and $n = 9$ Plotted as a Function of Frequency	65
Fig. 6.3	Variation of Equivalent Shunt Resistance of a 4X150A Caused by Lead Inductances and Transit Time	66
Fig. 6.4	Attenuation Constant Per Section of Grid Line Due to Small Signal Effects of a Distributed Amplifier Using 4X150A Tubes. $R_g = 50 \Omega$	68
Fig. 6.5	Variation of Grid Voltage as a Function of Frequency for a 300 MC, 4X150A Distributed Amplifier for Peak Grid Voltages Less Than 0 Volts	69
Fig. 6.6	Plate Characteristics for a 4X150A with $E_{c2} = 400$ Volts Load Lines Drawn for a 9-Tube Distributed Amplifier at Low Frequencies for Various Q-Points Considered in Graphical Analysis	71
Fig. 6.7	Dynamic Transfer Characteristic for a 9-Tube Distributed Amplifier with $E_{bb} = 800V$, $E_{c2} = 400V$.	72
Fig. 6.8	Grid Current as a Function of Grid Voltage for a 4X150A	73
Fig. 6.9	i_b VS ωt for $E_{bq} = 800V$, $E_{c2} = 400V$, $E_{c1} = -13.3V$ $E_{sig} = 33.3$ V peak	75
Fig. 6.10	$i_b \cos \omega t$ VS. ωt for $E_{bq} = 800V$, $E_{c2} = 400V$, $E_{c1} = -13.3V$ $E_{sig} = 33.3V$ Peak	76
Fig. 6.11	$i_b \cos 2\omega t$ VS. ωt for $E_{bq} = 800V$, $E_{c2} = 400V$, $E_{c1} = -13.3V$ $E_{sig} = 33.3V$ Peak	77
Fig. 6.12	Instantaneous Value of Grid Current as a Function of ωt for $E_{bq} = 800V$, $E_{c2} = 400V$, $E_{c1} = -13.3V$ Peak Signal Voltage = 33.3 Volts	78
Fig. 6.13	$i_{c1} \cos \omega t$ VS. ωt for $E_{bq} = 800V$, $E_{c2} = 400V$, $E_{c1} = -13.3V$ Peak Signal Voltage = 33.3 Volts	80
Fig. 6.14	Graphical Summary of Results Calculated for a 9-Tube Distributed Amplifier Using 4X150A Tubes for $E_{bq} = 800V$, $E_{c2} = 400V$, and a Maximum Instantaneous Grid Voltage of +20V	82
Fig. 6.15	Graphical Summary of Results Calculated for a 9-Tube Distributed Amplifier Using 4X150A Tubes for $E_{bq} = 800V$, $E_{c2} = 500V$, and a Maximum Instantaneous Grid Voltage of +25V	84

LIST OF FIGURES (Cont.)

	Page
Fig. 6.16 Graphical Summary of Results Calculated for a 9-Tube Distributed Amplifier Using 4X150A Tubes for $E_{bq} = 800V$, $E_{c2} = 600V$, and a Maximum Instantaneous Grid Voltage of +10V	85
Fig. 6.17 Graphical Summary of Results Calculated for a 9-Tube Distributed Amplifier Using 4X150A Tubes for $E_{bq} = 1000$ Volts, $E_{c2} = 400$ Volts, and a Maximum Instantaneous Grid Voltage of +20 Volts	86
Fig. 6.18 Graphical Summary of Results Calculated for a 9-Tube Distributed Amplifier Using 4X150A Tubes for $E_{bq} = 1000V$, $E_{c2} = 500V$, and a Maximum Instantaneous Grid Voltage of +25V	87
Fig. 6.19 Graphical Summary of Results Calculated for a 9-Tube Distributed Amplifier Using 4X150A Tubes for $E_{bq} = 1000V$, $E_{c2} = 600V$, and a Maximum Instantaneous Grid Voltage of +10V	88
Fig. B.1 Schematic Diagram for 15kc Distributed Amplifier	95
Fig. C.1 Block Diagram of Paired-Plate Distributed Amplifier	97
Fig. D.1 Equivalent Circuit of a Tube Used for the Determination of Input Conductance	100
Fig. F.1 i_b VS. ωt for $E_{bq} = 800V$, $E_{c2} = 400V$, $E_{c1} = -20V$, $E_{sig} = 40V$ Peak	108
Fig. F.2 $i_b \cos \omega t$ VS. ωt for $E_{bq} = 800V$, $E_{c2} = 400V$, $E_{c1} = -20V$, $E_{sig} = 40V$ Peak	109
Fig. F.3 $i_b \cos 2 \omega t$ VS ωt for $E_{bq} = 800V$, $E_{c2} = 400V$, $E_{c1} = -20V$, $E_{sig} = 40V$ Peak	110
Fig. F.4 Instantaneous Value of Grid Current as a Function of ωt for $E_{bq} = 800V$, $E_{c2} = 400V$, $E_{c1} = -20V$, Peak Signal Voltage = 40.0 Volts	111
Fig. F.5 $i_{c1} \cos \omega t$ VS ωt for $E_{bq} = 800V$, $E_{c2} = 400V$, $E_{c1} = -20.0V$, Peak Signal Volts = 40.0 Volts	112
Fig. F.6 i_b VS ωt for $E_{bq} = 800V$, $E_{c2} = 400V$, $E_{c1} = -26.6V$, $E_{sig} = 46.6V$ Peak	114
Fig. F.7 $i_b \cos \omega t$ VS ωt for $E_{bq} = 800V$, $E_{c2} = 400V$, $E_{c1} = -26.6V$, $E_{sig} = 46.6V$ Peak	115

LIST OF FIGURES (Cont.)

	Page	
Fig. F.8	$i_b \text{ COS } 2\omega t \text{ VS. } \omega t \text{ for } E_{bq} = 800V, E_{c2} = 400V,$ $E_{c1} = -26.6V, E_{sig} = 46.6V \text{ Peak}$	116
Fig. F.9	Instantaneous Value of Grid Current as a Function of ωt for $E_{bq} = 800V, E_{c2} = 400V, E_{c1} = -26.6V,$ Peak Signal Voltage = 46.6 Volts	117
Fig. F.10	$i_{c1} \text{ COS } \omega t \text{ VS. } \omega t \text{ for } E_{bq} = 800V, E_{c2} = 400V, E_{c1} = -26.6V,$ Peak Signal Voltage = 46.6 Volts	118
Fig. F.11	$i_b \text{ VS. } \omega t \text{ for } E_{bq} = 800V, E_{c2} = 400V, E_{c1} = -40V,$ $E_{sig} = 60V \text{ Peak}$	120
Fig. F.12	$i_b \text{ COS } \omega t \text{ VS. } \omega t \text{ for } E_{bq} = 800V, E_{c2} = 400V, E_{c1} = -40V,$ $E_{sig} = 60V \text{ Peak}$	121
Fig. F.13	$i_b \text{ COS } 2\omega t \text{ VS. } \omega t \text{ for } E_{bq} = 800V, E_{c2} = 400V, E_{c1} = -40V,$ $E_{sig} = 60V \text{ Peak}$	122
Fig. F.14	Instantaneous Value of Grid Current as a Function of $\omega t,$ for $E_{bq} = 800V, E_{c2} = 400V, E_{c1} = 40V,$ Peak Signal Voltage = 60.0 Volts	123
Fig. F.15	$i_{c1} \text{ COS } \omega t \text{ VS. } \omega t \text{ for } E_{bq} = 800V, E_{c2} = 400V, E_{c1} = -40V,$ Peak Signal Voltage = 60 Volts	124
Fig. F.16	$i_b \text{ VS. } \omega t \text{ for } E_{bq} = 800V, E_{c2} = 400V, E_{c1} = -53.3V,$ $E_{sig} = 73.3V \text{ Peak}$	126
Fig. F.17	$i_b \text{ COS } \omega t \text{ VS. } \omega t \text{ for } E_{bq} = 800V, E_{c2} = 400V, E_{c1} = -53.3V,$ $E_{sig} = 73.3V \text{ Peak}$	127
Fig. F.18	$i_b \text{ COS } 2\omega t \text{ VS. } \omega t \text{ for } E_{bq} = 800V, E_{c2} = 400V, E_{c1} = -53.3V,$ $E_{sig} = 73.3V \text{ Peak}$	128
Fig. F.19	Instantaneous Value of Grid Current as a Function of ωt for $E_{bq} = 800V, E_{c2} = 400V, E_{c1} = -53.3V,$ Peak Signal Voltage = 73.3 Volts	129
Fig. F.20	$i_{c1} \text{ COS } \omega t \text{ VS. } \omega t \text{ for } E_{bq} = 800V, E_{c2} = 400V, E_{c1} = -53.3V,$ Peak Signal Voltage = 73.3 Volts	130
Fig. F.21	i_b and $i_b \text{ COS } \omega t \text{ VS. } \omega t \text{ for } E_{bq} = 800V, E_{c2} = 400V,$ $E_{c1} = -66.6V, E_{sig} = 86.6V \text{ Peak}$	132
Fig. F.22	$i_b \text{ COS } 2\omega t \text{ VS. } \omega t \text{ for } E_{bq} = 800V, E_{c2} = 400V, E_{c1} = -66.6V,$ $E_{sig} = 86.6V \text{ Peak}$	133

LIST OF FIGURES (Cont.)

	Page	
Fig. F.23	Instantaneous Value of Grid Current as a Function of ωt for $E_{bq} = 800V$, $E_{c2} = 400V$, $E_{c1} = -66.6$ Volts, Peak Signal Voltage = 86.6 Volts	134
Fig. F.24	$i_{c1} \cos \omega t$ VS ωt for $E_{bq} = 800V$, $E_{c2} = 400V$, $E_{c1} = 66.6V$, Peak Signal Voltage = 86.6 Volts	135
Fig. F.25	i_b VS ωt for $E_{bq} = 800V$, $E_{c2} = 400V$, $E_{c1} = -80V$, $E_{sig} = 100V$ Peak	137
Fig. F.26	$i_b \cos \omega t$ VS ωt for $E_{bq} = 800V$, $E_{c2} = 400V$, $E_{c1} = -80V$, $E_{sig} = 100V$ Peak	138
Fig. F.27	$i_b \cos 2\omega t$ VS ωt for $E_{bq} = 800V$, $E_{c2} = 400V$, $E_{c1} = -80V$, $E_{sig} = 100V$ Peak	139
Fig. F.28	Instantaneous Value of Grid Current as a Function of ωt for $E_{bq} = 800V$, $E_{c2} = 400V$, $E_{c1} = -80V$, Peak Signal Voltage = 100 Volts	140
Fig. F.29	$i_b \cos \omega t$ VS ωt for $E_{bq} = 800V$, $E_{c2} = 400V$, $E_{c1} = -80.0V$, Peak Signal Voltage = 100.0V	141

LARGE SIGNAL ANALYSIS OF DISTRIBUTED AMPLIFIERS

CHAPTER I. INTRODUCTION

The primary importance of the distributed amplifier circuit is derived from its ability to operate in the frequency range above that covered by conventional amplifiers and below that covered by microwave amplifiers. The frequency range of conventional wide-band power amplifiers is generally limited to frequencies of the order of 10 mc. Microwave power amplifiers of the traveling-wave-tube type have been constructed to operate with lower frequency limits of the order of hundreds of megacycles. The distributed amplifier can be designed to operate from tens of megacycles to hundreds of megacycles, thus filling the gap between conventional techniques and microwave techniques.

1.1 Statement of Problem

Equations describing the behavior of distributed amplifiers when transmitting small signals have been derived and studied by Ginzton, Hewlett, Jasberg, Noe¹ and others²⁻⁹. They have described various methods of obtaining a specified frequency response, and have also described special design procedures necessary at high frequencies.

It is the purpose of this dissertation to extend the analysis of distributed amplifiers to account for large-signal effects, and to determine a graphical procedure for analyzing the non-linear operation of the tubes in a distributed amplifier. The efficiency of devices designed to deliver power is of major importance in comparing power amplifiers; therefore, the efficiency of the distributed amplifier is discussed in detail in this paper.

1.2 General Considerations of Distributed Amplifiers

Basically, distributed amplification¹ is based upon a physical distribution of vacuum tubes between two transmission lines. The grids of the tubes are connected to the input transmission and the plates are connected to the output transmission line. Adjacent grids and adjacent plates are connected to the transmission lines in such a manner that the phase shift of the input voltage in traversing the line between adjacent grids is equal to the phase shift in the output signal in traversing the plate line between the corresponding plates. All of the individual tube currents add in phase at the output.

The significant contribution of distributed amplifiers to wide-band amplification lies in the fact that the input and output capacities of the tubes are used as the shunt elements of artificial transmission lines in which the gain of the individual tubes add rather than multiply as in conventional cascaded amplifier. Hence, the gain of the individual tubes may be less than unity and yet the gain of the amplifier may be adjusted to any desired value by the number of tubes. This circuit essentially removes the gain-bandwidth limitation of conventional amplifiers.

The voltage gain of distributed amplifiers¹ may be written as

$$A = \frac{n g_m}{2} \sqrt{Z\pi_g} \cdot \sqrt{Z\pi_p} \quad (1.1)$$

where n = the number of tubes

g_m = the transconductance of the tubes

$Z\pi_g$ = the mid-shunt image impedance of the artificial grid line

and $Z\pi_p$ = the mid-shunt image impedance of the artificial plate line.

Equation (1.1) neglects the attenuation on the grid and plate lines. The voltage amplification has a very objectionable peak as the cut-off frequency is approached due to the nature of $Z\pi$. If the attenuation on the grid line is

caused by the transit time and other high frequency effects, it is possible to adjust the product of the number of tubes and the cut-off angular frequency² for a relatively flat amplification over the design frequency range.

$$n\omega_c = \frac{\omega^2 C_g}{G_{in}} \quad (1.2)$$

where ω_c = the cut-off angular frequency

G_{in} = the input conductance of the tube due to high-frequency effects measured at the angular frequency ω

and

C_g = the input capacity of the tube.

The large-signal analysis of any active network in general involves the characteristic curves for the active element. The normal procedure in a large-signal analysis is to plot the voltage-current locus of the passive network on the characteristics of the active element. This locus determines the operation of the active element and allows its operation to be calculated. A distributed amplifier differs from most active networks in that each of the tubes in the amplifier contributes to the operating locus of any given tube in the amplifier. Hence the operating locus of plate voltage versus plate current for each tube in a distributed amplifier is different from any other tube. Chapter II is devoted to the determination of this operating locus.

CHAPTER II. LARGE-SIGNAL ANALYSIS OF DISTRIBUTED AMPLIFIERS

The analyses of distributed amplifiers presented in the literature have concerned themselves with the small-signal theory. From the small-signal standpoint the voltage gain and the frequency response are of prime concern; however, in distributed power amplifiers, saturated power output level and efficiency are also factors of prime interest to the designer. In fact, in many large-signal applications more emphasis is placed on the saturated power output level than is placed on the gain. The saturated power output level can only be determined from the tube characteristics. Therefore, in large-signal analysis, the tube characteristic curves will normally be used instead of the small-signal concept of transconductance.

In order to be able to utilize the tube characteristic curves for calculations involving distributed amplifiers it is necessary to know the operating locus of plate voltage versus plate current for each tube. This locus is generally referred to as the operating load line or as defining the plate load impedance. In the low-pass distributed amplifier circuit shown schematically in Figure 2.1 it is easily ascertained that all of the tubes are essentially in parallel at frequencies sufficiently low so that the phase shift between sections (i.e., between adjacent plates or grids) may be neglected. If all the tubes are identical, and if the grid voltage applied to each tube does not vary with the position of the tube in the amplifier, then each tube will deliver identical currents to the plate line. The voltage across the output resistance will be greater by a factor n (the number of tubes in the distributed amplifier) than the output voltage would be if only one tube were operating. This voltage also appears across each tube in the distributed amplifier. Hence the impedance seen by each tube is n times the impedance that tube would see if it were the

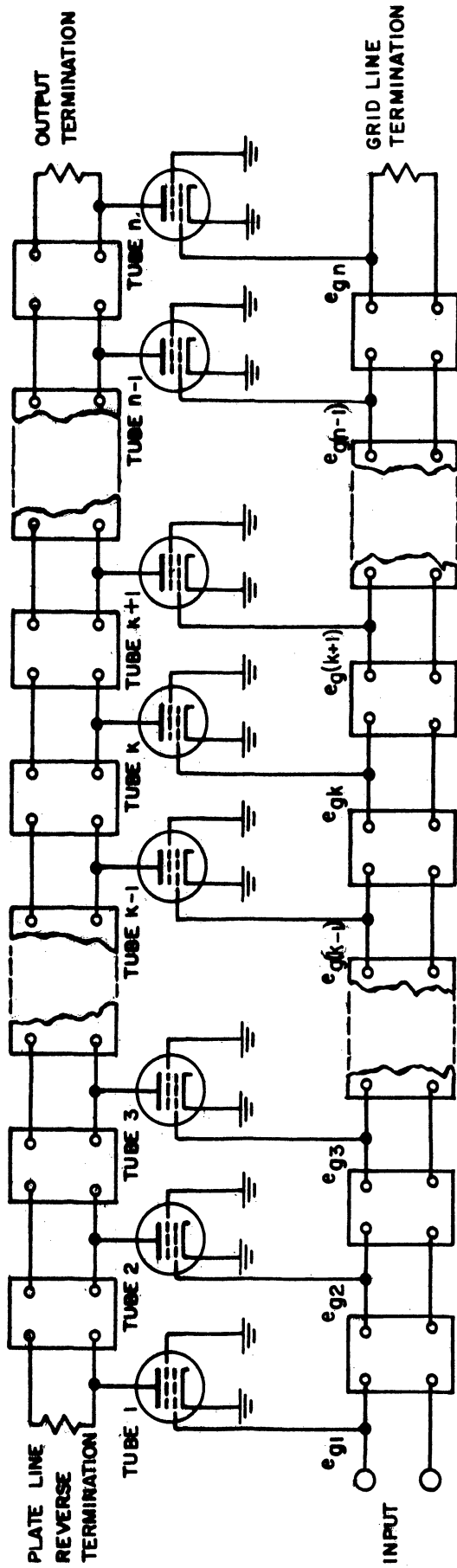


FIG. 2.1. BLOCK DIAGRAM OF AN n -TUBE DISTRIBUTED AMPLIFIER.

only one operating, or

$$Z = n \frac{Z_0}{2} \quad (2.1)$$

This equation is valid for operating frequencies sufficiently close to zero so that all the grids and all the plates are essentially in parallel.

As the operating frequency increases, the phase angle between the voltages on adjacent grids becomes more important since the grid voltages determine the phase angle of the currents that are fed into the plate line. In a conventional distributed amplifier the phase shift per section of the plate line is the same as the phase shift per section of the grid line, so that each of the paths a signal may pursue through a distributed amplifier produces the same amount of phase shift on the signal. The voltages appearing between plate and cathode of an individual tube will vary with the operating frequency, the position of the tube in the distributed amplifier, and the characteristic impedance of the plate line.

Tetrodes or pentodes are generally used in distributed amplifiers because of their inherently low capacitance between plate and grid. This low inter-electrode capacitance minimizes coupling between the plate line and the grid line and increases the stability of the distributed amplifier. This restriction of the choice of tube types to tetrodes or pentodes means that the tubes used in distributed amplifiers approximate constant-current devices in which the output current is independent of the plate voltage over a large region of operation. The output current is dependent only on the grid voltage.

The plate load impedance of each tube will be calculated as the ratio of the voltage appearing between the plate and cathode of the particular tube in question to the plate current of the same tube. This plate load impedance can then be used in conjunction with the plate characteristics of the tube to determine the operating path of the tube, the point at which the tube will begin to saturate, and the amount of distortion generated in the tube. The efficiency of the

distributed amplifier can be calculated, given the operating locus of each tube and the plate characteristics.

2.1 Assumptions

Four assumptions were made in order to simplify the analysis. These assumptions are discussed in some detail in this section.

The first assumption is that the grid line has no loss; this means that the signal voltage is the same on every tube in the distributed amplifier. The errors incurred in using this assumption will be analyzed later; however, when the distributed amplifier is designed to operate at higher frequencies, it is obvious that many factors will influence the loss in the grid line. The input impedance of the tubes used in the distributed amplifier is one of the major factors involved in the grid-line dissipation. The input impedance of the tube can be considered as a capacity in parallel with a resistance connected between grid and cathode. The capacity remains fairly constant with frequency, but the resistive component decreases as the square of frequency. This resistive component arises from the fact that the cathode lead inductance, in conjunction with the capacity between the grid and the cathode, gives rise to grid current that has an in-phase component. In addition, the inductance in series with the screen, and the capacity between the screen and the grid, give rise to an in-phase current. However, the latter in-phase component of current is 180° out-of-phase with the applied voltage, which leads to a negative resistance. Also there will be some radiation from the grid line which will have the same effect as increased dissipation; however, this radiation can be reduced to a point where it is negligible by proper shielding. The series coils in the grid line give rise to some loss, but this loss can be kept small in comparison with that caused by the grid loading. Most of the effects discussed here are high-frequency effects that are common to any wide-band high-frequency amplifier.

The second assumption is that the plate line has no dissipation, and also that it has a constant transfer characteristic with frequency up to the cut-off frequency. The characteristic impedance of the plate line is assumed to be Z_0 . However, the magnitude of Z_0 may vary with frequency, but it is assumed to be resistive over the operating frequency range. The plate line is assumed to be matched at both ends. These assumptions are met fairly well in practice with the constant-k line with m-derived terminations. Radiation from the plate line can be a serious problem, but again, by adequate shielding, it is possible to reduce this loss so that it is negligible. The loss due to skin effect can be reduced by increasing the size of the wire used to wind the plate line.

The third assumption made in this analysis is that the tubes are identical. This implies that all of the tubes have the same transconductance and the same input and the same output capacitances. Variation of transconductance can change the results of the calculation of plate load impedance since a cancellation takes place at some frequencies which reduces the voltage between the plate and cathode of the first few tubes. The variation of input and output capacities from tube to tube will affect the frequency response of the amplifier and the characteristic impedance of the artificial transmission lines. However, the major effect of variation between tubes in input and output capacitances is to introduce ripple in the frequency response of the amplifier.

The final assumption is that the tube characteristics are ideal constant-current curves in that the output current is independent of the plate voltage as long as the plate voltage is positive. This still allows the idea of clipping to be introduced since the point where the operating load line intersects the $E_p = 0$ axis can be determined. This assumption allows the use of the transconductance of the tube as a measure of the output current, and also assures that the plate current is a function of the grid voltage alone.

2.2 Plate Load Impedance

An expression for the plate load impedance (the ratio of the plate-cathode voltage to the plate current) of any tube in an n-tube distributed amplifier is derived in the following analysis. It should be noted that the four assumptions discussed in Section 2.1 apply to this analysis. From these plate load impedances the efficiency of a given amplifier can be determined from the characteristics of the tubes involved. Once the operating path is known, it is a simple matter to determine also the point at which the amplifier begins to saturate.

As the frequency of operation increases the phase shift along the grid and plate lines cannot be neglected, and the plate load impedance becomes markedly different from that given in Equation 2.1. Since it has been assumed (Section 2.1) that there is no dissipation in the grid line, the individual grid voltages differ only in phase. If an equivalent large-signal transconductance (G_m) is defined as the ratio of the fundamental component of plate current to the fundamental component of grid voltage, the plate current of each tube can be written as

$$\begin{aligned}
 i_1 &= G_m E_{gm} \sin \omega t \\
 i_2 &= G_m E_{gm} \sin (\omega t - \phi) \\
 \vdots & \\
 i_k &= G_m E_{gm} \sin [\omega t - (k-1)\phi] \\
 \vdots & \\
 i_n &= G_m E_{gm} \sin [\omega t - (n-1)\phi]
 \end{aligned} \tag{2.2}$$

where $E_{gm} \sin \omega t$ is the instantaneous value of the grid voltage on the first tube of the distributed amplifier and ϕ is the phase shift per section of the grid and plate lines at the operating angular frequency ω .

The plate voltage on the k^{th} tube as a result of the application of a signal voltage to the input of the grid line can be calculated, by the Superposition Principle, as the sum of the voltages that would appear there as the tubes are turned on one at a time.

$$e_k = \sum_{j=1}^n e_{kj} \quad (2.3)$$

where j = the number of the tube that is operating.

If no loss is assumed in the plate line, the voltages appearing on each tube will have the same magnitude; however, the phase of the voltage appearing on the k^{th} tube plate will be dependent on the phase shift per section of the plate line and the number of sections the current traverses in arriving at the plate of the k^{th} tube. From tube number one, up to and including the k^{th} tube, the total number of sections of both grid line and plate line that are traversed by an input signal in arriving at the plate of the k^{th} tube (as these tubes are turned on one at a time) are equal. Hence the voltage on the k^{th} tube that results from any tube from one to k is equal to the plate current of the particular tube turned on multiplied by half the characteristic impedance of the plate line. The phase angle with respect to the grid voltage on the first tube will be $(k-1)$ times the phase shift per section of the filter networks that constitute the grid and plate lines. This results from the fact that the input signal must traverse $(k-1)$ filter sections in arriving at the plate of the k^{th} tube.

$$\begin{aligned} e_{k1} &= G_m E_{gm} \frac{Z_0}{2} \sin [\omega t - (k-1)\phi] \\ &\vdots \\ e_{kk} &= G_m E_{gm} \frac{Z_0}{2} \sin [\omega t - (k-1)\phi] \end{aligned} \quad (2.4)$$

The contribution of the plate currents of tubes $k+1$ to n to the plate voltage across the k^{th} tube are all different in phase since the number of sections of filter traversed in going from the input to the plate of the k^{th} tube is different for **each** path. The voltages due to tubes $(k+1)$ through n operating alone are

$$\begin{aligned} e_{k(k+1)} &= G_m E_{gm} \frac{Z_0}{2} \sin [\omega t - (k-1)\phi - 2\phi] \\ &\vdots \\ e_{kn} &= G_m E_{gm} \frac{Z_0}{2} \sin [\omega t - (k-1)\phi - 2(n-k)\phi] \end{aligned} \quad (2.5)$$

Substituting Equations 2.4 and 2.5 into Equation 2.3, and summing the resulting finite series as shown in Appendix A, yields

$$e_k = G_m E_{gm} \frac{Z_0}{2} \left\{ k \sin [\omega t - (k-1)\phi] + \frac{\sin(n-k)\phi}{\sin \phi} \sin [\omega t - (k-1)\phi - (n-k+1)\phi] \right\} \quad (2.6)$$

The plate load impedance that the k^{th} tube sees is given by the ratio of the plate voltage to the plate current (see Equation 2.2).

$$Z_k = \frac{e_k}{i_k} = \frac{Z_0}{2} \left[k + \frac{\sin(n-k)\phi}{\sin \phi} e^{-j(n-k+1)\phi} \right] \quad (2.7)$$

Equation 2.7 shows that the plate load impedances of all except the n^{th} tube possesses a phase angle which is different from zero except at discrete frequencies. The plate-voltage plate-current locus will in general be an ellipse, or over the majority of the frequency range all the tubes with the exception of the last tube operate with elliptical load lines.

2.3 Plate Load Impedance for Specific Cases

Equation 2.7 is plotted for each tube of a six-tube distributed amplifier in Figures 2.2 through 2.7. It can be seen in Figure 2.2 that the phase angle of the plate load impedance is greater than 90° in some regions. This indicates that in these regions the first tube is absorbing power from the plate line rather than delivering power to it. This power is dissipated in the form of heat at the plate of the first tube (in the case of a six-tube distributed amplifier). This increase in plate dissipation can give rise to serious tube burnout problems in practical distributed amplifiers where the amplifier is operated under full dc input conditions. Figure 2.8 shows the magnitude of the plate load impedances for each tube of a 9-tube distributed amplifier. The regions in which the angle of the plate load impedance is greater than 90° is indicated by the regions of increased width of the curves. It will be noted

ANGLE OF PLATE IMPEDANCE, θ

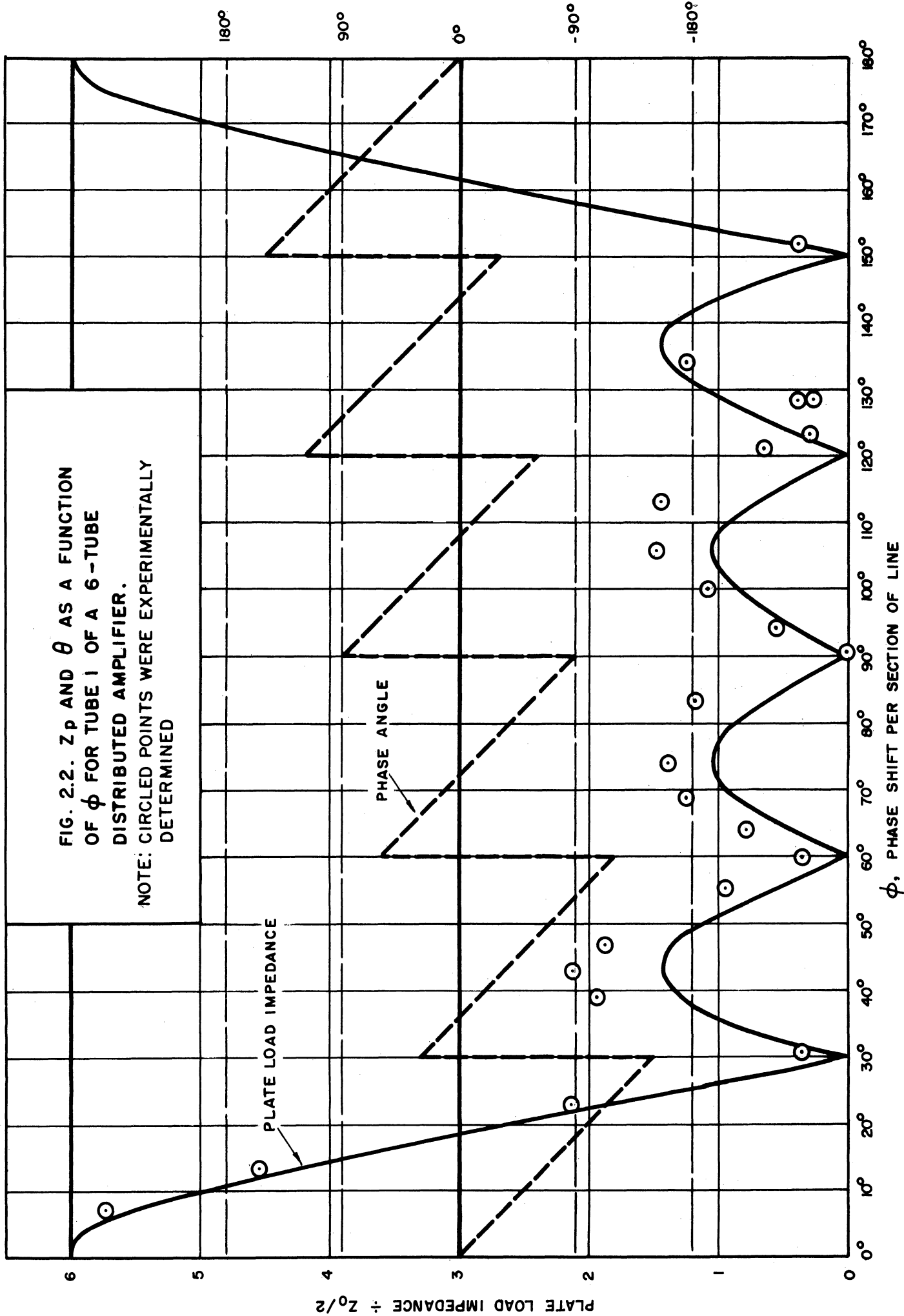


FIG. 2.2. Z_p and θ as a function of ϕ for tube 1 of a 6-tube distributed amplifier.

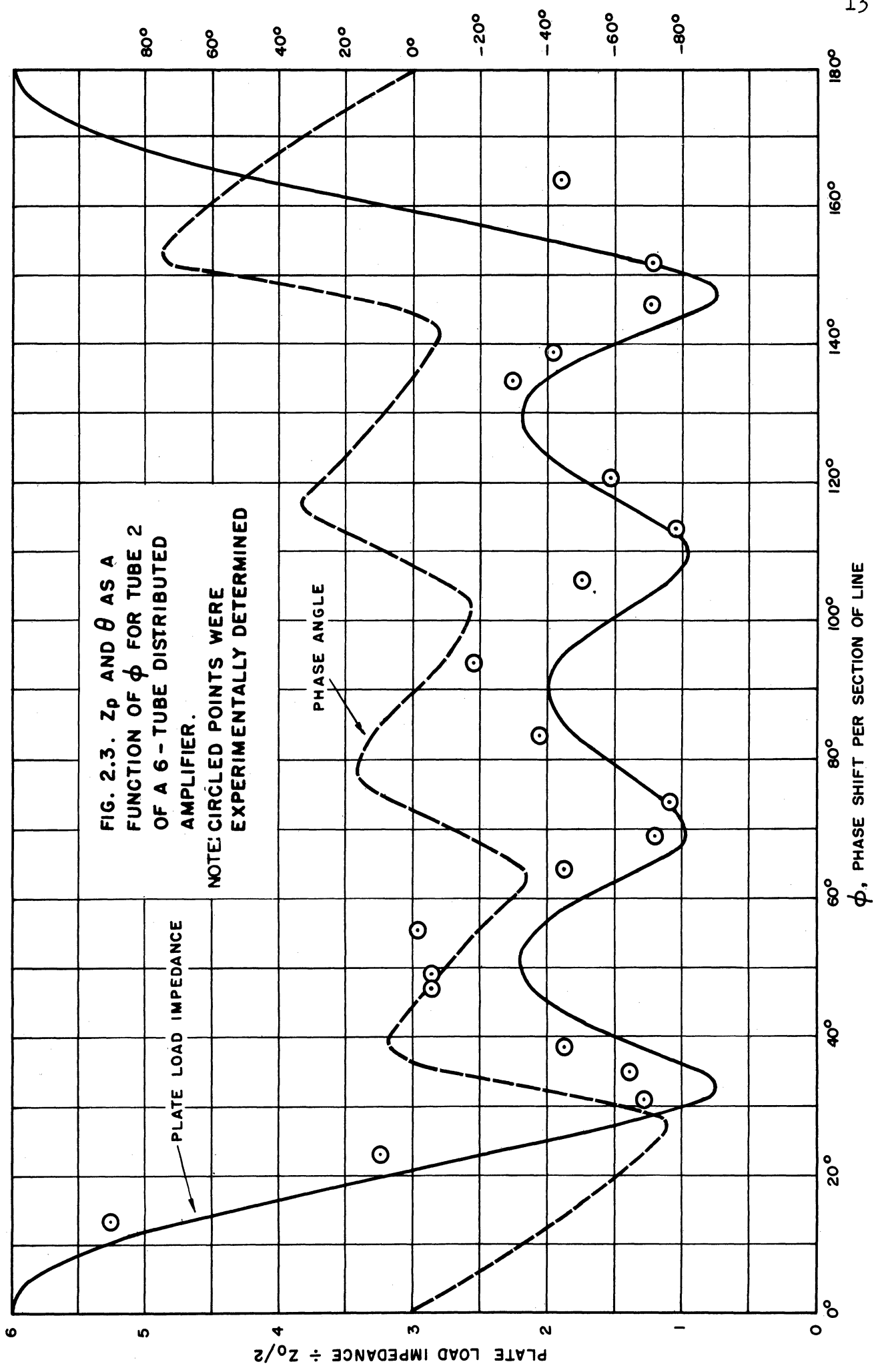
NOTE: CIRCLED POINTS WERE EXPERIMENTALLY DETERMINED

PLATE LOAD IMPEDANCE

PHASE ANGLE

ϕ , PHASE SHIFT PER SECTION OF LINE

PLATE LOAD IMPEDANCE $\div Z_0/2$



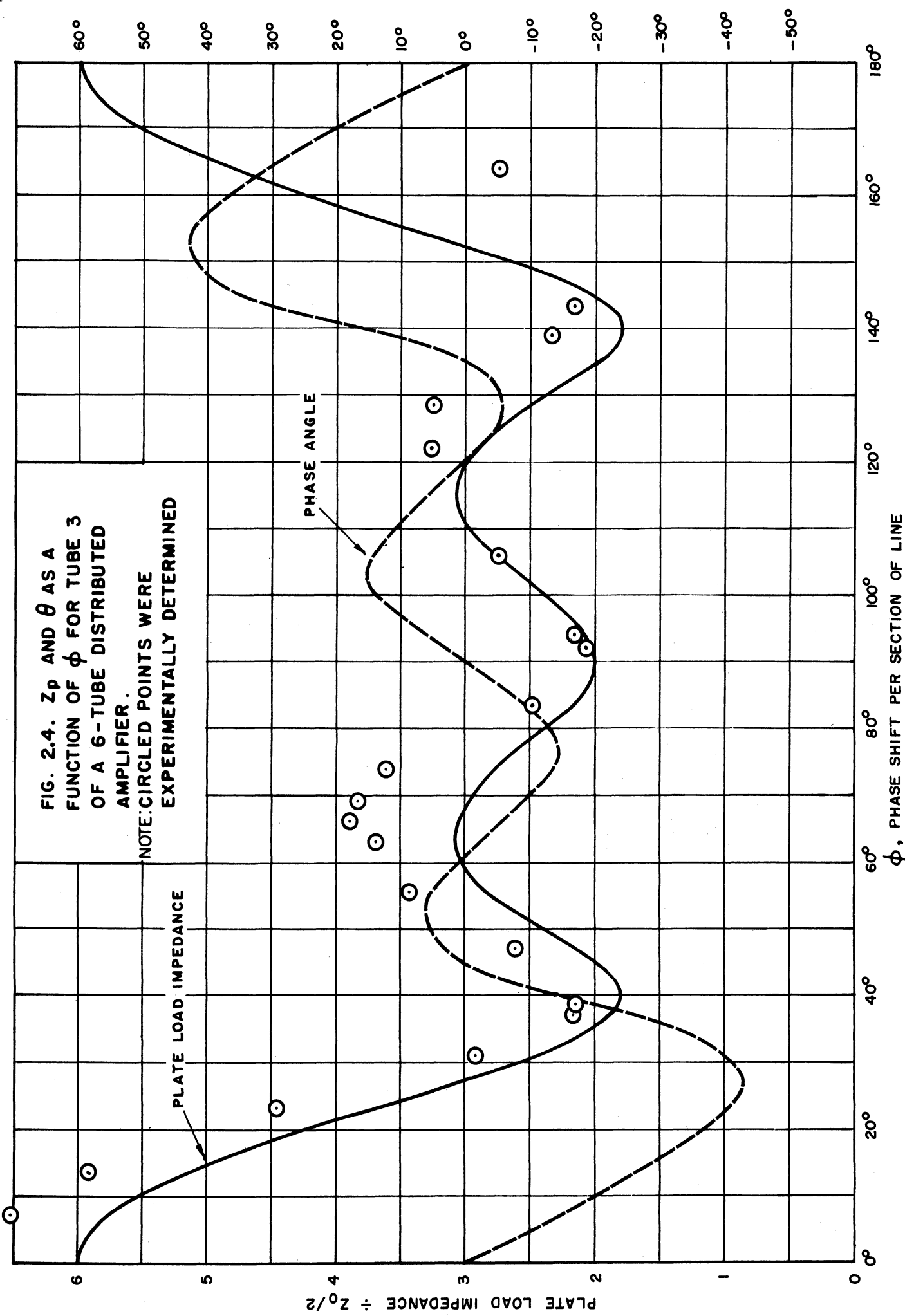
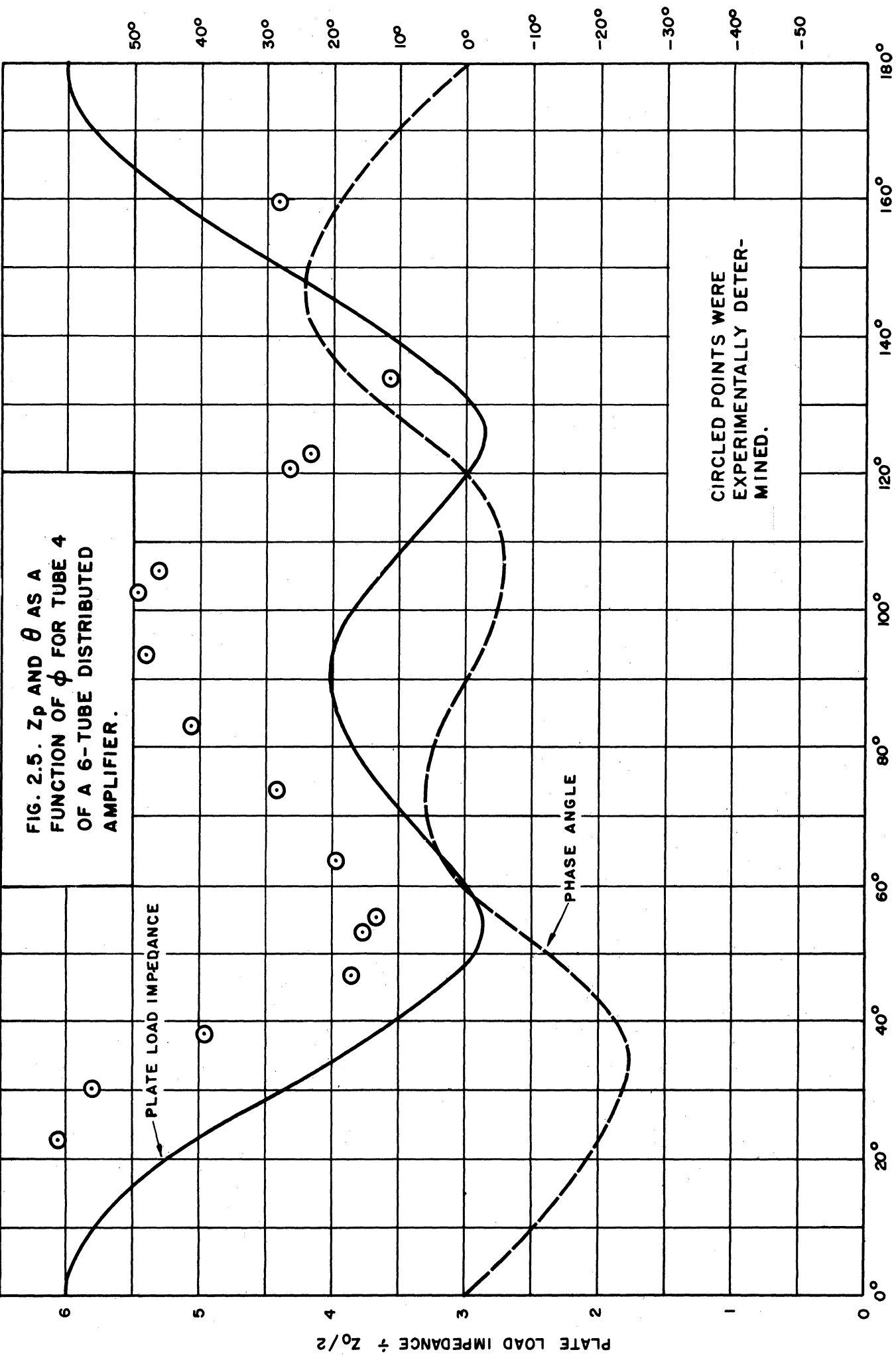


FIG. 2.5. Z_p AND θ AS A FUNCTION OF ϕ FOR TUBE 4 OF A 6-TUBE DISTRIBUTED AMPLIFIER.



CIRCLED POINTS WERE EXPERIMENTALLY DETERMINED.

PLATE LOAD IMPEDANCE

PHASE ANGLE

ϕ , PHASE SHIFT PER SECTION OF LINE

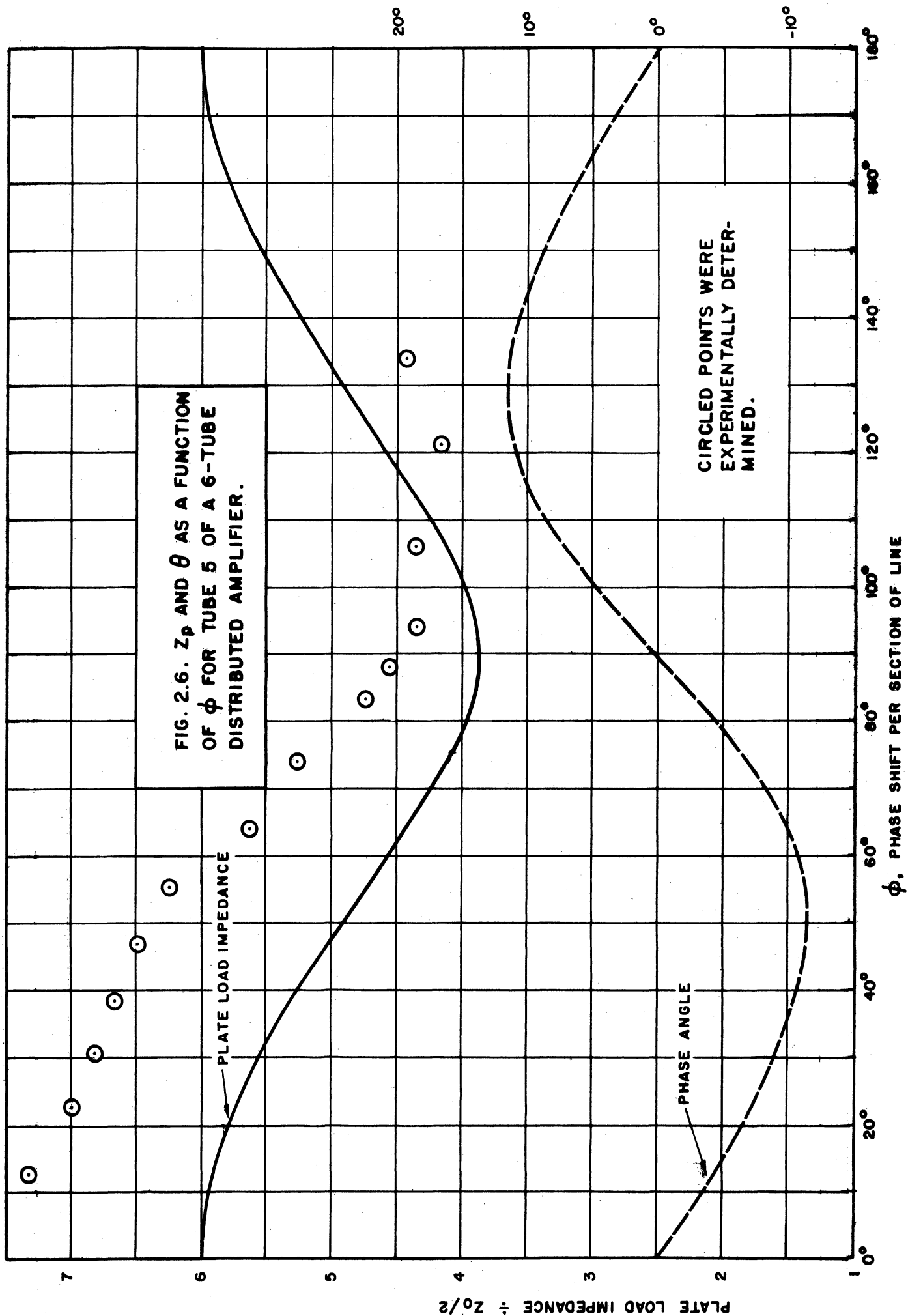


FIG. 2.6. Z_p AND θ AS A FUNCTION OF ϕ FOR TUBE 5 OF A 6-TUBE DISTRIBUTED AMPLIFIER.

CIRCLED POINTS WERE EXPERIMENTALLY DETERMINED.

PLATE LOAD IMPEDANCE

PHASE ANGLE

ϕ , PHASE SHIFT PER SECTION OF LINE

PLATE LOAD IMPEDANCE $\div Z_0/2$

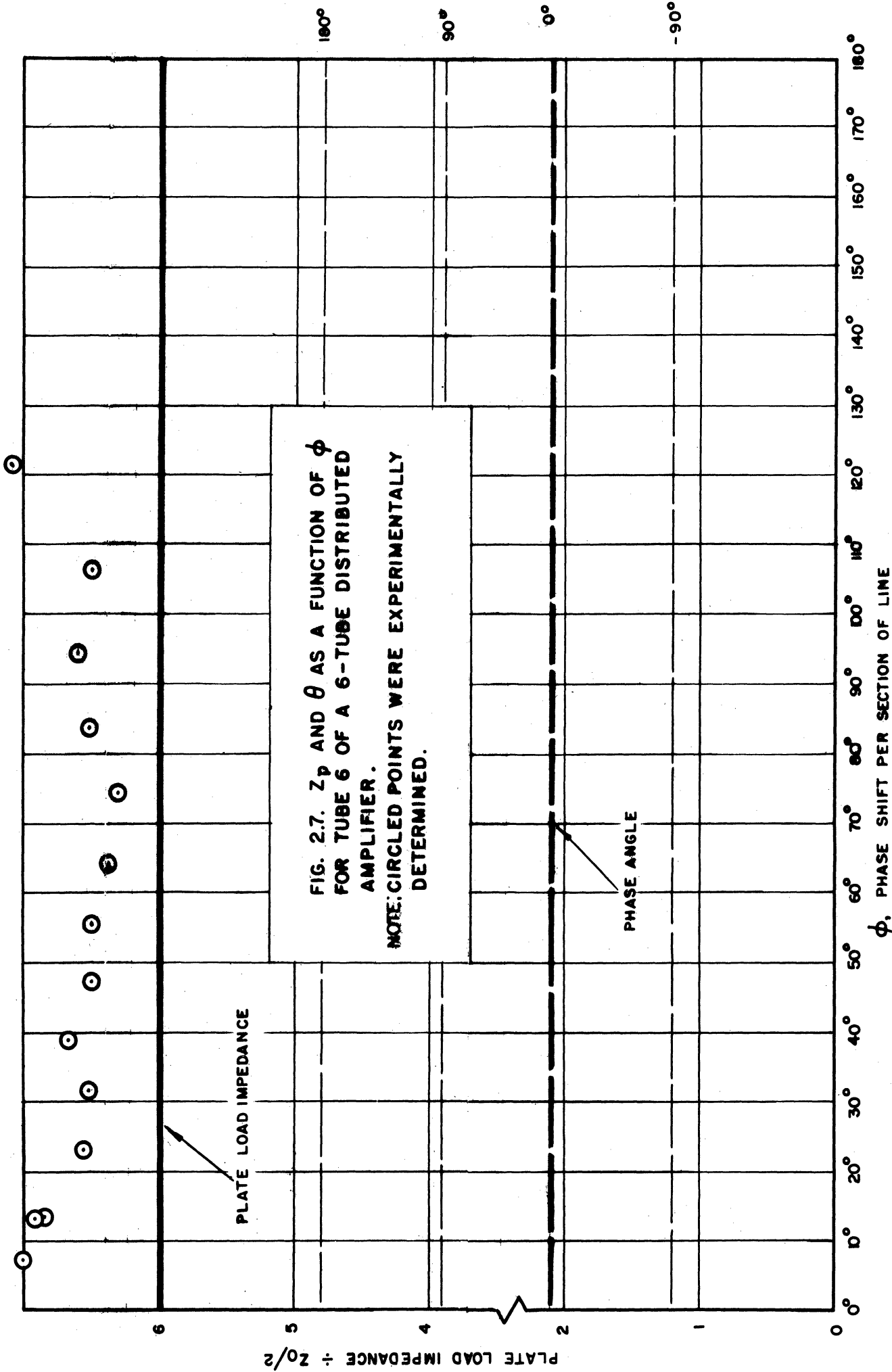


FIG. 2.7. Z_p AND θ AS A FUNCTION OF ϕ FOR TUBE 6 OF A 6-TUBE DISTRIBUTED AMPLIFIER.
 NOTE: CIRCLED POINTS WERE EXPERIMENTALLY DETERMINED.

PLATE LOAD IMPEDANCE

PHASE ANGLE

ϕ , PHASE SHIFT PER SECTION OF LINE

PLATE LOAD IMPEDANCE $\div Z_0/2$

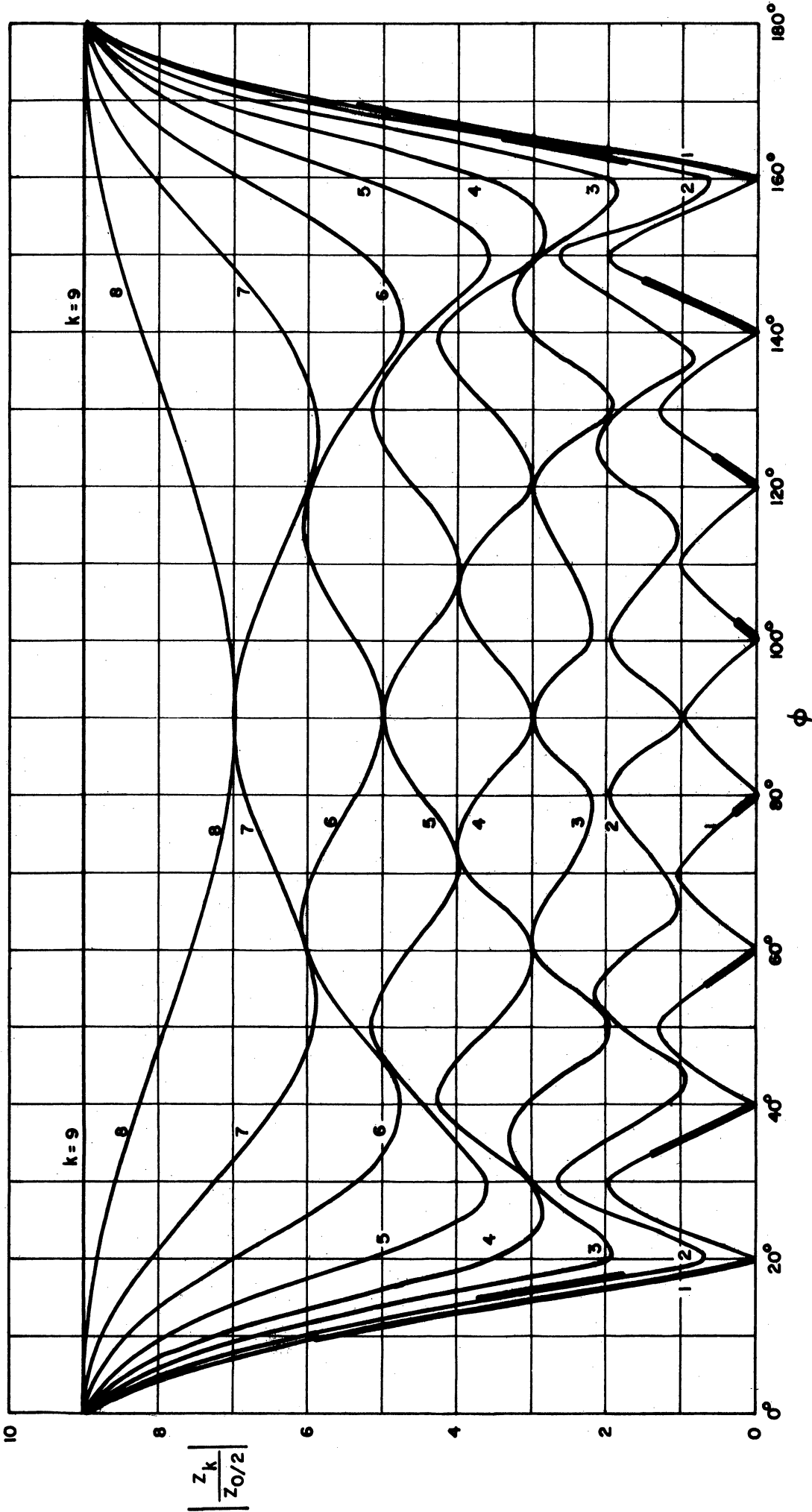


FIG. 2.8. PLATE LOAD IMPEDANCE FOR A 9-TUBE DISTRIBUTED AMPLIFIER .

$$Z_k = \frac{Z_0}{2} \left[k + \frac{\sin(n-k)\phi}{\sin \phi} e^{-j(n-k+1)\phi} \right]$$

$n = 9$

$k = 1, 2, 3, \dots, 7, 8, \& 9$

MAGNITUDE $\left[\frac{Z_k}{Z_0/2} \right]$ VS. ϕ .

NOTE: WIDER LINES INDICATE REGIONS IN WHICH PHASE ANGLE OF PLATE LOAD IMPEDANCE IS GREATER THAN 90° .

here that the plate load impedance has a negative resistance component for certain regions of the second tube as well as for the first tube. Hence some special precautions must be taken in order to prevent overheating of the first few tubes in long-string distributed amplifiers.

A low-frequency model of a distributed amplifier was constructed in order to verify experimentally this analysis of plate load impedance as determined by Equation 2.7. The design of this low frequency distributed amplifier, as well as the method of data reduction, are shown in Appendix B. The points on Figures 2.2 through 2.7 were experimentally obtained.

The experimentally determined points are, in general, higher than the theoretical curve. The disagreement of the curves is caused by three factors. First, it is impossible to match the transconductance of the tubes exactly. Second, the dissipation in the grid line was neglected in the theoretical curves. And third, the low-frequency model has more dissipation in the plate line than a wide-band distributed amplifier, and it affects the plate load impedance. However, the experimental points are in general agreement with the theoretical curves.

Figure 2.9 shows the plate load impedance for a six-tube paired-plate distributed amplifier. The derivation of the equations for this figure are shown in Appendix C. In addition the schematic diagram for a paired-plate distributed amplifier is shown in Appendix C (Figure C.1). Figure 2.9 is included to show the effects of one variation (the paired-plate) to the standard distributed amplifier circuit. Many other variations are possible and for each one a plate load impedance plot such as shown in Figure 2.9 could be calculated by the techniques described above.

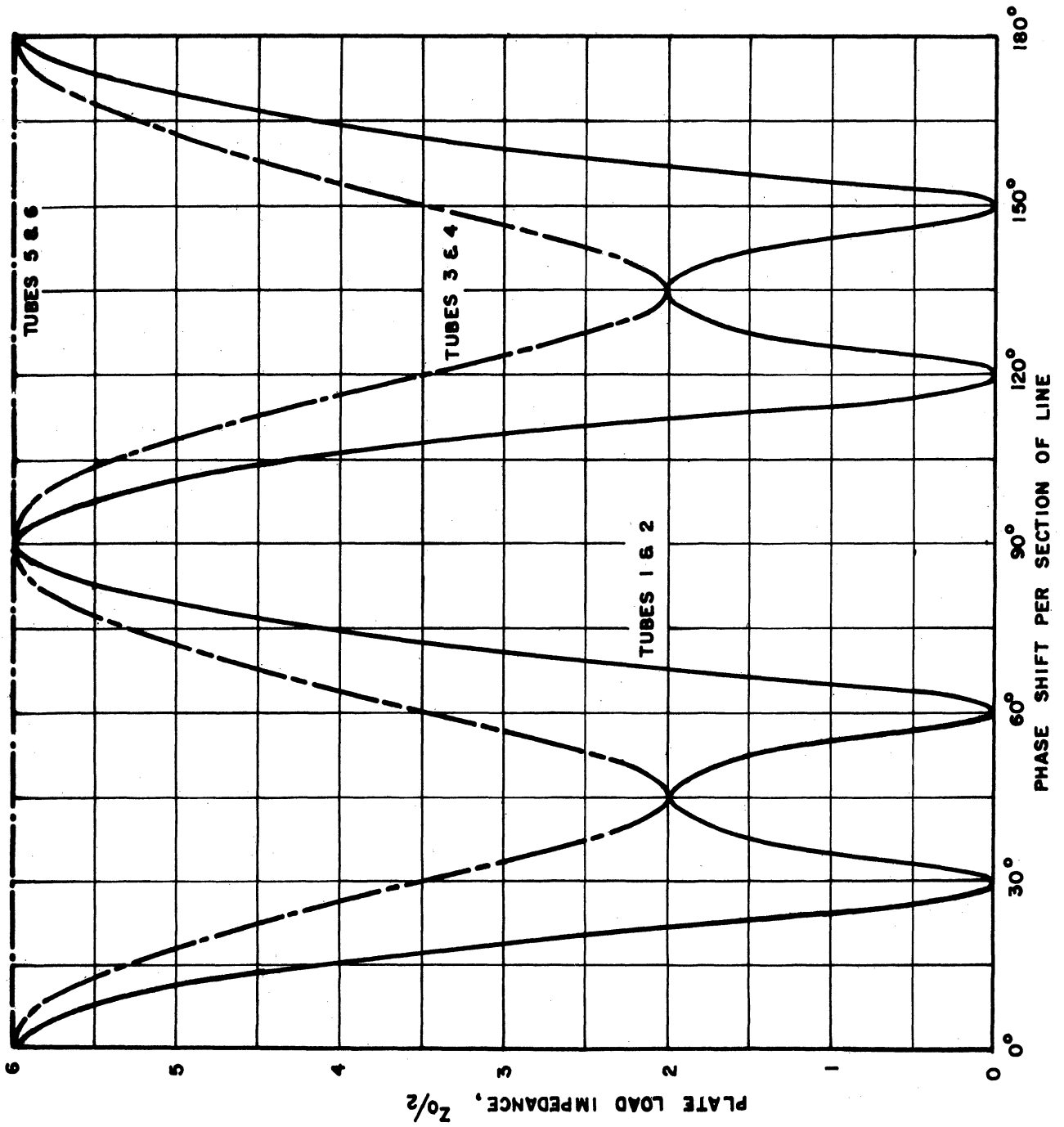


FIG. 2.9. PLATE LOAD IMPEDANCE FOR A 6-TUBE PAIRED-PLATE DISTRIBUTED AMPLIFIER.

CHAPTER III. FREQUENCY LIMITATIONS IN DISTRIBUTED AMPLIFIERS

Standard distributed amplifiers use constant-k filter sections between adjacent grids and also between adjacent plates. The impedance levels of the plate and grid lines are adjusted so that the phase shift per section of the grid line and the plate line are the same at any frequency in the operating range of the amplifier. The following formulas for constant-k low-pass filters can be found in many text books.^{10, 11}

The mid-shunt image impedance

$$Z_{\pi} = R \frac{1}{\sqrt{1 - \left(\frac{\omega}{\omega_c}\right)^2}} \quad (3.1)$$

The phase shift per section

$$\varphi = 2 \sin^{-1} \left(\frac{\omega}{\omega_c} \right) \quad (3.2)$$

where

$$\omega_c = \frac{2}{\sqrt{LC}}$$

$$R = \sqrt{\frac{L}{C}}$$

Multiplying the equations for R and ω_c the following useful equation is obtained.

$$R\omega_c = \frac{2}{C} \quad (3.3)$$

L and C are defined by the schematic of a constant-k filter shown in Figure 3.1.

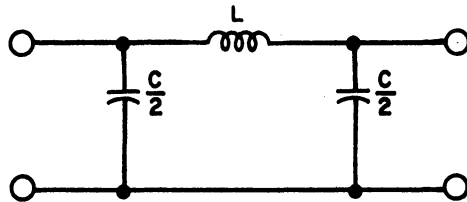


FIG. 3.1 . SCHEMATIC DIAGRAM FOR A LOW-PASS, PI-SECTION, CONSTANT-k, FILTER.

Since the phase shift per section of the filter sections in the plate line and the grid line must be equal, it can be seen from Equation 3.2 that the cut-off frequency of the grid section must be the same as the cut-off frequency for the corresponding plate line section. In the usual distributed amplifier all the sections of the plate line are identical and all the sections of the grid line are identical. If Equation 3.3 for the plate line is divided by a similar equation for the grid line, it can be seen that the impedance level of the plate and grid lines are directly proportional to the input and output capacities of the tubes, or

$$\frac{R_p}{R_g} = \frac{C_g}{C_p} \quad (3.4)$$

The above equations would seem to indicate that there is no upper limit for the cut-off frequency for which a distributed amplifier can be designed. Equation 3.3 leads one to the conclusion that with a given tube capacitance the cut-off frequency can be raised as far as is desired if the impedance of the line is reduced so that the product of the angular cut-off frequency and the impedance level of the line remain equal to twice the reciprocal of the tube capacitance. However, the realization of the constant-k structure in a practical wide-band amplifier is, in general, dependent upon the cancellation of the inductance of the grid lead and the inductance of the plate lead.

3.1 Cancellation of Lead Inductances

The standard procedure in cancelling lead inductances is to utilize air core transformers with negative mutual inductance as shown in Figure 3.3. Here the lead inductance is represented by L_l and the capacitance between tube elements by C . The mutual inductance is adjusted so that it is equal in magnitude to the lead inductance. Figure 3.2 shows the negative mutual transformer and its "T" equivalent.

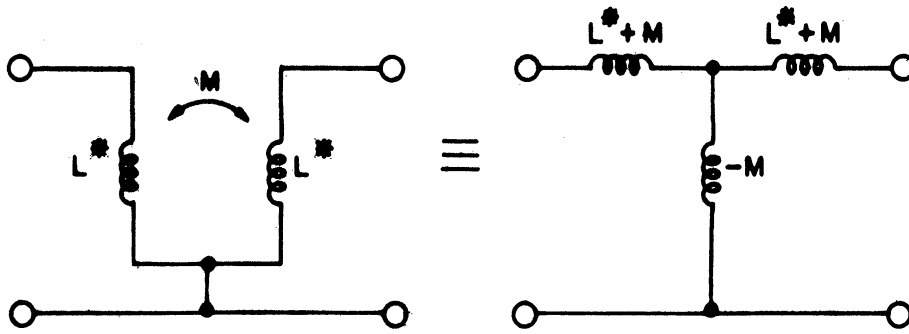


FIG.3.2 . NEGATIVE MUTUAL TRANSFORMER AND ITS EQUIVALENT "T".

It can be seen from Figure 3.2 that half the constant-k inductance is given by

$$\frac{L}{2} = L^* + M \quad (3.5)$$

where: L^* = primary or secondary inductance of transformer

M = mutual inductance between primary and secondary of transformer.

The coefficient of coupling is defined as

$$k = \frac{|M|}{\sqrt{L_p L_s}} = \frac{|M|}{L^*} \quad (3.6)$$

If Equation 3.6 is solved for M and the result substituted in Equation 3.5,

$$\frac{L}{2} = L^*(1-k) \quad (3.7)$$

The magnitude of the mutual inductance is made equal to the lead inductance in order to cancel the effect of the lead inductance. When this equality is substituted into Equation 3.6 and the result applied to Equation 3.7, the constant-k inductance becomes

$$L = 2L_l \left[\frac{1+k}{k} \right] \quad (3.8)$$

If this value for the inductance of the constant-k section is substituted into

Equation 3.2 for the cut-off angular frequency, then

$$\omega_c = \frac{2}{\sqrt{2L_\ell \left[\frac{1+k}{k} \right] C}} = \sqrt{\frac{2k}{1+k}} \cdot \frac{1}{\sqrt{L_\ell C}} \quad (3.9)$$

If the series resonant angular frequency of the tube element being considered is designated by ω_0 ,

$$\frac{\omega_c}{\omega_0} = \sqrt{\frac{2k}{1+k}} \quad (3.10)$$

Equation 3.10 is plotted in Figure 3.3. It can be seen from this figure that it is theoretically possible to operate an amplifier up to the series resonant frequency of the controlling element of the tubes; however, this requires a coupling coefficient of unity. In air-core coils it is possible to realize a coupling coefficient of about 0.5. Hence the upper cut-off frequency of the amplifier is limited to about 0.8 of the series resonant frequency of the controlling element of the tube.

In most tetrodes and pentodes the input capacity is larger than the output capacity, and the lead inductance of the grid is of the same order of magnitude as that of the plate (in most power tubes the lead inductance of the grid is larger than that of the plate lead). Therefore, in general, the grid circuit is the controlling element as far as frequency is concerned. As a rule of thumb, the highest cut-off frequency can be taken as

$$f_c \cong 0.8 f_0 \quad (3.11)$$

3.2 Conductive Loading of the Grid Line Due to High Frequency Effects

There are three major frequency-dependent factors that contribute to attenuation in the grid line. Each of these factors have been considered in the literature and are repeated here only for the sake of completeness.^{12,13}

In general, the effect of cathode lead inductance within the tube is to provide a common element through which both the output current and the input current flow.

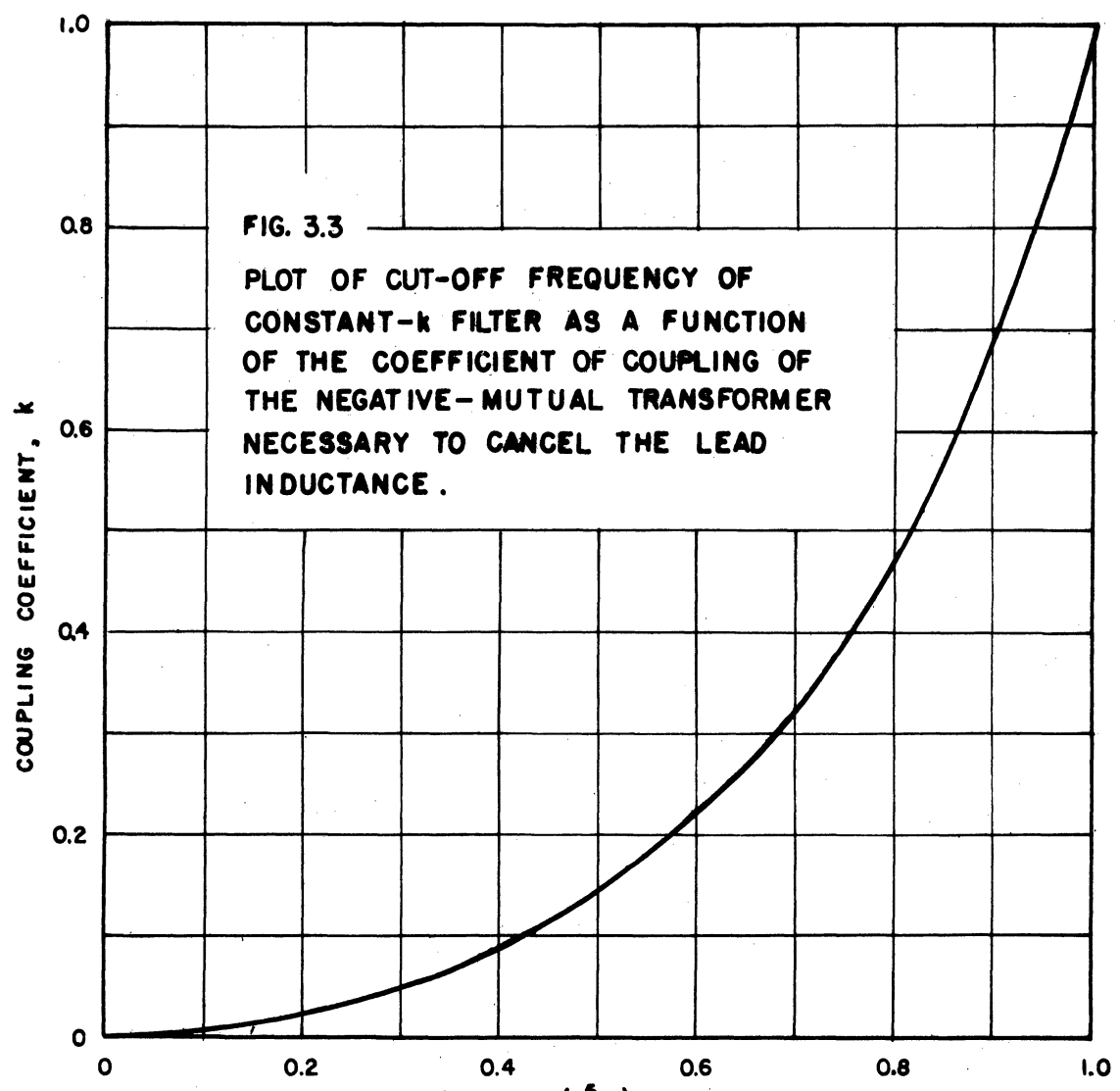
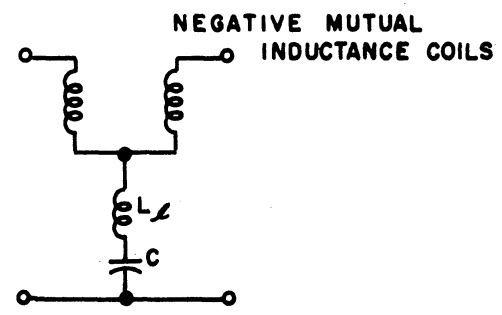


FIG. 3.3
PLOT OF CUT-OFF FREQUENCY OF
CONSTANT-k FILTER AS A FUNCTION
OF THE COEFFICIENT OF COUPLING OF
THE NEGATIVE-MUTUAL TRANSFORMER
NECESSARY TO CANCEL THE LEAD
INDUCTANCE .

RATIO OF THE CUT-OFF
 FREQUENCY TO SERIES
 RESONANT FREQUENCY
 OF L_2 AND C.



This feedback within the tube affects the input conductance of the tube (Equation 3.12).

$$G_{in} = g_m \omega^2 C_g L_k \frac{(1 - \omega^2 C_p L_k)}{g_m^2 \omega^2 L_k^2 + [\omega^2 L_k (C_g + C_p) - 1]^2} \quad (3.12)$$

The constants in this equation are defined by Figure 3.4. g_m is the transconductance of the tube and ω is the operating angular frequency. This equation is derived in Appendix D and involves the assumption that the impedance in the

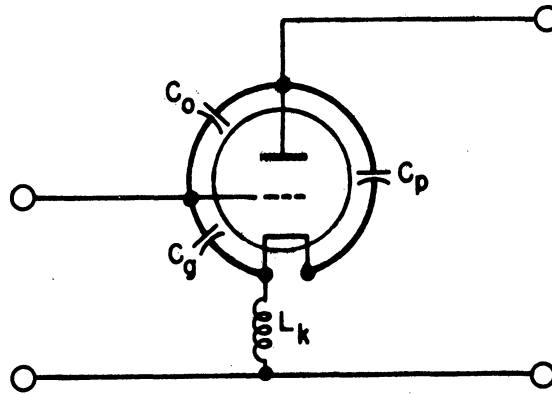


FIG. 3.4 . EQUIVALENT CIRCUIT FOR THE DETERMINATION OF INPUT CONDUCTANCE CAUSED BY THE FEEDBACK RESULTING FROM CATHODE LEAD INDUCTANCE .

plate circuit is so small that the Miller Effect is negligible. If the corrective term is neglected, Equation 3.12 simplifies to Equation 3.13, which is the one most quoted in the literature.

$$G_{in} \approx g_m \omega^2 C_g L_k \quad (3.13)$$

In order to neglect the corrective term the resonant frequency of the cathode lead inductance and the capacitance from grid to cathode must be high in comparison to the operating frequency. If this term is not negligible, Equation 3.12 must be used.

Inductance in the screen grid lead results in a negative conductive component in the input to the tube. In some amplifiers this fact has been used to

offset, to a certain extent, the effect of cathode lead inductance. Equation 3.14 shows the manner in which the input conductance varies if the screen lead inductance alone is considered¹⁴.

$$G_{in} \cong -g_{m2}\omega^2 L_{g2} C_{gs} \quad (3.14)$$

where g_{m2} is the transconductance from the control grid to the screen grid, L_{g2} is the inductance of the screen lead, and C_{gs} is the capacity between the control grid and the screen grid. Equation 3.14 neglects all the impedances associated with the tube with the exception of the screen lead inductance and the capacitance between the control grid and the screen grid.

At frequencies above 30 mc transit time affects the operation of tubes. As the transit time becomes a measurable fraction of the period of the input frequency, the current induced in the grid due to the passage of the electrons will contain a fundamental component that no longer leads the grid voltage by 90° . As a result the input admittance of the tube contains a conductive component. The input conductance is given approximately by¹⁵

$$G_{in} \cong K g_m \omega^2 T^2 \quad (3.15)$$

where T is the electron transit time.

The three effects mentioned above can be represented in Equation 3.16.

$$G_{in} \cong \omega^2 \left[g_m C_g L_k + g_m K T^2 - g_{m2} L_{g2} C_{gs} \right] \quad (3.16)$$

This equation contains the most important loading effects present in a small-signal distributed amplifier. These loading effects are present in a large-signal amplifier also, but Equation 3.16 must be modified by the substitution of the equivalent large-signal transconductance (G_m) for the transconductance (g_m). However, in power distributed amplifiers there is an additional effect in that the tubes are generally driven into the positive grid region where a considerable grid current flows. This gives rise to an additional loading effect on the grid line; however, this loading is independent of frequency being dependent on the

magnitude of grid voltage to a first approximation. This effect will be considered in a later chapter.

3.3 Frequency Tolerance

Equation 3.1 shows the variation of the mid-shunt image impedance of a constant-k filter as a function of frequency. This equation is plotted in Figure 3.5. It was shown in Chapter II that the plate load impedance of the various tubes in a distributed amplifier is dependent upon the value of the characteristic impedance of the plate line. For a constant-k plate line, this value is the mid-shunt image impedance of the constant-k filter sections. This gives rise to a plate load impedance which increases rapidly as the cut-off frequency is approached. This is particularly true of the last few tubes in a distributed amplifier, where the plate load impedance does not vary as radically with frequency as it does for the first few tubes. This rising plate load impedance can result in plate clipping in the last few tubes in a distributed amplifier, and cause the large-signal response to be different from the small-signal response. This is shown in Figure 3.6 where the plate load line for the last tube in a six-tube distributed amplifier is drawn for four different frequencies. It will be noted from Figure 3.6 that for the particular operating point chosen, if the grid is driven 20 volts positive, clipping will begin to occur at a frequency of 0.685 of the cut-off frequency. However, if the grid drive is such that the grid maximum positive excursion is only 15 volts, then clipping will occur above about 0.8 the cut-off frequency.

Since the frequency at which plate clipping occurs is a function of both the operating point and the grid drive, the proper determination of the operating point and the grid drive is not a simple procedure. In order to facilitate the location of the operating point, an additional parameter, called

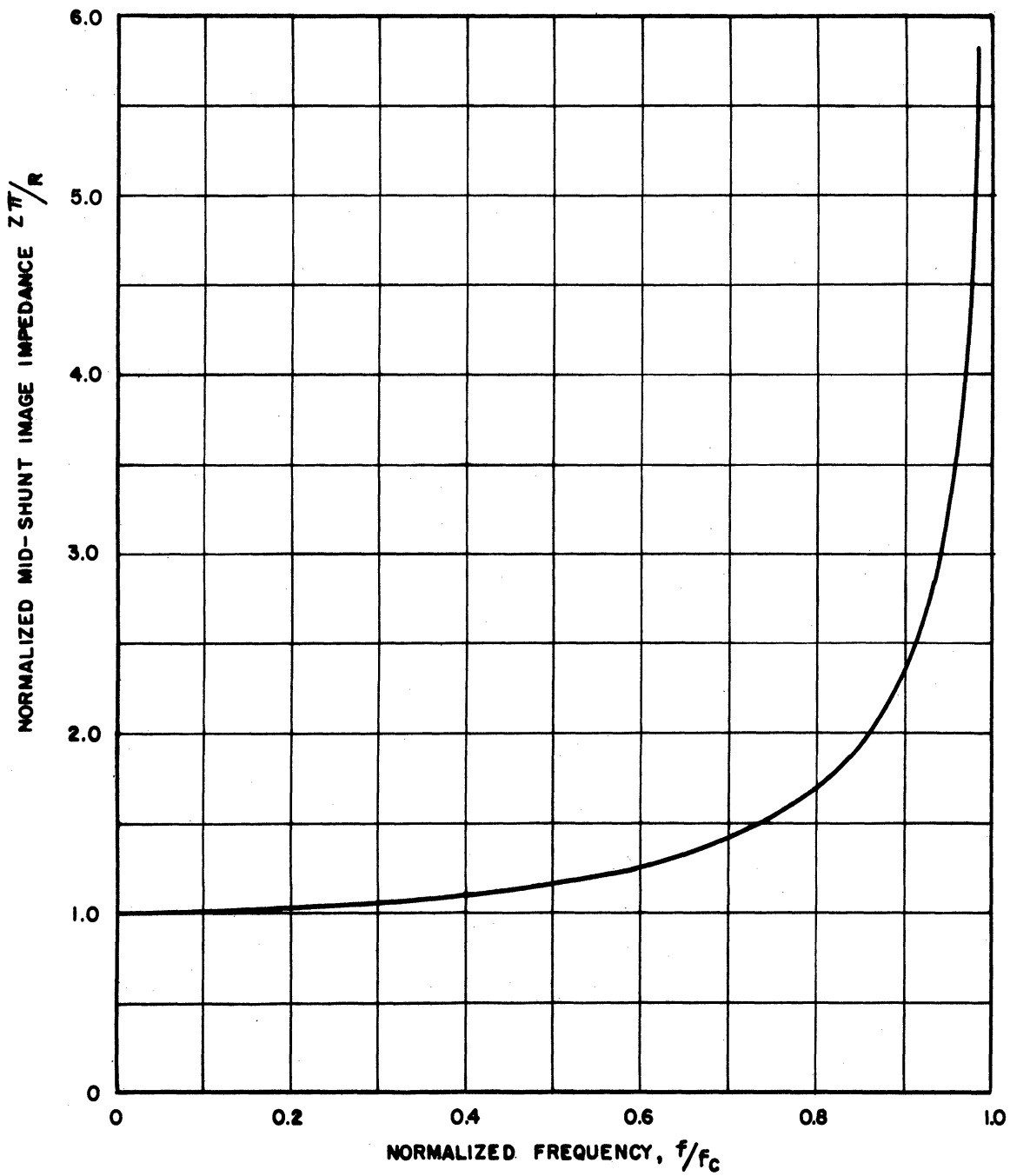


FIG. 3.5. VARIATION OF MID-SHUNT IMAGE IMPEDANCE AS A FUNCTION OF FREQUENCY .

2262 A-61-148 JEM 6-3-55

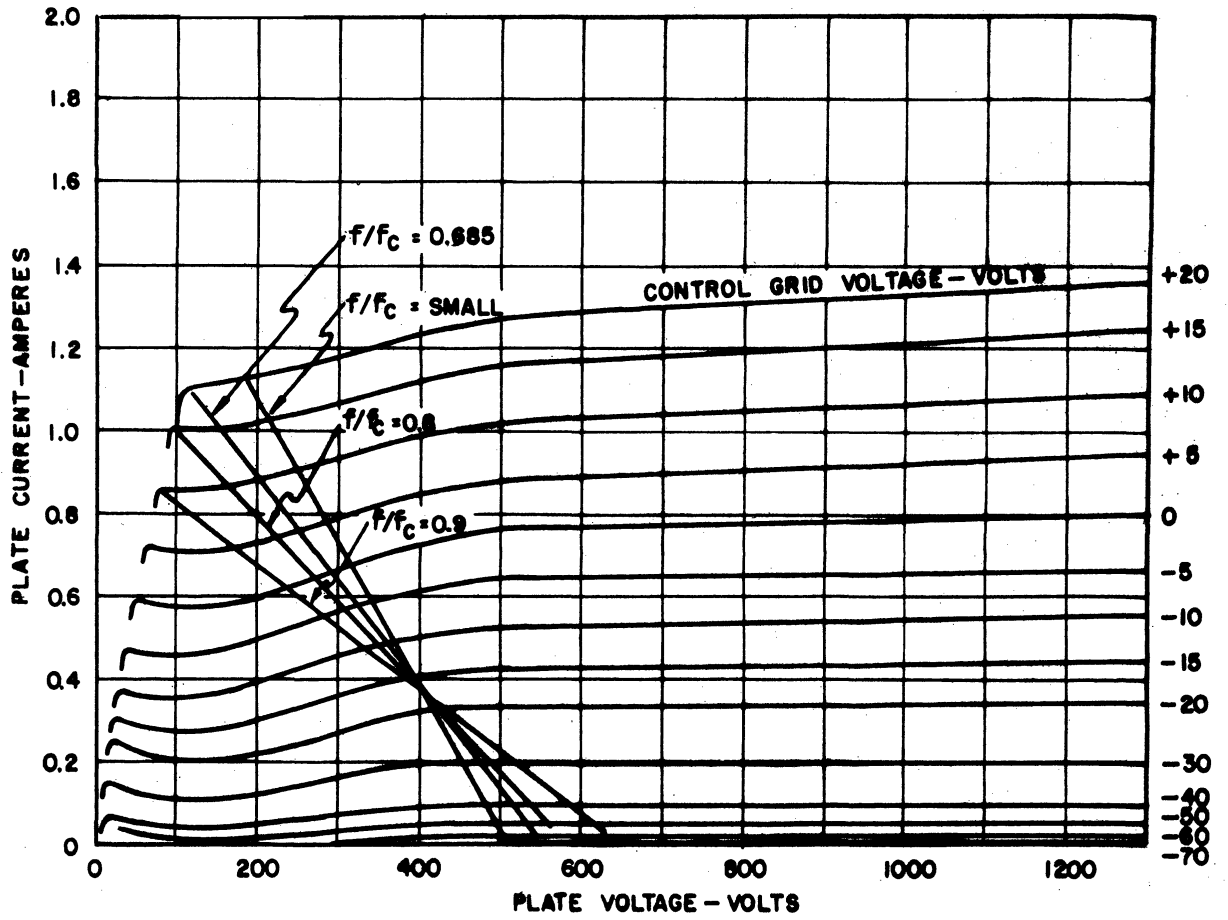


FIG. 3.6 . VARIATION OF THE PLATE LOAD IMPEDANCE OF THE LAST TUBE OF A 6 TUBE DISTRIBUTED AMPLIFIER AS A FUNCTION OF FREQUENCY.

the frequency tolerance, is defined. Frequency tolerance is defined as that frequency above which clipping will be present in the last tube of a low-pass distributed amplifier. This concept will be explored further in a later chapter.

3.4 Summary

The high-frequency effects discussed in this chapter can be classified into two main categories. One of these categories deals with an upper limit to the cut-off frequency for the constant-k filter sections used as the plate line and the grid line of distributed amplifiers. This limit is imposed by the finite grid and plate lead inductances. However, this frequency limit could be increased considerably if tubes possessing satisfactory high-frequency characteristics were constructed with two grid leads and two plate leads. These leads should preferably come out opposite sides of the tube. The second category includes the high-frequency effects which tend to distort the normal frequency response curve of the amplifier. The loading on the grid line due to the input conductance of the tubes can serve the useful function of flattening the normally rising frequency response of distributed amplifiers without losses.² However, for wide-band distributed amplifiers, every effort should be made to reduce the input conductance of the tubes as much as possible. This implies tubes with as small an inductance in the cathode lead as possible and with small transit time. Some inductance in the screen lead is a definite advantage; however, care must be taken to insure stable operation of the tube. Also included in this category is the frequency coverage of power distributed amplifiers, which is determined by the onset of clipping in the final tube of the distributed amplifier. The frequency tolerance is determined by the location of the Q-point and the amplitude of the grid drive. For a given frequency tolerance and grid drive (this is the same as requiring a certain power output) the operating point for the tubes is determined.

CHAPTER IV. GRID LOSSES

4.1 Attenuation Constant of Constant-k Filters with Losses

All of the analytical assumptions discussed in Section 2.1 are close approximations to the real situation with the exception of the lossless grid line assumption. The losses associated with the input impedance of the tubes in a distributed amplifier give rise to attenuation in the grid line. At the higher frequencies this attenuation is serious enough so that it cannot be neglected. In distributed amplifiers designed to deliver power, the grids will, in general, be driven positive giving rise to an additional loading effect on the grid line. Consequently, the attenuation on the grid line will be a function of the grid driving voltage and of frequency.

The constant-k filter sections of the grid can be represented as shown in Figure 3.2 with the addition of a resistance across the capacities representing the input admittance of the tube. If it is desired to take the losses in the coils into account, a resistance in series with the coils can represent this loss. R is defined as the resistance in series with the inductances comprising the grid line, and G is defined as the conductance shunting the input capacity of the tubes in the distributed amplifier. The attenuation constant per section of the grid line, α , may be written as¹⁶

$$\alpha = \left(\frac{R}{2L} + \frac{G}{2C} \right) \frac{d\varphi}{d\omega} + \left(\frac{R}{2L} + \frac{G}{2C} \right)^2 \frac{1}{2} \frac{d^2\varphi}{d\omega^2} + \dots, \quad (4.1)$$

providing

$$\left(\frac{R}{2\omega L} - \frac{G}{2\omega C} \right) \ll 1.$$

or a constant-k filter Equation 4.1 becomes

$$\alpha = \left(\frac{R}{2L} + \frac{G}{2C} \right) \frac{2}{\omega_c} \frac{1}{\sqrt{1 - \left(\frac{\omega}{\omega_c} \right)^2}} + \left(\frac{R}{2L} + \frac{G}{2C} \right)^2 \frac{\omega}{\omega_c^3} \frac{1}{\left[1 - \left(\frac{\omega}{\omega_c} \right)^2 \right]^{3/2}} + \dots \quad (4.2)$$

To a high degree of approximation in wide-band power distributed amplifiers $\frac{R}{2L}$ is negligibly small in comparison to $\frac{G}{2C}$. Therefore, α may be written approximately as

$$\alpha \approx \frac{G_g}{\omega_c C} \frac{1}{\sqrt{1 - \left(\frac{\omega}{\omega_c} \right)^2}} + \left(\frac{G_g}{2\omega_c C} \right)^2 \left(\frac{\omega}{\omega_c} \right) \frac{1}{\left[1 - \left(\frac{\omega}{\omega_c} \right)^2 \right]^{3/2}} \approx \frac{G_g Z \pi}{2} + \left(\frac{G_g Z \pi}{4} \right)^2 \frac{\left(\frac{\omega}{\omega_c} \right)}{\sqrt{1 - \left(\frac{\omega}{\omega_c} \right)^2}} \quad (4.3)$$

where G_g is the input conductance of the individual tubes. Over the major portion of the frequency region the second term in Equation 4.3 may be neglected in comparison to the first term. However, this assumption is not valid if the amplifier is operating near cut-off frequency.

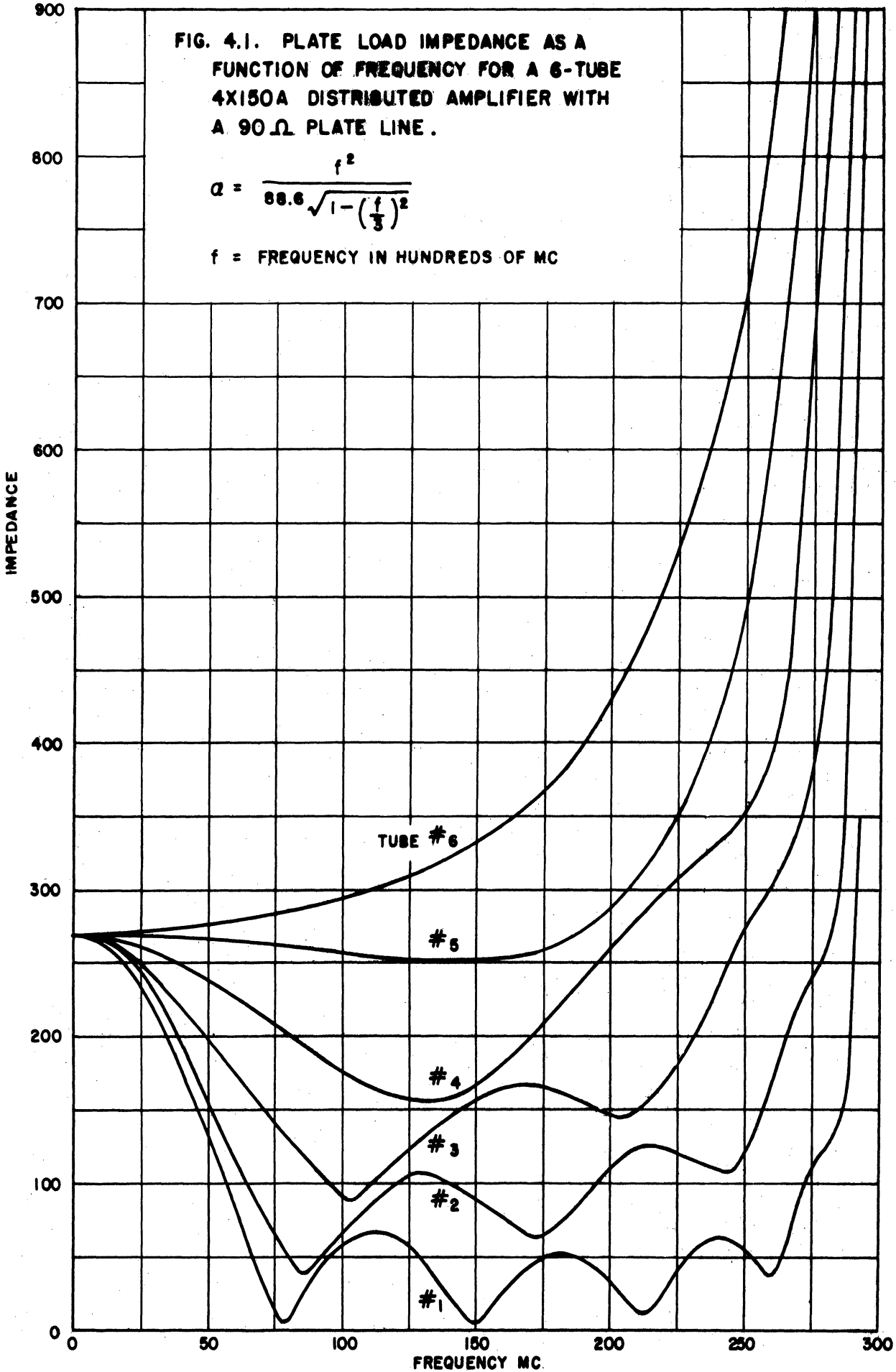
4.2 Determination of the Plate Load Impedance with Attenuation in the Grid Line

The voltages on adjacent grids in the distributed amplifier will possess approximately the same phase angle relative to one another as they did in the lossless case. However, their amplitudes will differ by e^α , where e is the natural logarithm base and α is the attenuation constant described in the preceding section. The plate load impedance for any tube, k , in an n -tube distributed amplifier can be calculated in a manner that is analogous to the derivation in

Chapter II. In this derivation it is assumed that there is no attenuation in the plate line, that the attenuation constant for each section of the grid line is the same, that each artificial transmission line is matched at the ends, and that each of the tubes have identical large-signal transconductances. This analysis is carried out in Appendix E, and only the results are given here.

$$Z_k = \frac{Z_0}{2} \left[\frac{\sinh \frac{k\alpha}{2}}{\sinh \frac{\alpha}{2}} e^{(k-1)\frac{\alpha}{2}} + \frac{\sinh \left[(n-k)\frac{\alpha}{2} + j(n-k)\phi \right]}{\sinh \left[\frac{\alpha}{2} + j\phi \right]} e^{-(n-k+1)\frac{\alpha}{2} - j(n-k+1)\phi} \right] \quad (4.4)$$

Figure 4.1 is a plot of Equation 4.4 for a six-tube distributed amplifier using type 4X150A tubes. In order to determine these curves it was necessary to know the input impedance of the 4X150A tube in the circuit in which it is finally to be used, i.e., with the same lead lengths and the same by-pass condensers. This measurement indicated that the input circuit of the 4X150A may be approximated by a resistance of $\frac{2260}{f^2}$ ohms (where f is the frequency of measurement expressed in hundreds of megacycles) in parallel with a capacity of about 20 micro-microfarads. These curves represent the plate load impedance with no dc grid current. The curves will vary to some extent when the grids are driven positive with respect to the cathode. The magnitude of the plate load impedance will increase somewhat for small grid currents. The curves of Figure 4.1 represent the plate load impedance of the six-tube amplifier to a reasonable degree of approximation even under large-signal conditions. Note that the plate load impedance on the first few tubes is quite low over the major portion of the frequency range; hence, it would seem feasible to utilize a lower supply voltage for the first few tubes without appreciably affecting the power output. This would increase the overall efficiency of the amplifier. Calculations indicate that it should be possible to increase the efficiency of a standard distributed amplifier by about 30% by staggering the plate supply voltages.



The plate load impedance for the first and sixth tube are plotted in Figure 4.2. The solid curves are reproduced from Figure 4.1 and the dashed curves indicate the plate load impedance calculated for no attenuation in the grid line. It can be seen from Figure 4.2 that the plate load impedance of the first tube is not affected appreciably by attenuation in the grid line; however, the plate load impedance for the sixth tube is seen to rise faster as frequency increases.

4.3 Modification of Gain Equation to Account for Losses in the Grid Line

Without loss in the grid line the voltages on the various tubes of a distributed amplifier are the same. The grid voltages are related to the driving power as shown in Equation 4.5.

$$E_g = \sqrt{P_{dr}} \cdot \sqrt{Z\pi_g} \quad (4.5)$$

This expression holds if matched conditions are assumed on the input and output of the grid line. Here, P_{dr} is the driving power. However, if the grid line has attenuation, the voltages on the individual tubes will be given by Equation 4.6.

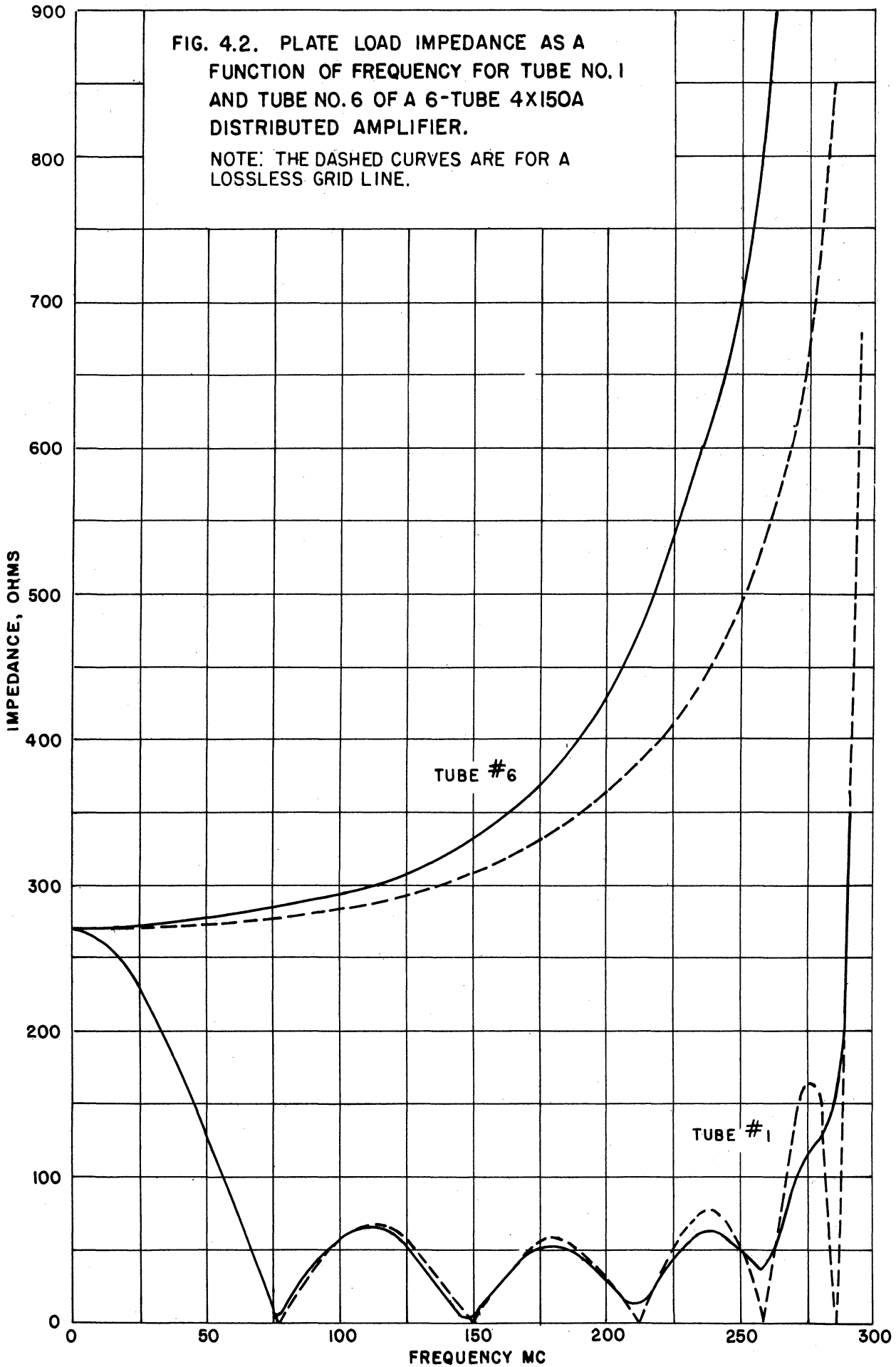
$$\begin{aligned} E_{g1} &= \sqrt{P_{dr}} \cdot \sqrt{Z\pi_g} \cdot e^{-\alpha_1} \\ E_{g2} &= \sqrt{P_{dr}} \cdot \sqrt{Z\pi_g} \cdot e^{-(\alpha_1+\alpha_2)} \\ &\cdot \\ &\cdot \\ E_{gn} &= \sqrt{P_{dr}} \cdot \sqrt{Z\pi_g} \cdot e^{-(\alpha_1+\alpha_2+\dots+\alpha_n)} \end{aligned} \quad (4.6)$$

where E_{gk} is the grid voltage on the k^{th} tube, α_1 is the attenuation constant for the first half section filter, and α_k is the attenuation constant for the filter section terminating on the k^{th} tube. The current flowing into the output half-section filter of the plate line can be written as shown in Equation 4.7.

$$I_o = \frac{G_m \sqrt{P_{dr}} \cdot \sqrt{Z\pi_g}}{2} \left[e^{-\alpha_1} + e^{-(\alpha_1+\alpha_2)} + \dots + e^{-(\alpha_1+\alpha_2+\dots+\alpha_n)} \right] \quad (4.7)$$

FIG. 4.2. PLATE LOAD IMPEDANCE AS A FUNCTION OF FREQUENCY FOR TUBE NO. 1 AND TUBE NO. 6 OF A 6-TUBE 4X150A DISTRIBUTED AMPLIFIER.

NOTE: THE DASHED CURVES ARE FOR A LOSSLESS GRID LINE.



The output power is given by the square of the current flowing into the last half-section of the plate line multiplied by the mid-shunt image impedance of the plate line.

$$P_{\text{out}} = I_0^2 Z_{\pi_p} \quad (4.8)$$

The output power can be calculated for any given set of operating conditions on the tubes in a distributed amplifier from Equation 4.8; however, the procedure is rather long and tedious. The main difficulty arises from the fact that the attenuation constants are different for each section of the grid line.

From Equation 4.3, α can be expressed approximately as one-half the product of the input conductance of the tube and the mid-shunt image impedance of the grid line.

$$\alpha \approx \frac{G_g Z_{\pi_g}}{2} \quad (4.9)$$

The input conductance of the tube contains two components. One varies as the square of frequency and the other depends on the magnitude of the driving voltage.

$$G_g = G_0 \omega^2 + G_{\text{dr}} \quad (4.10)$$

Equation 4.9 can be written in terms of G_0 and G_{dr} as shown in Equation 4.11

$$\begin{aligned} \alpha &\approx \left[\frac{G_0 \omega^2}{2} + \frac{G_{\text{dr}}}{2} \right] Z_{\pi} \\ &= \frac{G_0 \omega_c^2 R_g}{2} \frac{\left(\frac{\omega}{\omega_c} \right)^2}{\sqrt{1 - \left(\frac{\omega}{\omega_c} \right)^2}} + \frac{G_{\text{dr}} R_g}{2} \frac{1}{\sqrt{1 - \left(\frac{\omega}{\omega_c} \right)^2}} \end{aligned} \quad (4.11)$$

Let

$$\alpha_0 = \frac{G_0 \omega_c^2 R_g}{2} = \frac{G_{\text{in}}}{\omega^2} \frac{\omega_c}{C_g} \quad (4.12)$$

and

$$\alpha_{\text{odr}} = \frac{G_{\text{dr}} R_g}{2} \quad (4.13)$$

α_{in} is the small-signal input conductance of the tube at the frequency ω , and α_{odr} is the effective conductance of the tubes due to the flow of grid current in the positive grid region. Equation 4.11 can be written as

$$\alpha \cong \alpha_o \frac{\left(\frac{\omega}{\omega_c}\right)^2}{\sqrt{1 - (\omega/\omega_c)^2}} + \alpha_{odr} \frac{1}{\sqrt{1 - (\omega/\omega_c)^2}}$$

$$= \alpha_o \left[\frac{(\omega/\omega_c)^2}{\sqrt{1 - (\omega/\omega_c)^2}} + \frac{\alpha_{odr}}{\alpha_o} \frac{1}{\sqrt{1 - (\omega/\omega_c)^2}} \right] \quad (4.14)$$

If the variation of α_{odr} for the various tubes in a distributed amplifier is assumed small and, in addition, the variation of α_{odr} with frequency is assumed small, the same value of α can be used in Equation 4.7 for $\alpha_2 \dots$, and α_n . α_1 would be half this value since it is for the input half-section. With this assumption, Equation 4.7 can be written as

$$I_o = \frac{G_m \sqrt{P_{dr}} \cdot \sqrt{Z\pi_g}}{2} e^{-\frac{\alpha}{2}} \left[1 + e^{-\alpha} + e^{-2\alpha} + \dots + e^{-(n-1)\alpha} \right] \quad (4.15)$$

The exponential series shown in brackets can be summed in a manner similar to the one shown in Appendix A, and the result is shown in Equation 4.16.

$$I_o = \frac{G_m \sqrt{P_{dr}} \cdot \sqrt{Z\pi_g}}{2} e^{-\frac{n\alpha}{2}} \frac{\sinh\left(\frac{n\alpha}{2}\right)}{\sinh\left(\frac{\alpha}{2}\right)} \quad (4.16)$$

From Equation 4.8 the output power can be written as

$$P_{out} = \frac{G_m^2 P_{dr} Z\pi_g Z\pi_p}{4} \left[e^{-\frac{n\alpha}{2}} \frac{\sinh\left(\frac{n\alpha}{2}\right)}{\sinh\left(\frac{\alpha}{2}\right)} \right]^2 \quad (4.17)$$

Substituting Equation 3.1 in Equation 4.17 the power output becomes

$$P_{out} = \frac{G_m^2 P_{dr} R_g R_p}{4} \left[\frac{e^{-\frac{n\alpha}{2}} \sinh\left(\frac{n\alpha}{2}\right)}{\sqrt{1 - (\omega/\omega_c)^2} \sinh\left(\frac{\alpha}{2}\right)} \right]^2 \quad (4.18)$$

The factor outside the brackets in Equation 4.18 is the power output from one tube operating alone in the distributed amplifier at low frequency and with no attenuation in the grid line. This factor is easily calculable from the characteristics for the particular tube as the square of one-half the rms value of the fundamental component of plate current times the nominal plate line impedance. The normalized value of the factor in the brackets in Equation 4.18 is plotted in Figures 4.3 through 4.11 as a function of frequency. From these curves it can be seen that a value of $\frac{n\alpha_0}{2}$ of about 0.5 should be used for a flat-gain characteristic. However, as the value of $\frac{\alpha_{odr}}{\alpha_0}$ increases, the value of $\frac{n\alpha_0}{2}$ for a flat response decreases. This change is slight for $\frac{\alpha_{odr}}{\alpha_0} \leq 0.25$.

If a value of $\frac{n\alpha_0}{2} = \frac{1}{2}$ is chosen as an approximate design parameter, the product of the number of tubes and the cut-off frequency for any given tube type is automatically determined.

$$n\omega_c = \frac{\omega_c^2}{G_{in}} \cdot C_g \quad (4.19)$$

where: n = the number of tubes

ω_c = the angular cut-off frequency

G_{in} = the input conductance to the tube at the frequency ω

C_g = the input capacity of the tube.

If α_{odr} is determined from the calculated value of the grid voltage on the first tube, the results calculated from Equation 4.18 will tend to be too low, since the value of α will actually be decreasing with k , where k is the number of the tube under consideration.

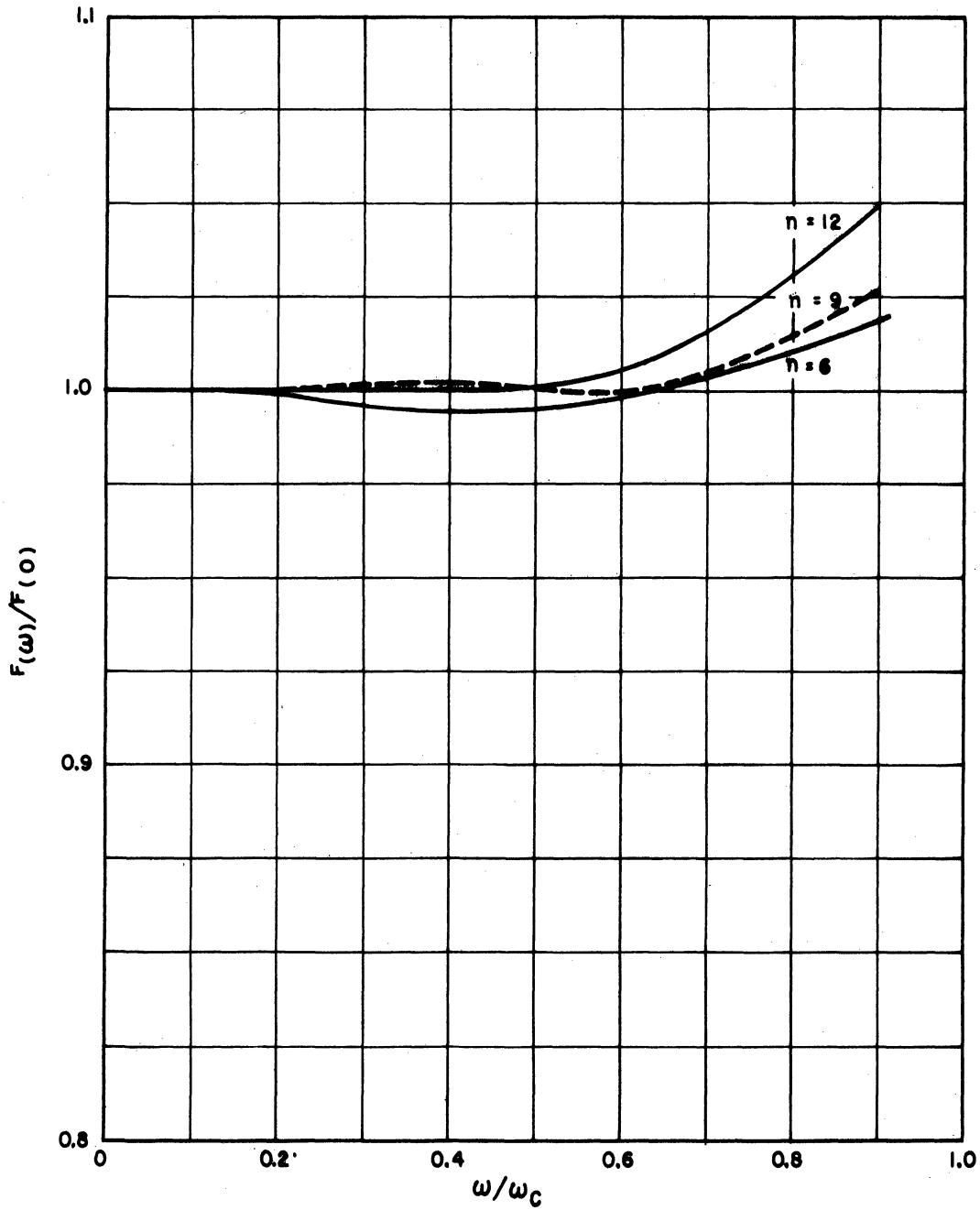


FIG. 4.3. NORMALIZED VOLTAGE AMPLIFICATION AS A FUNCTION OF FREQUENCY FOR $\frac{n a_0}{2} = 0.5$ AND $\frac{a_{odr}}{a_0} = 0.05$.

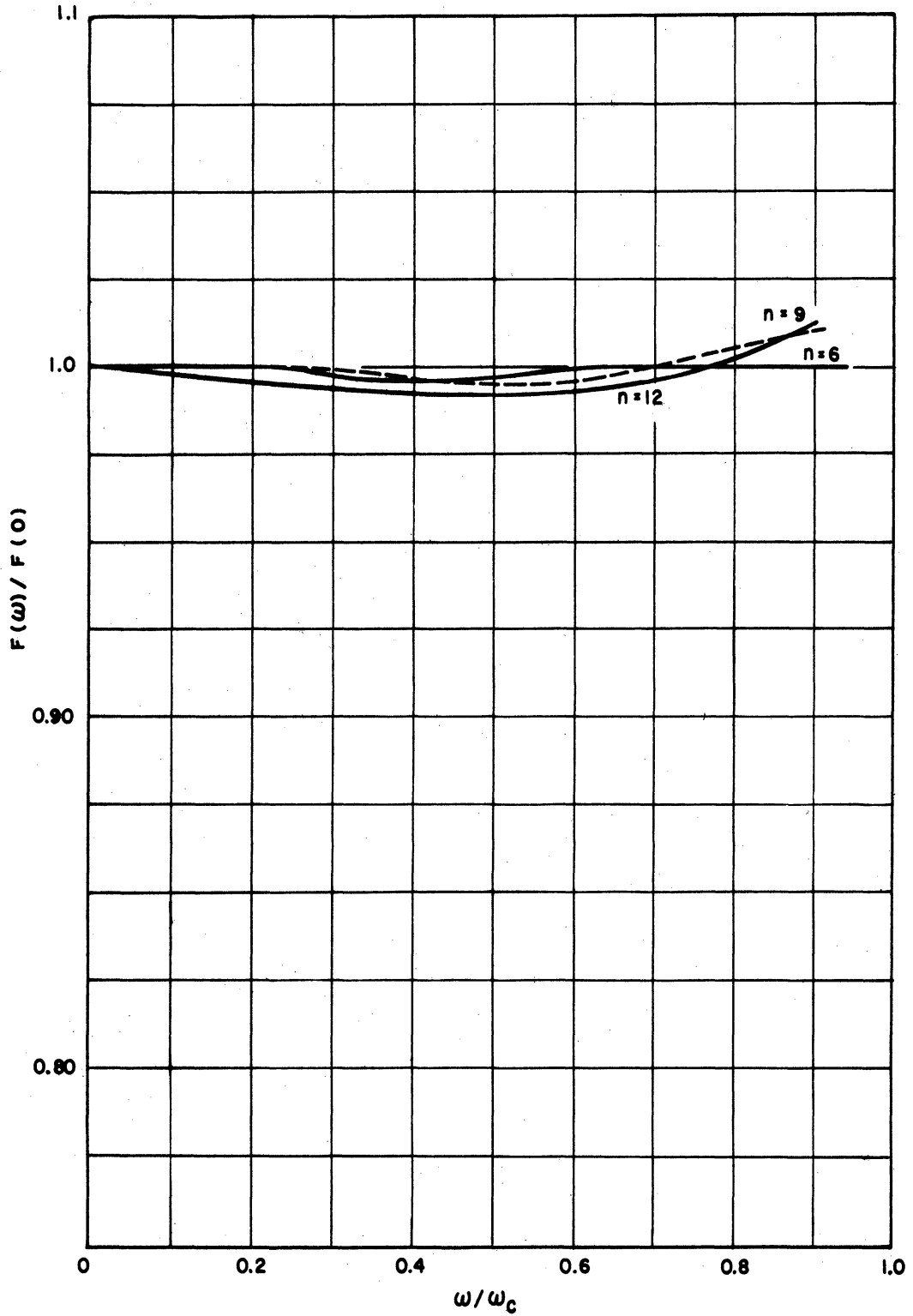


FIG. 4.4. NORMALIZED VOLTAGE AMPLIFICATION AS A FUNCTION OF FREQUENCY FOR $\frac{n\alpha_0}{2} = 0.5$ AND $\frac{\alpha_{odr}}{\alpha_0} = 0.10$.

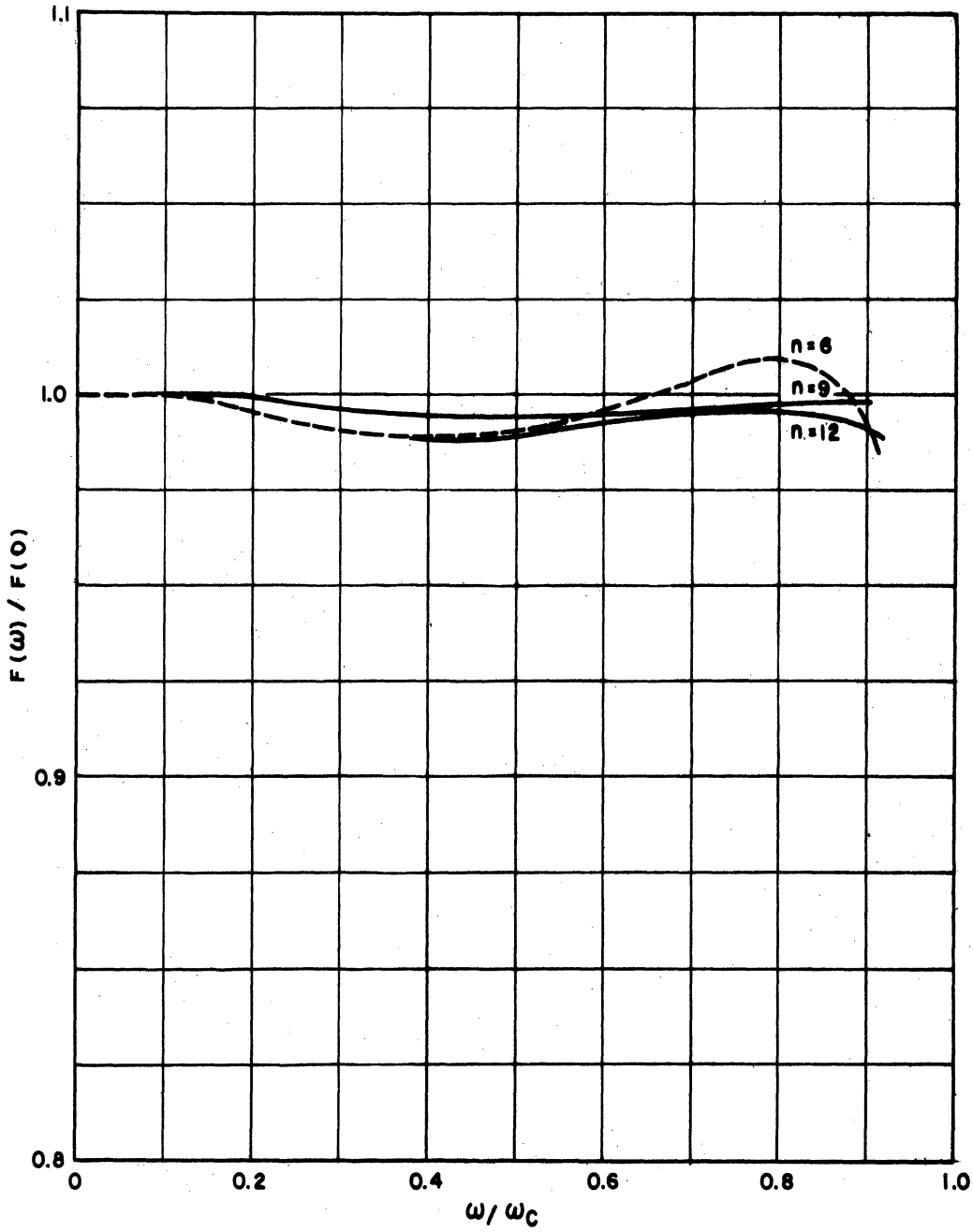


FIG. 4.5. NORMALIZED VOLTAGE AMPLIFICATION AS A FUNCTION OF FREQUENCY FOR $\frac{n a_0}{2} = 0.5$ AND $\frac{a_{odr}}{a_0} = 0.15$.

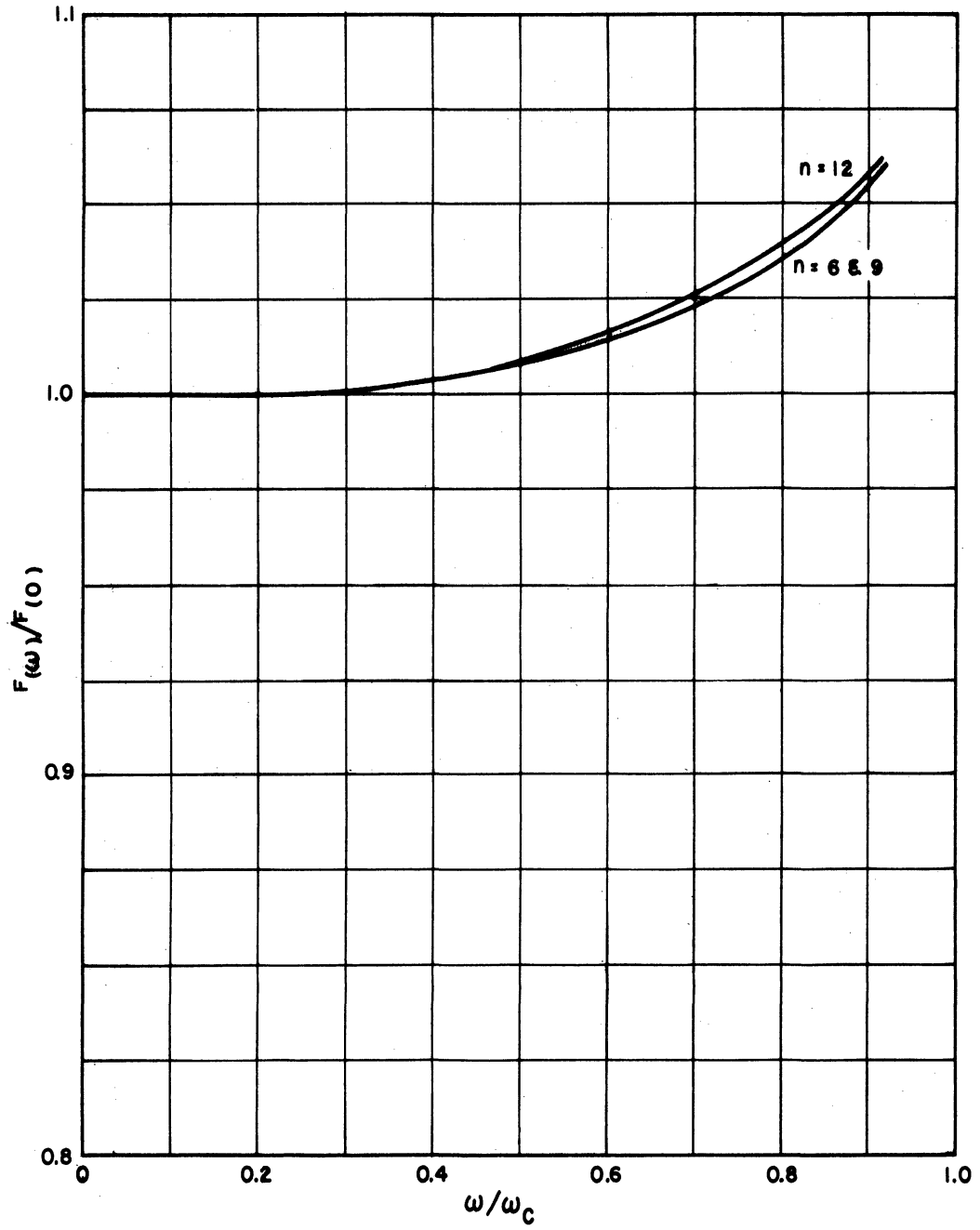


FIG. 4.6. NORMALIZED VOLTAGE AMPLIFICATION AS A FUNCTION OF FREQUENCY FOR $\frac{n\alpha_0}{2} = 0.45$ AND $\frac{\alpha_{odr}}{\alpha_0} = 0.20$.

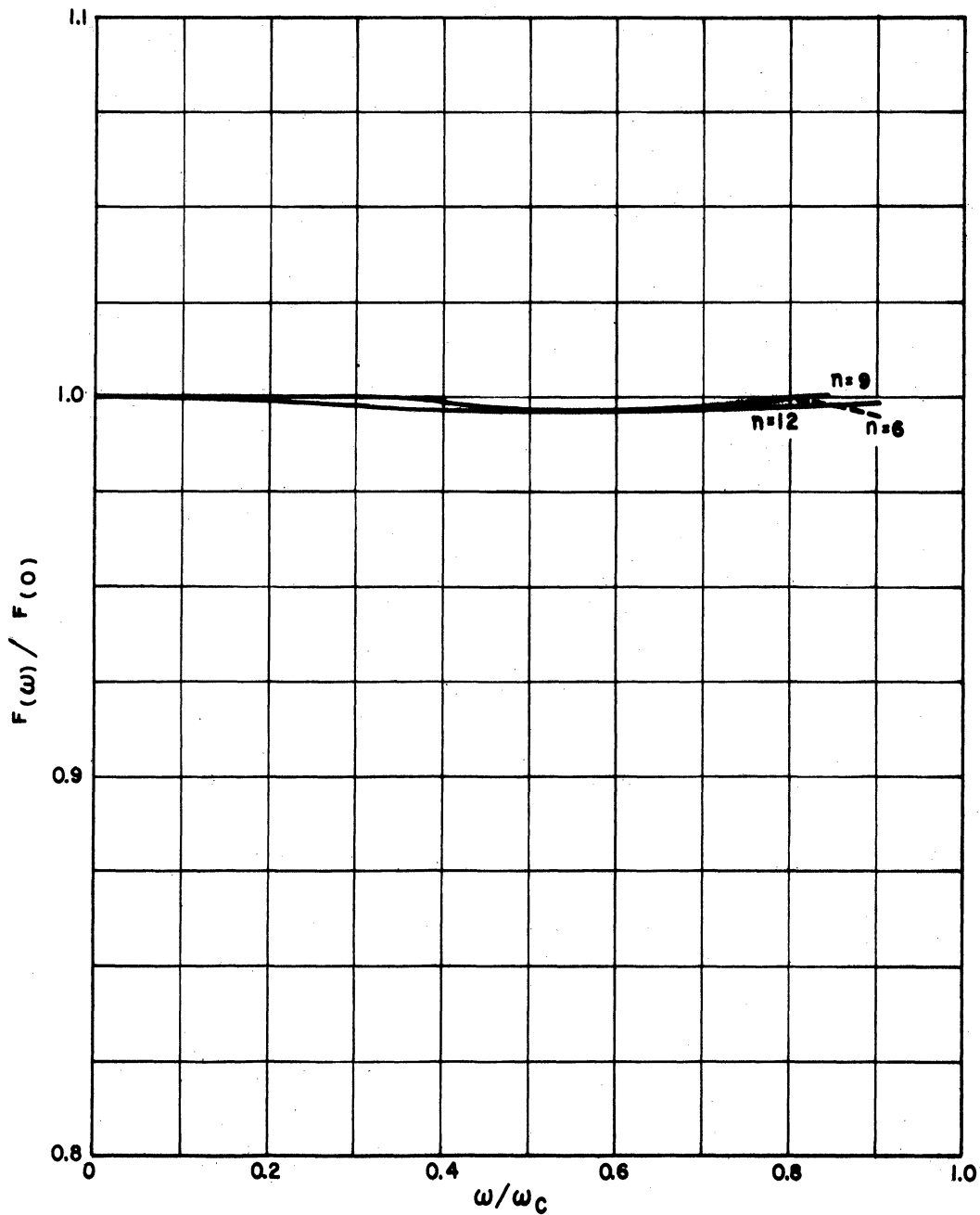


FIG. 4.7. NORMALIZED VOLTAGE AMPLIFICATION AS A FUNCTION OF FREQUENCY FOR $\frac{n\alpha_0}{2} = 0.49$ AND $\frac{\alpha_{odr}}{\alpha_0} = 0.20$.

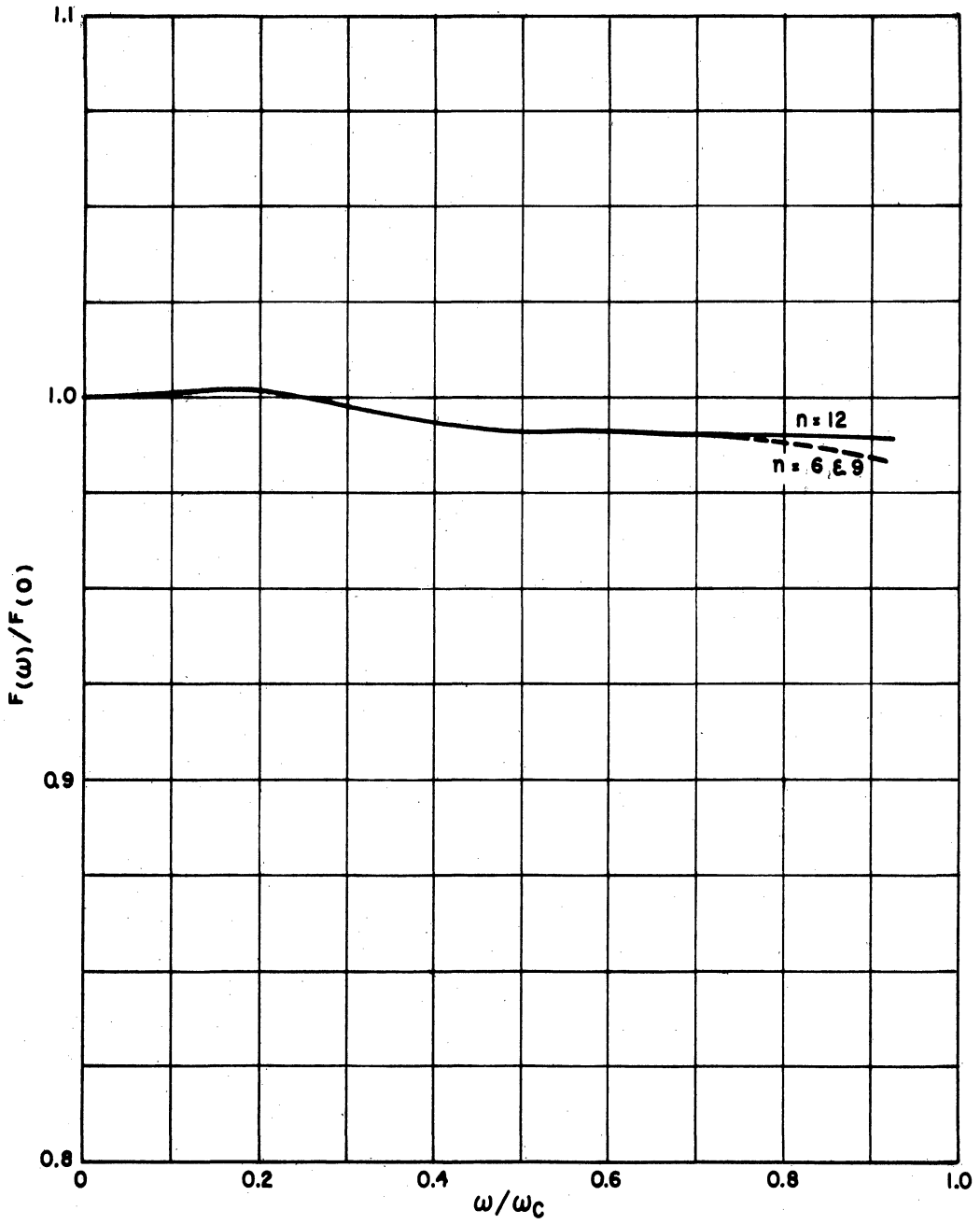


FIG. 4.8. NORMALIZED VOLTAGE AMPLIFICATION AS A FUNCTION OF FREQUENCY FOR $\frac{n\alpha_0}{2} = 0.5$ AND $\frac{\alpha_{odr}}{\alpha_0} = 0.20$.

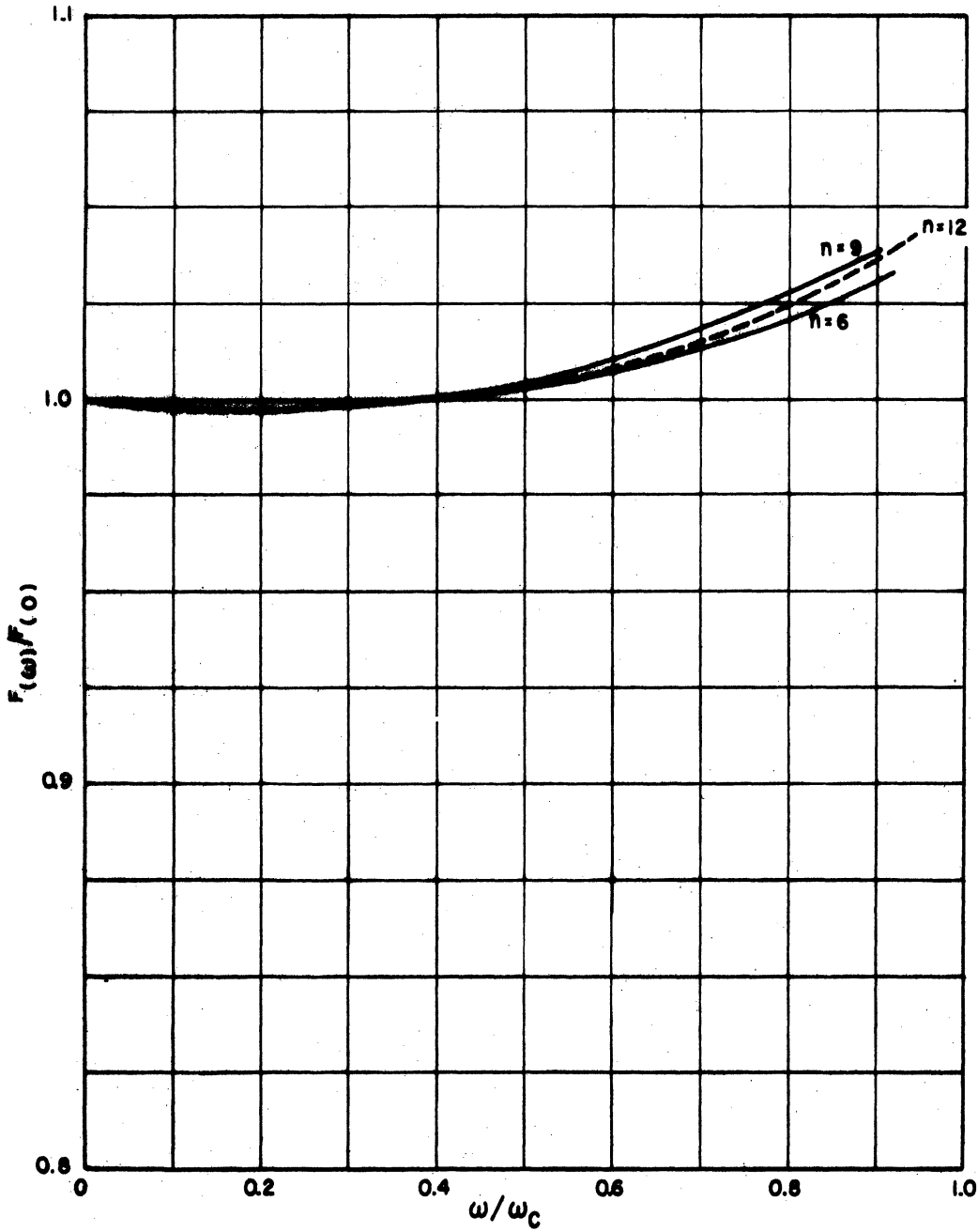


FIG. 4.9. NORMALIZED VOLTAGE AMPLIFICATION AS A FUNCTION OF FREQUENCY FOR $\frac{n\alpha_0}{2} = 0.45$ AND $\frac{\alpha_{odr}}{\alpha_0} = 0.25$.

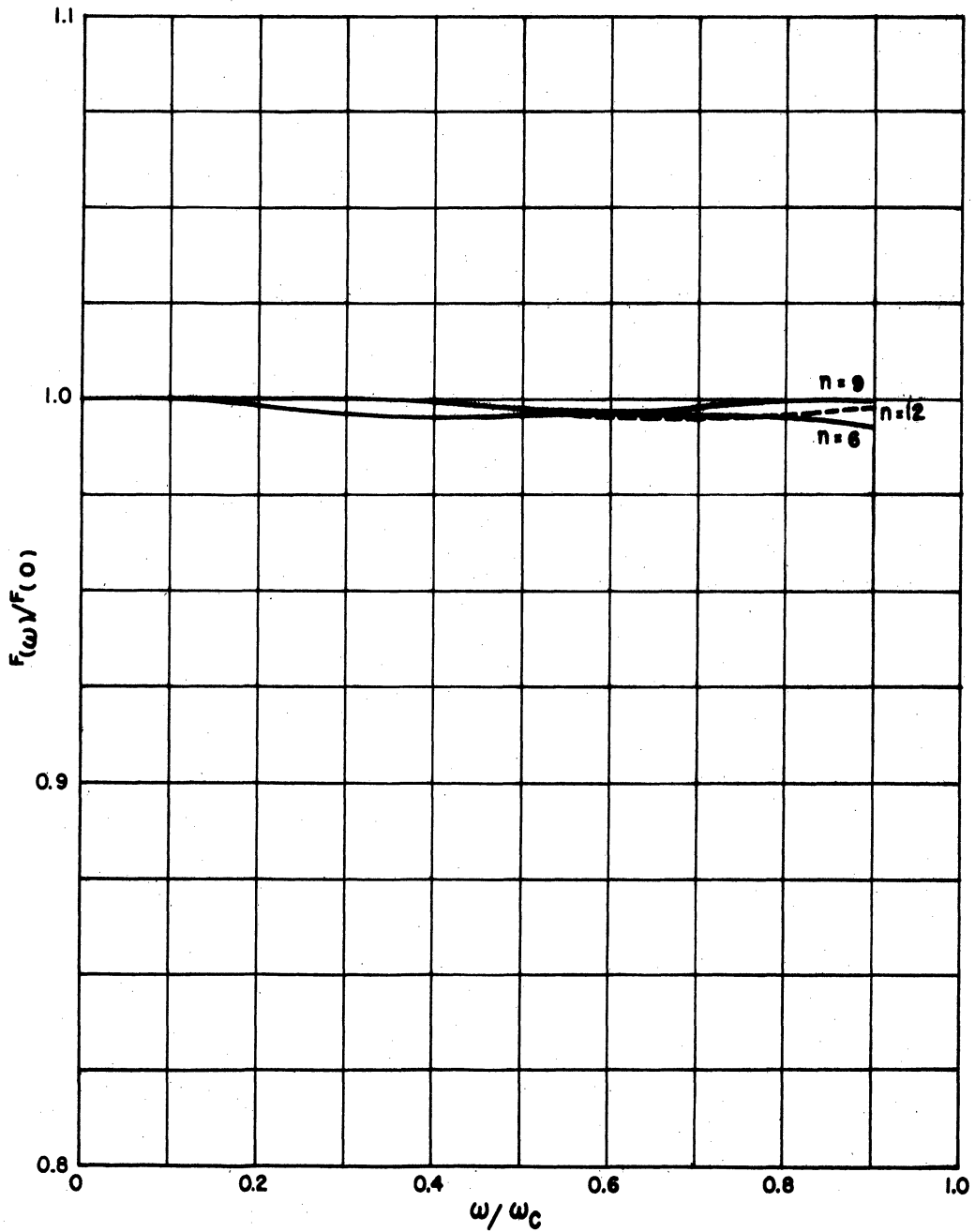


FIG. 4.10. NORMALIZED VOLTAGE AMPLIFICATION AS A FUNCTION OF FREQUENCY FOR $\frac{na_0}{2} = 0.48$ AND $\frac{a_{odr}}{a_0} = 0.25$.

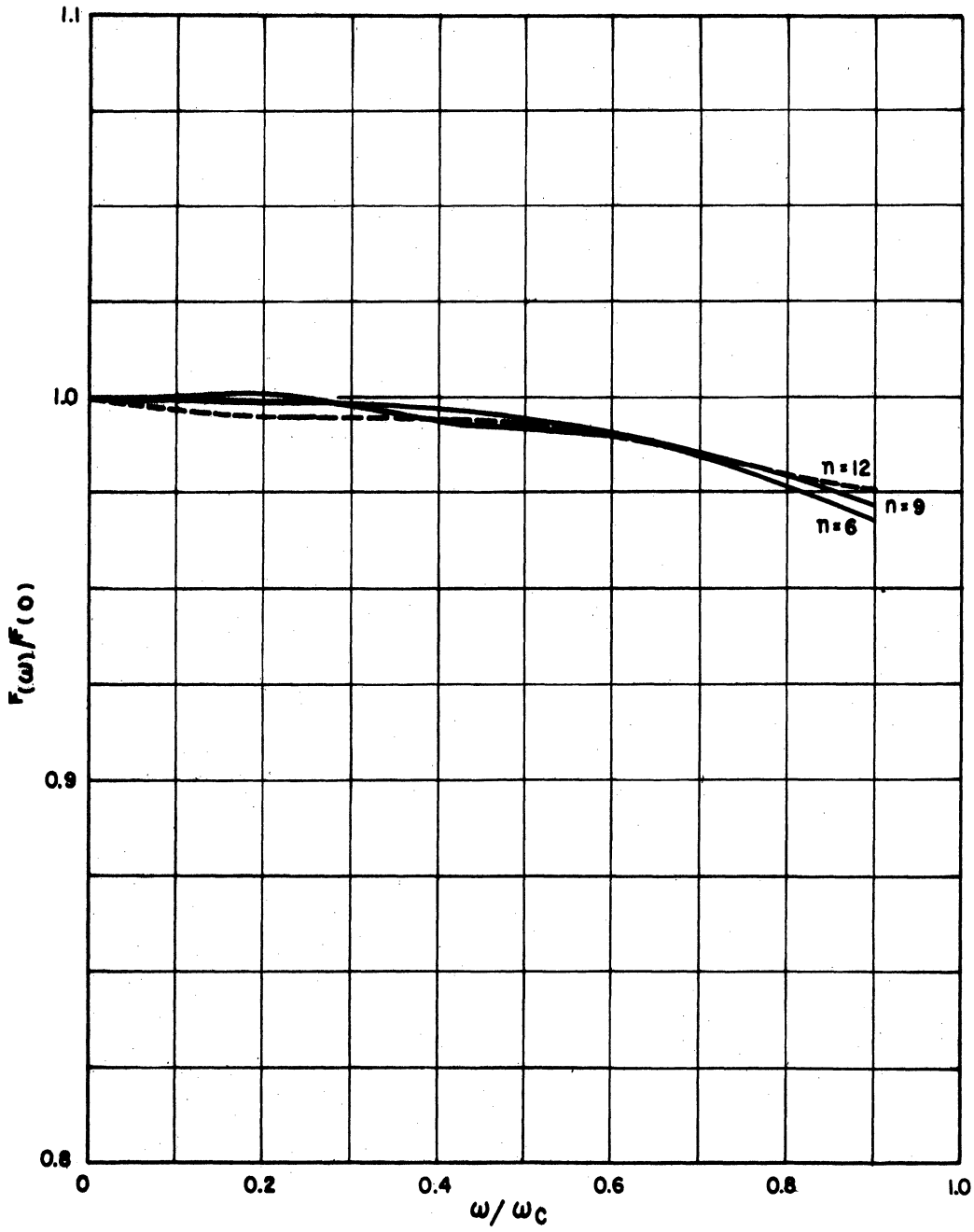


FIG. 4.11. NORMALIZED VOLTAGE AMPLIFICATION AS A FUNCTION OF FREQUENCY FOR $\frac{n\alpha_0}{2} = 0.5$ AND $\frac{\alpha_{odr}}{\alpha_0} = 0.25$.

CHAPTER V. EFFICIENCY

If the attenuation in the grid line is neglected in order to obtain a general analysis of distributed amplifiers operating as large-signal devices, rather elementary reasoning will suffice to show that the power output varies as the square of the number of tubes. This comes from the fact that all of the tube currents add in-phase as they progress toward the output end of the amplifier; consequently, the output current is just n times the current that one tube produces in the output resistance. Hence, the output power varies as the square of the number of tubes. This is in contrast to the dc power input which varies directly with the number of tubes. The above reasoning leads to the conclusion that the efficiency increases directly with the number of tubes. Therefore, if the attenuation in the grid line is neglected, it would seem desirable to use as large a number of tubes as possible; the number being limited only by the plate load impedance and the plate characteristics of the tube under consideration.

5.1 Calculation of Efficiency

If attenuation in the grid line is taken into consideration in a distributed amplifier which is designed to have a relatively flat gain over the frequency region, the output power no longer increases as the square of the number of tubes. From Equation 4.18 the output power can be written as

$$P_{\text{out}} = P_{\text{ol}} \left[\frac{e^{-\frac{n\alpha}{2}}}{\sqrt{1 - (\omega/\omega_c)^2}} \frac{\sinh\left(\frac{n\alpha}{2}\right)}{\sinh\left(\frac{\alpha}{2}\right)} \right]^2 \quad (5.1)$$

where P_{ol} is the output power for one tube operating in the distributed amplifier without attenuation in the grid line. At low frequencies Equation 5.1 can be written as shown in Equation 5.2.

$$P_{out} = P_{ol} \left[\frac{e^{-\frac{nG_{dr}R_g}{4}} \sinh\left(\frac{nG_{dr}R_g}{4}\right)}{\sinh\left(\frac{G_{dr}R_g}{4}\right)} \right]^2 \quad (5.2)$$

$$\text{if } \frac{nG_{dr}R_g}{4} < 0.2 ,$$

$$\left[\frac{\sinh\left(\frac{nG_{dr}R_g}{4}\right)}{\sinh\left(\frac{G_{dr}R_g}{4}\right)} \right]^2 \approx n^2$$

the error involved here is less than 1.25 percent. The output power can be written approximately as

$$P_{out} \approx P_{ol} n^2 e^{-\frac{nG_{dr}R_g}{2}} \quad (5.3)$$

If the value of $\frac{n\alpha_0}{2}$ is chosen in a manner described in Chapter IV for constant power gain over the frequency region, the efficiency can be calculated by Equation 5.4.

$$\eta = \eta_1 n^2 e^{-\frac{nG_{dr}R_g}{2}} \quad (5.4)$$

here η_1 = the efficiency of one tube operating alone in the distributed amplifier.

The efficiency as calculated from Equation 5.4 is valid for low frequencies. Since the magnitude of the grid voltages varies with frequency, the average value of plate current will also vary with frequency if harmonic distortion is present. In a distributed amplifier designed for a relatively flat gain over the operating frequency range, the output power will be constant if the driving power is constant. However, the average value of the dc current drawn from the plate supply will decrease with frequency. Hence, the distributed amplifier will tend to become more efficient as the operating frequency increases. The change in efficiency is related to the change in the average plate current from no-signal conditions to full-signal conditions.

5.2 Maximum Theoretical Efficiency of Distributed Amplifiers

Figures 5.1 and 5.2 show idealized characteristics that are assumed for the calculations of maximum theoretical efficiency. The load lines that are drawn on these characteristics are for a pure resistance load on the tubes. At low frequencies the tubes in a distributed amplifier are operating in parallel as discussed in Chapter II. In a distributed amplifier designed for a flat frequency response the output power is constant with frequency as long as the driving power remains constant. Hence the output power calculated for low frequencies should apply for any frequency in the operating range. The instantaneous values of plate voltage and plate current are shown in Figure 5.3. The instantaneous value of the plate voltage may be written as

$$\begin{aligned} e_b &= E_m (1 - \cos \omega t) && \frac{\theta}{2} \leq \omega t \leq \frac{\theta}{2} \\ &= E_m \left[1 - \cos \left(\frac{\theta}{2} \right) \right] && \frac{\theta}{2} \leq \omega t \leq 2\pi - \frac{\theta}{2} \end{aligned} \quad (5.5)$$

The instantaneous value of the plate current may be written as

$$\begin{aligned} i_b &= I_m \left[\cos \omega t - \cos \left(\frac{\theta}{2} \right) \right] && -\frac{\theta}{2} \leq \omega t \leq \frac{\theta}{2} \\ &= 0 && \frac{\theta}{2} \leq \omega t \leq 2\pi - \frac{\theta}{2} \end{aligned}$$

The dc value of the plate voltage must be equal to the plate supply voltage, E_{bb} .

$$\begin{aligned} E_{bb} &= \frac{E_m}{2\pi} \left[\int_{-\frac{\theta}{2}}^{+\frac{\theta}{2}} [1 - \cos \omega t] d\omega t + [2\pi - \theta] \left[1 - \cos \frac{\theta}{2} \right] \right] \\ &= \frac{E_m}{\pi} \left[\pi + \frac{\theta}{2} \cos \left(\frac{\theta}{2} \right) - \pi \cos \left(\frac{\theta}{2} \right) - \sin \left(\frac{\theta}{2} \right) \right] \end{aligned} \quad (5.7)$$

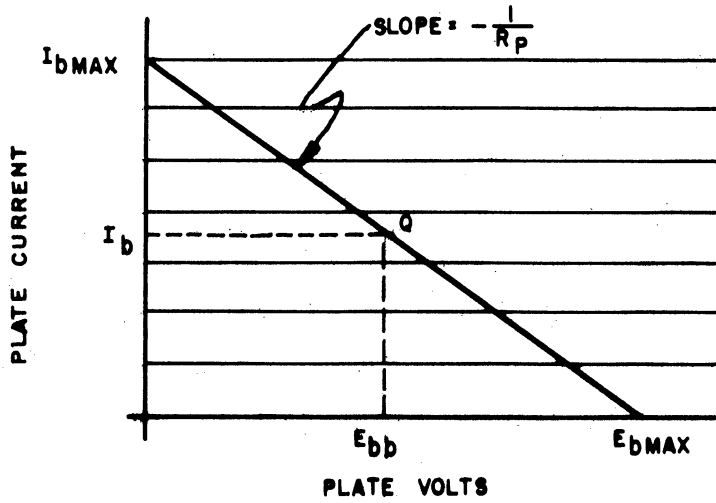


FIG. 5.1. IDEALIZED CONSTANT-CURRENT TUBE PLATE CHARACTERISTICS WITH LOAD LINE DRAWN FOR CLASS A OPERATION.

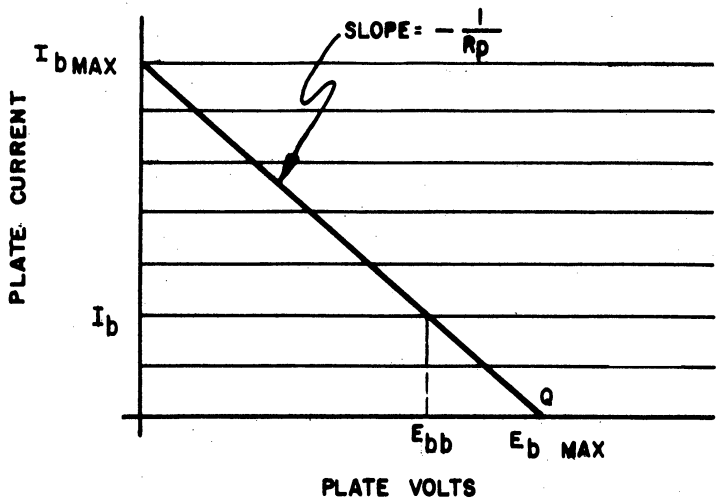


FIG. 5.2 IDEALIZED CONSTANT-CURRENT TUBE PLATE CHARACTERISTICS WITH LOAD LINE DRAWN FOR CLASS B OPERATION.

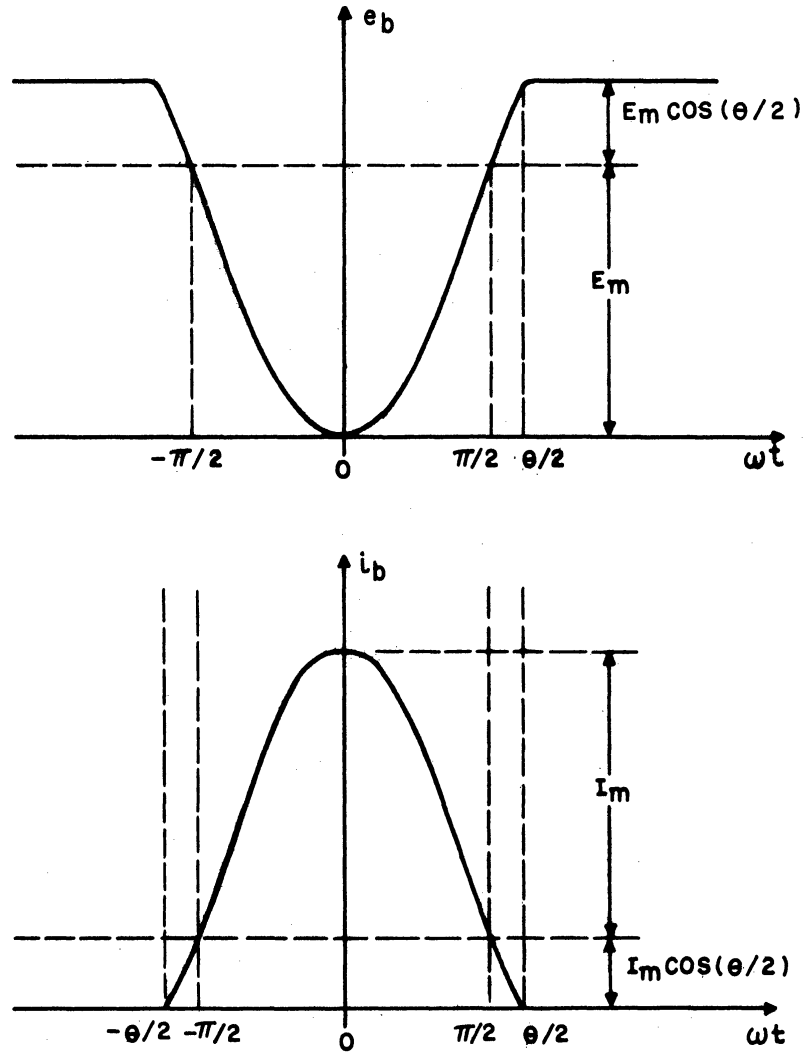


FIG. 5.3. INSTANTANEOUS VALUE OF PLATE VOLTAGE AND PLATE CURRENT.

The dc plate current is the average value of the instantaneous plate current.

$$\begin{aligned}
 I_b &= \frac{I_m}{2\pi} \int_{-\frac{\theta}{2}}^{+\frac{\theta}{2}} \left[\cos \omega t - \cos \left(\frac{\theta}{2} \right) \right] d\omega t \\
 &= \frac{I_m}{\pi} \left[\sin \left(\frac{\theta}{2} \right) - \frac{\theta}{2} \cos \frac{\theta}{2} \right] \quad (5.8)
 \end{aligned}$$

The peak value of the fundamental component of plate voltage is given by Equation

5.9.

$$\begin{aligned}
 E_1 &= \frac{E_m}{\pi} \left[2 \int_0^{\theta/2} (1 - \cos \omega t) \cos \omega t d\omega t + \int_{\frac{\theta}{2}}^{2\pi-\theta/2} \left[1 - \cos \frac{\theta}{2} \right] \cos \omega t d\omega t \right] \\
 &= \frac{E_m}{2\pi} \left[\sin \theta - \theta \right] \quad (5.9)
 \end{aligned}$$

The peak value of the fundamental component of plate current is given by Equation

5.10.

$$\begin{aligned}
 I_1 &= \frac{I_m}{\pi} \int_{-\frac{\theta}{2}}^{+\frac{\theta}{2}} \left[\cos \omega t - \cos \left(\frac{\theta}{2} \right) \right] \cos \omega t d\omega t \\
 &= \frac{I_m}{2\pi} \left[\theta - \sin \theta \right] \quad (5.10)
 \end{aligned}$$

The efficiency can be calculated as the ratio of the output power to the input dc

power. At low frequencies the plate circuit of distributed amplifiers is only

50 percent efficient since half the output power from the tubes is dissipated in

the reverse termination. The output power is one-half the product of the fundamental

current and fundamental voltage.

$$\eta = \frac{1}{2} \frac{\frac{E_1 I_1}{2}}{E_{bb} I_b} \quad (5.11)$$

$$= \frac{1}{8} \frac{[\theta - \sin \theta]^2}{\left[\pi + \frac{\theta}{2} \cos\left(\frac{\theta}{2}\right) - \pi \cos\left(\frac{\theta}{2}\right) - \sin\left(\frac{\theta}{2}\right) \right] \left[2 \sin\frac{\theta}{2} - \theta \cos\left(\frac{\theta}{2}\right) \right]}$$

Equation 5.11 is plotted in Figure 5.4 as a function of conduction angle of the plate current. The maximum theoretical efficiency is seen to be about 30 percent and occurs with a plate current conduction angle of about 225 degrees.

5.3 Staggering the Plate Supply Voltages for Individual Tubes

The curves of plate load impedance as a function of frequency show that the impedance for the first few tubes of a distributed amplifier remain low over an appreciable portion of the frequency range. If the actual operating frequency range is limited to a value somewhat below cut-off, and also at the low-frequency end of the nominal region of operation, the dc voltage supplying the first few tube can be decreased from that used for the last tubes with very little effect on the output of the distributed amplifier, but a corresponding increase in efficiency will be realized.

The efficiency of distributed amplifiers is inherently low due mainly to the inefficiency of the plate line. However when the distributed amplifier circuit is compared with other wide-band amplifiers, it is seen that the distributed amplifier, the wide-band video power amplifier, and the traveling wave amplifier have comparable efficiencies.

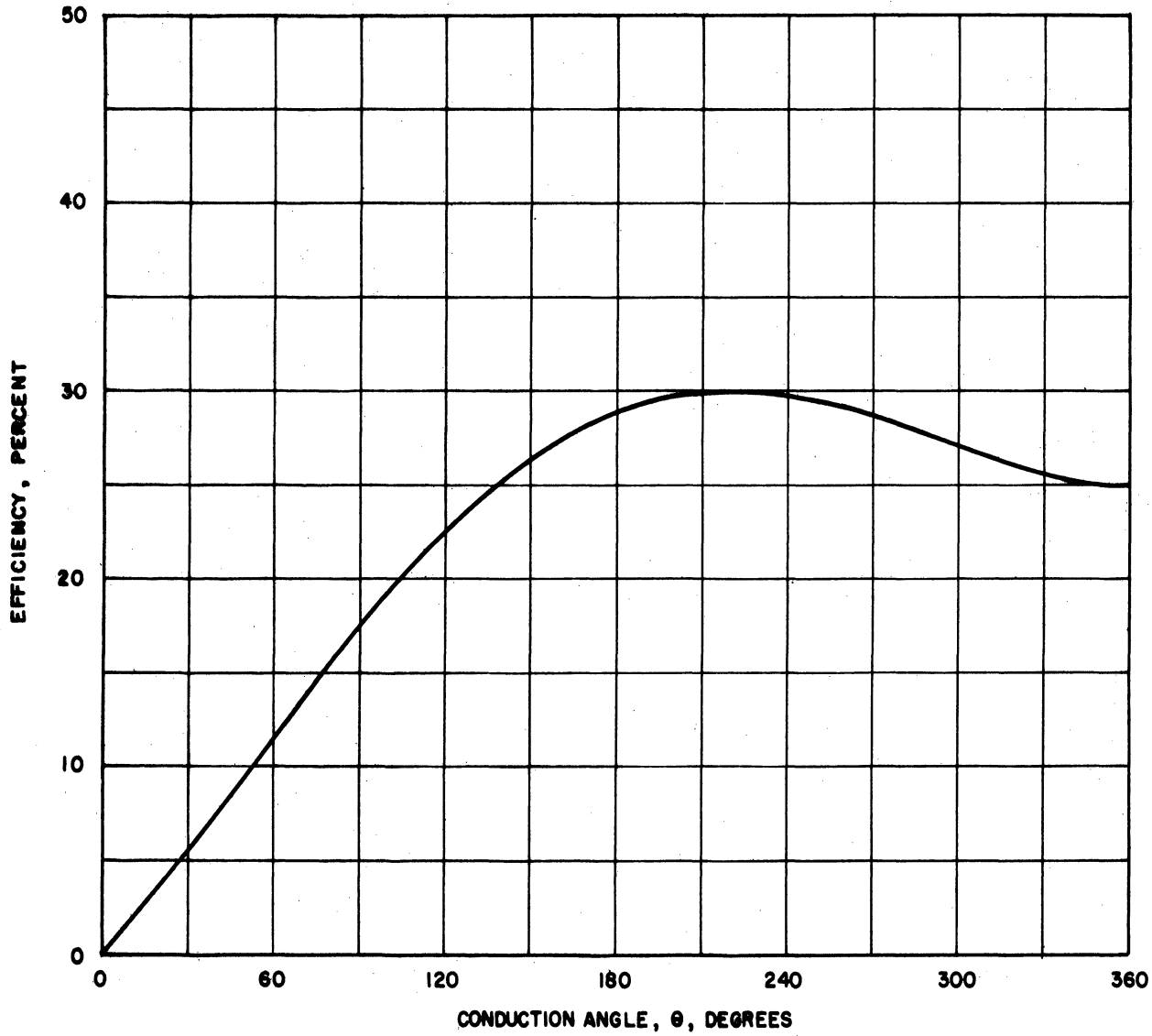


FIG. 5.4. VARIATION OF MAXIMUM THEORETICAL EFFICIENCY OF A DISTRIBUTED AMPLIFIER AS A FUNCTION OF THE CONDUCTION ANGLE OF PLATE CURRENT.

CHAPTER VI. GRAPHICAL ANALYSIS

6.1 Introduction

In any large-signal device utilizing vacuum tubes a graphical analysis is required to account for the non-linearity of the tubes. In this chapter a graphical method for the determination of the output power and efficiency of distributed amplifiers is outlined, and the frequency tolerance and second harmonic distortion problems encountered in distributed amplifiers are considered. It is further shown that under the proper operating conditions, the graphical analysis procedure may be simplified into one of reasonable length. A sample design of a distributed amplifier is given in order to illustrate the graphical analysis procedure.

6.2 Graphical Determination of Power Output and Efficiency

The design of a distributed amplifier having essentially constant power gain over the design frequency range was discussed in Chapter IV. If a distributed amplifier is designed in this manner, the output power calculated at low frequency will be valid for any frequency in the operating range as long as clipping does not occur. Clipping at the plate of the last few tubes is considered in Section 6.4.

Equation 4.6 shows the method of calculation of the grid voltages on any tube in the distributed amplifier. The value of the various α 's in this equation can be determined from Equation 4.3. The value of G_g becomes G_{dr} and can be calculated for any given operating condition of the tubes in a distributed amplifier. However, in actual calculations it is easier to start with the last tube in the distributed amplifier. For an assumed voltage applied to the last tube, and an assumed bias condition, the fundamental component of grid current is calculable by

standard graphical Fourier Analysis techniques. The ratio of the fundamental component of grid current to the grid voltage yields the equivalent grid conductance. This determines the value of α_n . The voltage on the grid of tube (n-1) is e^{α_n} times the voltage assumed on the last tube. This procedure is repeated for each tube in the distributed amplifier.

If the equivalent large-signal transconductance (the ratio of the fundamental component of plate current to grid voltage) of each tube is assumed to be equal, the plate load impedance of the k^{th} tube at low frequencies (see Equations 4.6 and 4.7) may be written as

$$R_k = \frac{R_p}{2} \left[e^{(\alpha_2 + \alpha_3 + \dots + \alpha_k)} + e^{(\alpha_3 + \alpha_4 + \dots + \alpha_k)} + \dots + e^0 + \dots + e^{-(\alpha_{k+1} + \dots + \alpha_n)} \right] \quad (6.1)$$

These load lines may be drawn through the operating Q-point and the fundamental component of plate current determined from a graphical Fourier analysis. The currents so determined may now be used to determine to a closer degree of approximation the plate load impedance on each tube. The above procedure is continued until the change in the fundamental component of plate current between successive approximations is negligible.

The power output can be determined as the square of one-half the sum of the fundamental components of plate current found above multiplied by the nominal impedance of the plate line, R_p .

The efficiency at low frequencies may be determined as the ratio of the output power calculated above and the dc power input. The dc power input is the product of the sum of the average values of the plate current and the plate supply voltage.

In general, the efficiency of large-signal distributed amplifiers will not be constant with frequency since the grid voltage on each tube varies with frequency, and hence the average value of the plate current will be a function of frequency. In a distributed amplifier designed for a flat frequency response the

efficiency will increase to some extent with frequency since the magnitude of the majority of grid voltages decreases with frequency which results in a lower dc supply current.

6.3 Approximate Graphical Solution

If the variation in the α 's at low frequencies between the various tubes in a distributed amplifier is small, a single value for the α 's may be used with the exception of α_1 which would be one-half this value since it is for a half-section of the grid-line filter networks. α may be determined by a method discussed in Section 6.2.

If the equivalent large-signal transconductances are assumed to be the same for all the tubes, the plate load impedance (See Equation 4.4) on the k^{th} tube is given by

$$R_k = \frac{R_p}{2} \left[e^{(2k-n-1)\frac{\alpha}{2}} \left[\frac{\sinh(\frac{n\alpha}{2})}{\sinh(\frac{\alpha}{2})} \right] \right] \quad (6.2)$$

If α is small,

$$R_k \approx \frac{R_p}{2} n \quad (6.3)$$

The approximate load line may be drawn through the operating Q-point and the fundamental component of plate current determined from a graphical Fourier analysis.

The output power can be determined from Equation 4.18, or as rewritten in Equation 6.4 for low frequencies.

$$P_{\text{out}} = P_{\text{ol}} \left[e^{-\frac{n\alpha}{2}} \frac{\sinh(\frac{n\alpha}{2})}{\sinh(\frac{\alpha}{2})} \right]^2 \quad (6.4)$$

where P_{ol} is the output power of one tube operating alone in the distributed amplifier without any attenuation in the grid line. However, if

$$\frac{nG_{\text{dr}}R_g}{4} < 0.2,$$

$$\left[\frac{\sinh(\frac{n\alpha}{2})}{\sinh(\frac{\alpha}{2})} \right]^2 \approx n^2$$

The output power can be written approximately as

$$P_{\text{out}} = P_{\text{ol}} n^2 e^{-n\alpha} \quad (6.5)$$

6.4 Frequency Tolerance

Frequency tolerance as defined in Chapter III is the frequency above which clipping occurs in the last tube of the distributed amplifier. This frequency may be found with the aid of the plate characteristics of the tube and two equations. If n is substituted for k in Equation 4.4 the plate load impedance for the last tube is given by

$$Z_n = \frac{Z_{\pi p}}{2} e^{(n-1)\frac{\alpha}{2}} \frac{\sinh \frac{n\alpha}{2}}{\sinh \frac{\alpha}{2}} \quad (6.6)$$

The grid voltage on the last tube of the distributed amplifier can be calculated from Equation 4.6. However, if all the α 's are assumed to be equal, the voltage on the last tube can be written as

$$E_n = \sqrt{P_{\text{dr}}} \cdot \sqrt{Z_{\pi g}} e^{-(2n-1)\frac{\alpha}{2}} \quad (6.7)$$

The plate load impedance for several different frequencies can be drawn on a set of plate characteristics using Equation 6.6. The grid voltage on these load lines is determined from Equation 6.7. As an example of these calculations, Figure 6.1 shows the final tube load line for a six-tube 4X150A distributed amplifier with a nominal grid line impedance of 50 ohms and a plate line impedance of 90 ohms. The dotted line crossing the load lines indicates the extent of the grid excursion. It will be noticed that above a frequency of about 250 mc, clipping begins to occur in the plate circuit of the final tube, and as a result the power output begins to decrease. It is interesting to note that the same frequency is obtained as the frequency tolerance if the normal increase in Z_{π} is used without attenuation in the grid line. This is indicated by the dashed curve in Figure 6.1.

2262 A-61-188 JEM 6-10-56

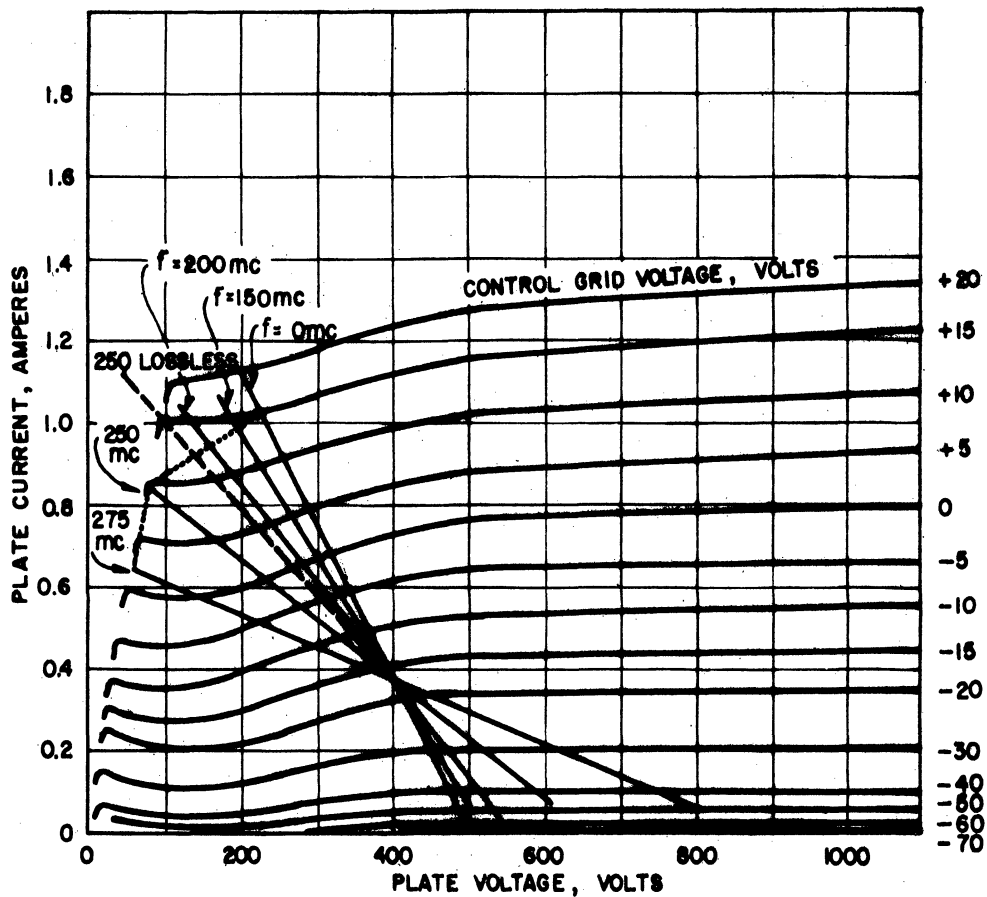


FIG. 6.1. FREQUENCY VARIATION OF THE PLATE LOAD IMPEDANCE OF THE 6th TUBE IN A DISTRIBUTED AMPLIFIER USING 6, 4X150A TUBES WITH A. NOMINAL GRID LINE IMPEDANCE OF 50 OHMS AND A NOMINAL PLATE LINE IMPEDANCE OF 90 OHMS.

6.5 Second Harmonic Distortion

In a distributed amplifier operating under specified conditions it is possible to determine the shape of the plate current waveform, and, by means of a graphical Fourier analysis, to determine the value of the second harmonic component of plate current. In order to determine the second harmonic output power it is necessary to take into account the phase difference of the individual currents as they appear at the output tube. Once the magnitude of the current which enters the filter section between the last tube and the output termination has been determined, the second harmonic power can be calculated by multiplying the square of this current by Z_{π} of the plate line.

If the attenuation in the grid line is neglected over the frequency range where the second harmonic would be transmitted by the plate line, the second harmonic component of the individual tubes can be written as

$$\begin{aligned} i_1 &= I_2 \sin 2\omega t \\ i_2 &= I_2 \sin 2(\omega t - \varphi) \\ &\vdots \\ &\vdots \\ i_n &= I_2 \sin 2(\omega t - [n-1] \varphi) \end{aligned} \quad (6.8)$$

where φ is the phase shift per section of the grid line at an angular frequency of ω , and I_2 is the peak value of the second harmonic component of plate current.

If the phase shift per section of the plate line at the second harmonic is designated as φ_2 , the current entering the last filter section is

$$\begin{aligned} i_{\text{out}} &= \frac{i_1}{2} \left[-\frac{(n-1)\varphi_2}{2} \right] + \frac{i_2}{2} \left[-\frac{(n-2)\varphi_2}{2} + \dots + \frac{i_n}{2} \right] \\ &= \frac{I_2}{2} e^{j2\omega t} \left[e^{-j(n-1)\varphi_2} + e^{-j[2\varphi + (n-2)\varphi_2]} + \dots \right. \\ &\quad \left. + e^{-j2(n-1)\varphi} \right] \end{aligned} \quad (6.9)$$

This finite exponential series may be summed in a manner similar to those of Appendix A, and Equation (6.9) can be written in closed form as shown in Equation 6.10

$$\begin{aligned}
 i_{\text{out}} &= \frac{I_2}{2} e^{j\left[2\omega t - (n-1)\left(\varphi + \frac{\varphi_2}{2}\right)\right]} \frac{\sin n\left(\frac{\varphi_2}{2} - \varphi\right)}{\sin\left(\frac{\varphi_2}{2} - \varphi\right)} \\
 &= \frac{I_2}{2} F_n\left(\frac{\omega}{\omega_c}\right) e^{j\left[2\omega t - (n-1)\left(\varphi + \frac{\varphi_2}{2}\right)\right]} \quad (6.10)
 \end{aligned}$$

where

$$\varphi = 2 \sin^{-1}\left(\frac{\omega}{\omega_c}\right) \text{ and } \varphi_2 = 2 \sin^{-1}\left(\frac{2\omega}{\omega_c}\right) \quad (6.11)$$

Figure 6.2 shows $F_n\left(\frac{\omega}{\omega_c}\right)$ for a six-tube and a nine-tube distributed amplifier. It can be seen from Figure 6.2 that the variation of $F_n\left(\frac{\omega}{\omega_c}\right)$ as a function of frequency is not great over the major portion of the frequency range where the second harmonic distortion is of interest. However, at the higher frequencies the phase angles of the second harmonic component of plate current of the individual tubes which appears in the output cause a cancellation effect and $F_n\left(\frac{\omega}{\omega_c}\right)$ decreases.

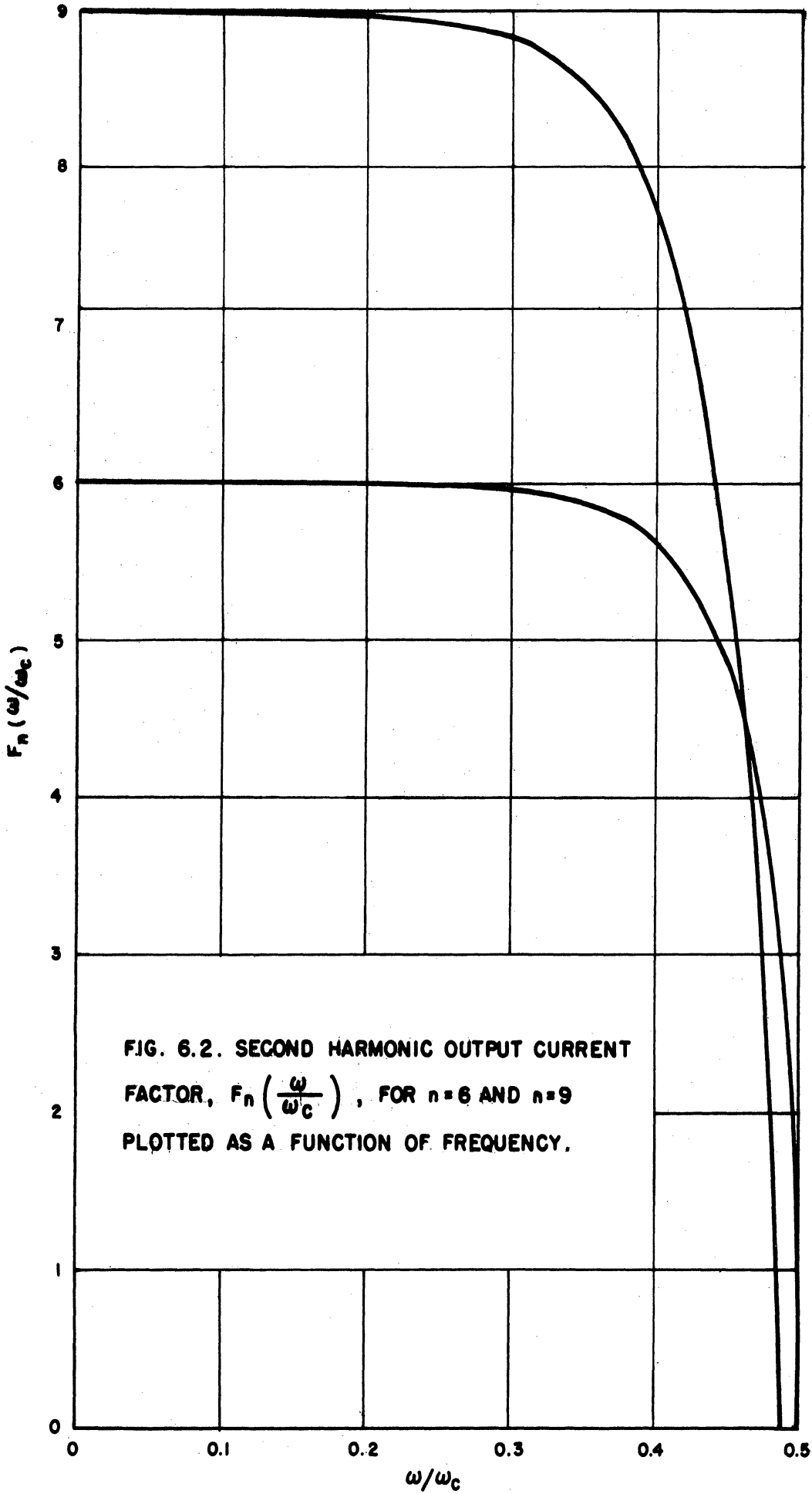
The second harmonic output power can be calculated from Equation 6.12.

$$P_{2\text{out}} = \left(\frac{I_2 F_n\left(\frac{\omega}{\omega_c}\right)}{2\sqrt{2}}\right)^2 Z_{\pi}(2\omega) \quad (6.12)$$

where $Z_{\pi}(2\omega)$ is the mid-shunt image impedance of the plate line evaluated at the second harmonic frequency.

6.6 Sample Design of a Distributed Amplifier Using 4X150A Tubes

After the tube type has been picked, the first step in the design procedure is to measure the small-signal effects. Figure 6.3 shows the input resistance for a 4X150A as a function of frequency. The input capacity of a 4X150A was measured as 21.2 micro-microfarads. If the experimentally determined values above are substituted in Equation 4.19, the product of the angular cut-off frequency and



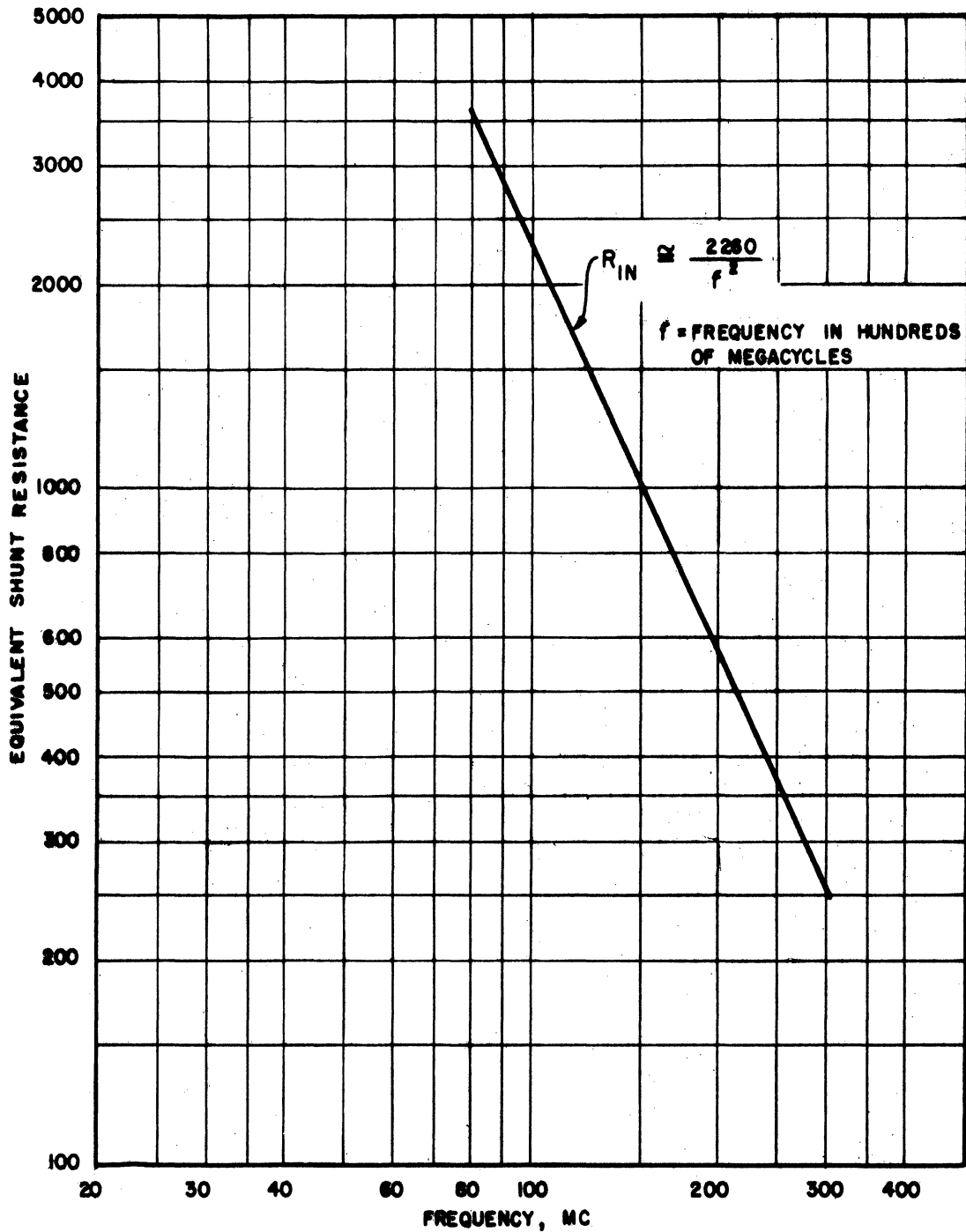


FIG. 6.3. VARIATION OF EQUIVALENT SHUNT RESISTANCE OF A 4X150A CAUSED BY LEAD INDUCTANCES AND TRANSIT TIME.

the number of tubes for a 4X150A is

$$n\omega_c = 189 \times 10^8 \quad (6.13)$$

The inductance of the grid lead of the 4X150A is about 0.007 microhenrys. The series resonant frequency of the grid lead inductance and the input capacity of the tube is 410 mc. Equation 3.11 indicates a maximum cut-off frequency of about 330 mc. The solution of Equation 6.13 with 330 mc for the cut-off frequency yields a value of nine tubes. The impedance level of the grid and plate lines can be determined from Equation 3.3.

$$R_g = \frac{2}{\omega_c C_g} = 45 \Omega$$

$$R_p = \frac{2}{\omega_c C_p} = 81.5 \Omega$$

for $C_p = 11.8 \mu\text{f}$. In order to simplify the impedance matching problem the upper cut-off frequency is modified so that the grid line has a nominal impedance of 50 ohms. This lowers the cut-off frequency to 300 mc and raises the nominal impedance of the plate line to 90 ohms.

The values of the inductances for the grid line and the plate line can be determined from Equation 3.2 and the coefficient of coupling of the negative mutual coils from Equation 3.10.

The attenuation of the grid line can be calculated for small signals from Equation 4.3, and the results of Figure 6.3. Figure 6.4 is a plot of the attenuation per section of the grid line under small-signal conditions. If the values of α from Figure 6.4 are substituted into Equation 4.6, the value of the various grid voltages can be found as a function of frequency. The results of this calculation are plotted in Figure 6.5.

The next step in the design of a distributed amplifier is to determine the operating voltages. Unfortunately there is no quick and easy method for graphically

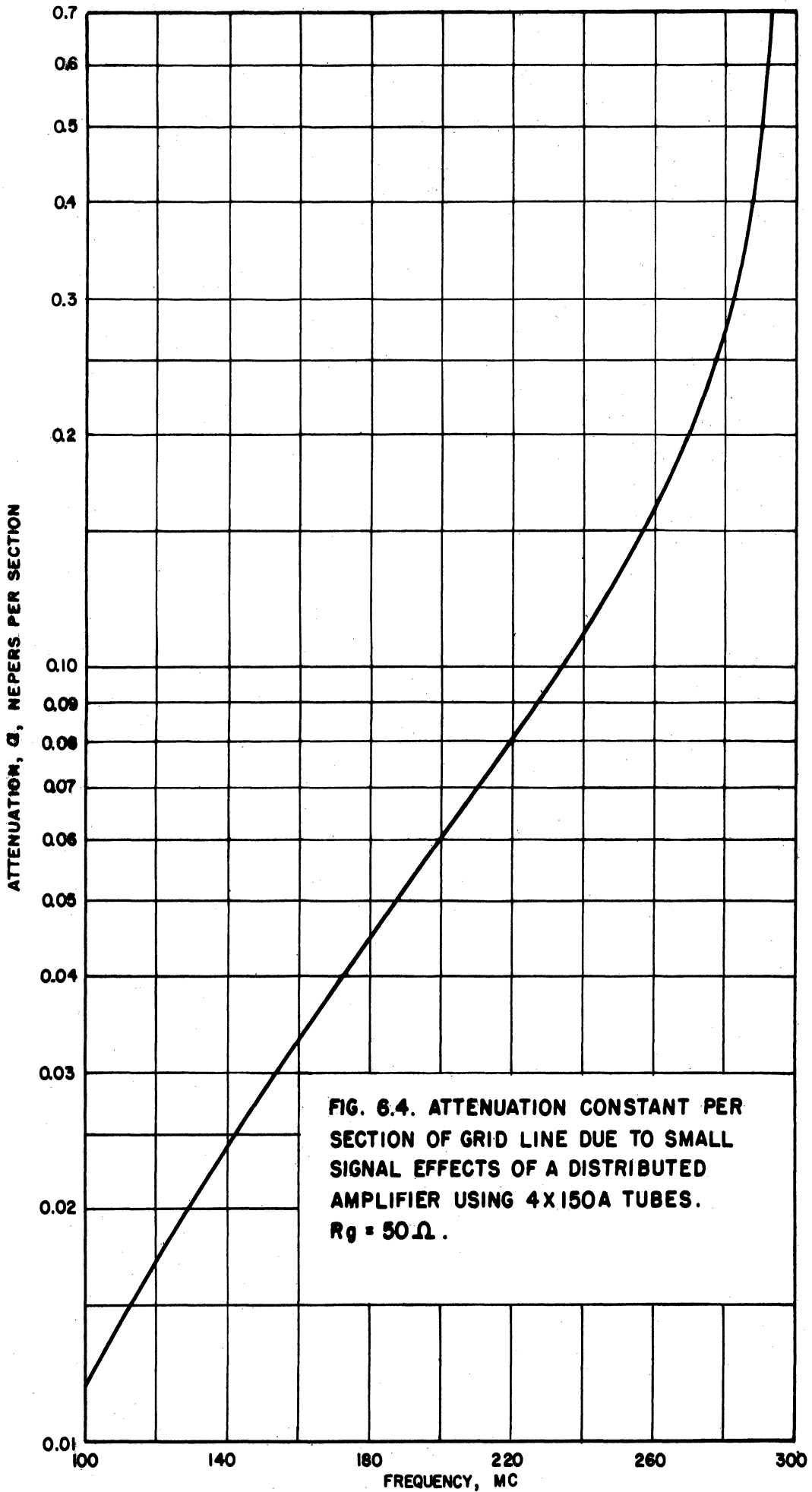
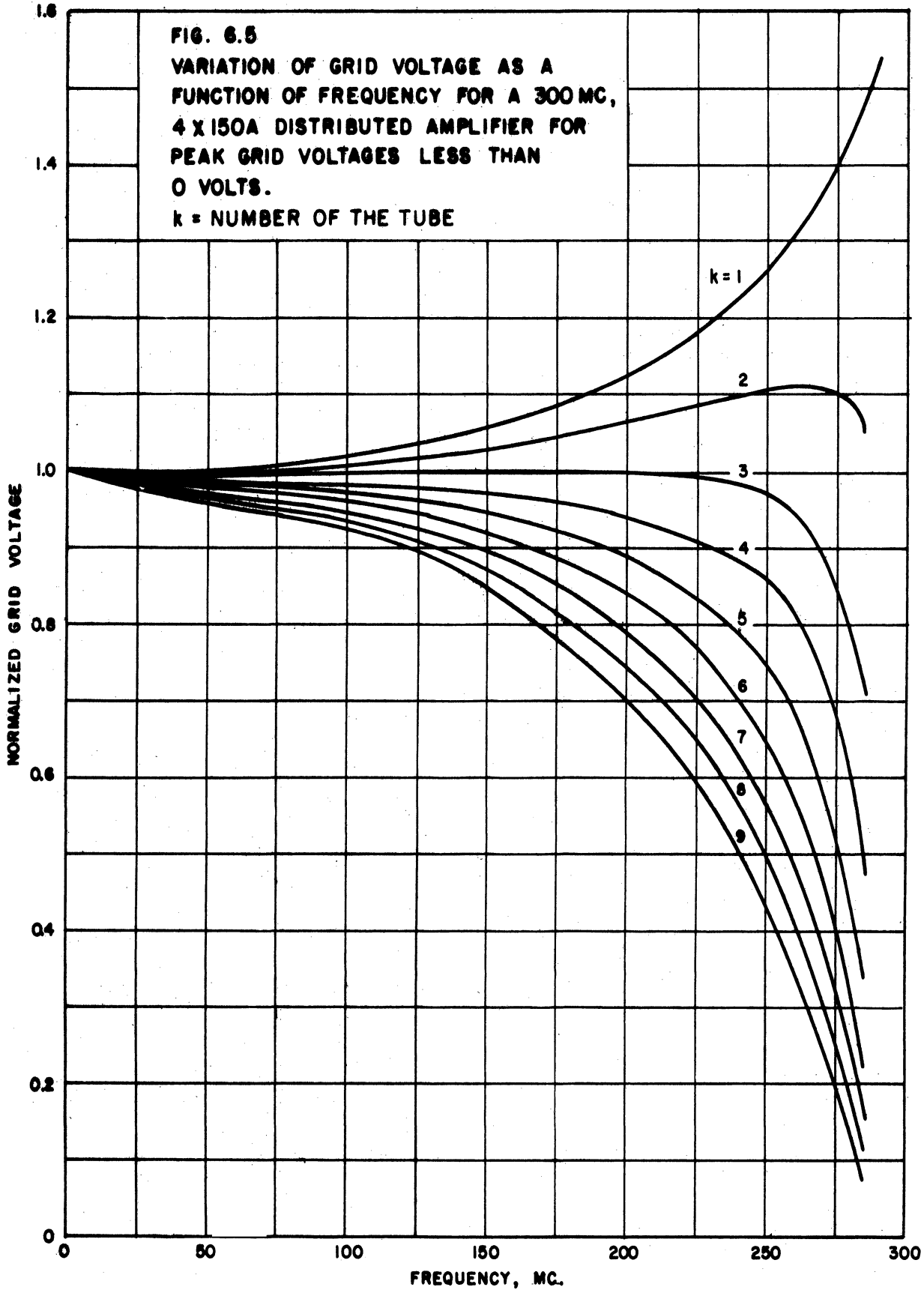


FIG. 6.5
VARIATION OF GRID VOLTAGE AS A
FUNCTION OF FREQUENCY FOR A 300 MC,
4 X 150A DISTRIBUTED AMPLIFIER FOR
PEAK GRID VOLTAGES LESS THAN
0 VOLTS.
k = NUMBER OF THE TUBE



determining the proper operating conditions for the distributed amplifier. The final operating conditions will in general represent a compromise between efficiency, power output, frequency tolerance, and driving power. The weighting of each of these parameters depends upon the application. One method of attack is illustrated in the graphical analysis that follows.

A plate voltage at the Q-point, E_{bq} , of 800 volts and a screen voltage of 400 volts were assumed. Figure 6.6 shows the plate characteristics for a 4X150A extrapolated to a screen voltage of 400 volts. This extrapolation process is described in detail in the Eimac tube handbook. Several possible values for the grid bias were assumed and the plate load line drawn. For this first approximation the load line is drawn with a slope of $-\frac{1}{405}$ mhos (attenuation in the grid line is neglected). The dynamic transfer characteristic is obtained from these lines and is plotted in Figure 6.7. It will be noticed from Figure 6.7 that the 4X150A is a good approximation to a constant-current device in that all the curves lie very close to one another. Figure 6.8 shows the variation of grid current with grid voltage for a 4X150A operating with a screen voltage of 400 volts. This curve will be used to determine the equivalent loading resistance due to grid current.

Table 6.1 shows the instantaneous values of plate current and grid current for a bias voltage of -13.3 volts and a peak signal voltage of 33.3 volts. Figure 6.9 is a plot of the instantaneous value of plate current as a function of ωt . From this plot the dc plate current is found to be 0.86 amperes. Figure 6.10 is a plot of the instantaneous value of the plate current multiplied by $\cos \omega t$. Twice the average value of this curve is the peak value of the fundamental component of plate current. From this curve the fundamental value of plate current is found to be 0.75 amps. Figure 6.11 is a plot of the instantaneous value of plate current multiplied by $\cos 2\omega t$. Twice the average value of this curve is the peak value of the second harmonic component of plate current. Figure 6.12 is a plot of the

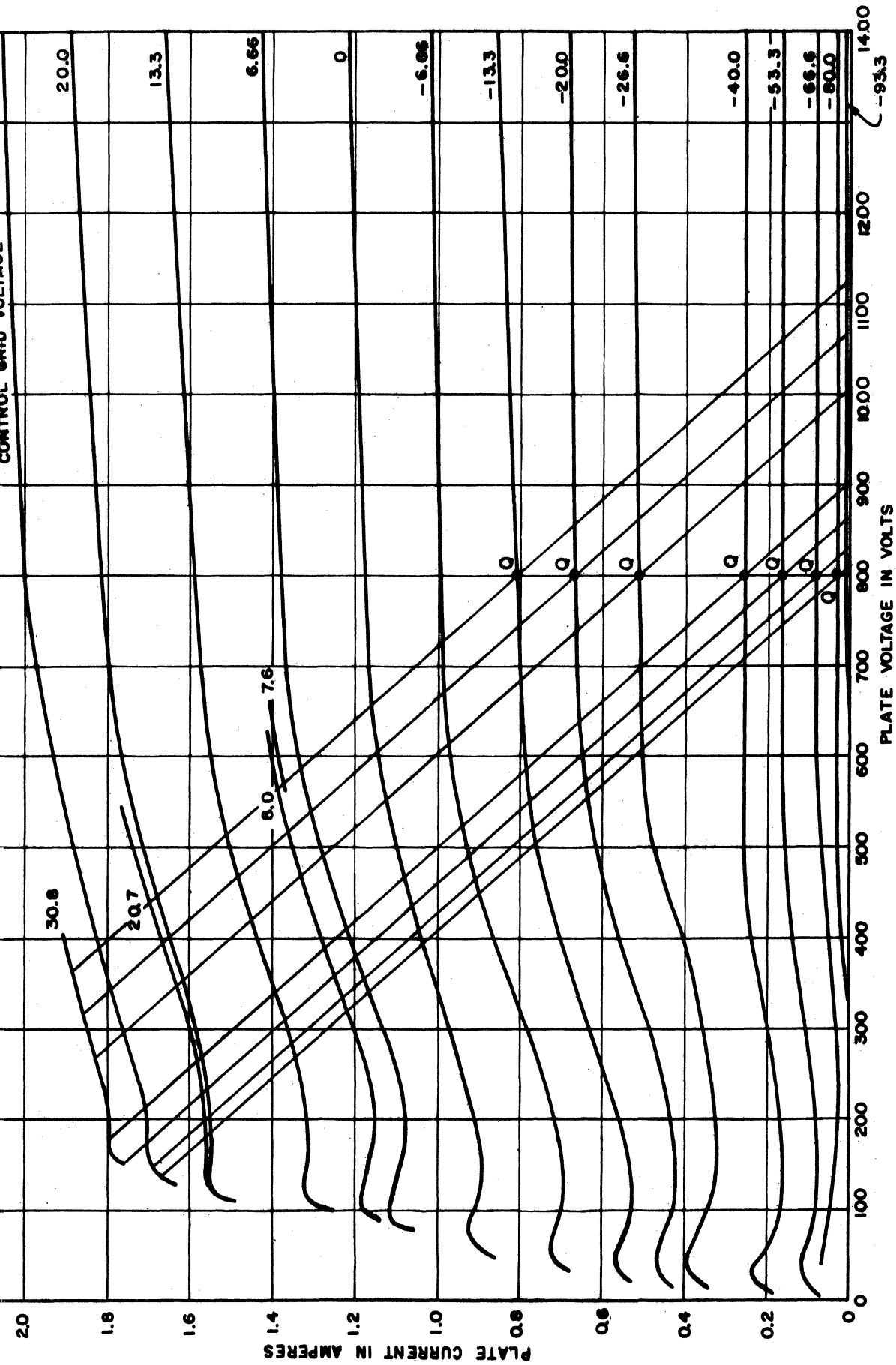
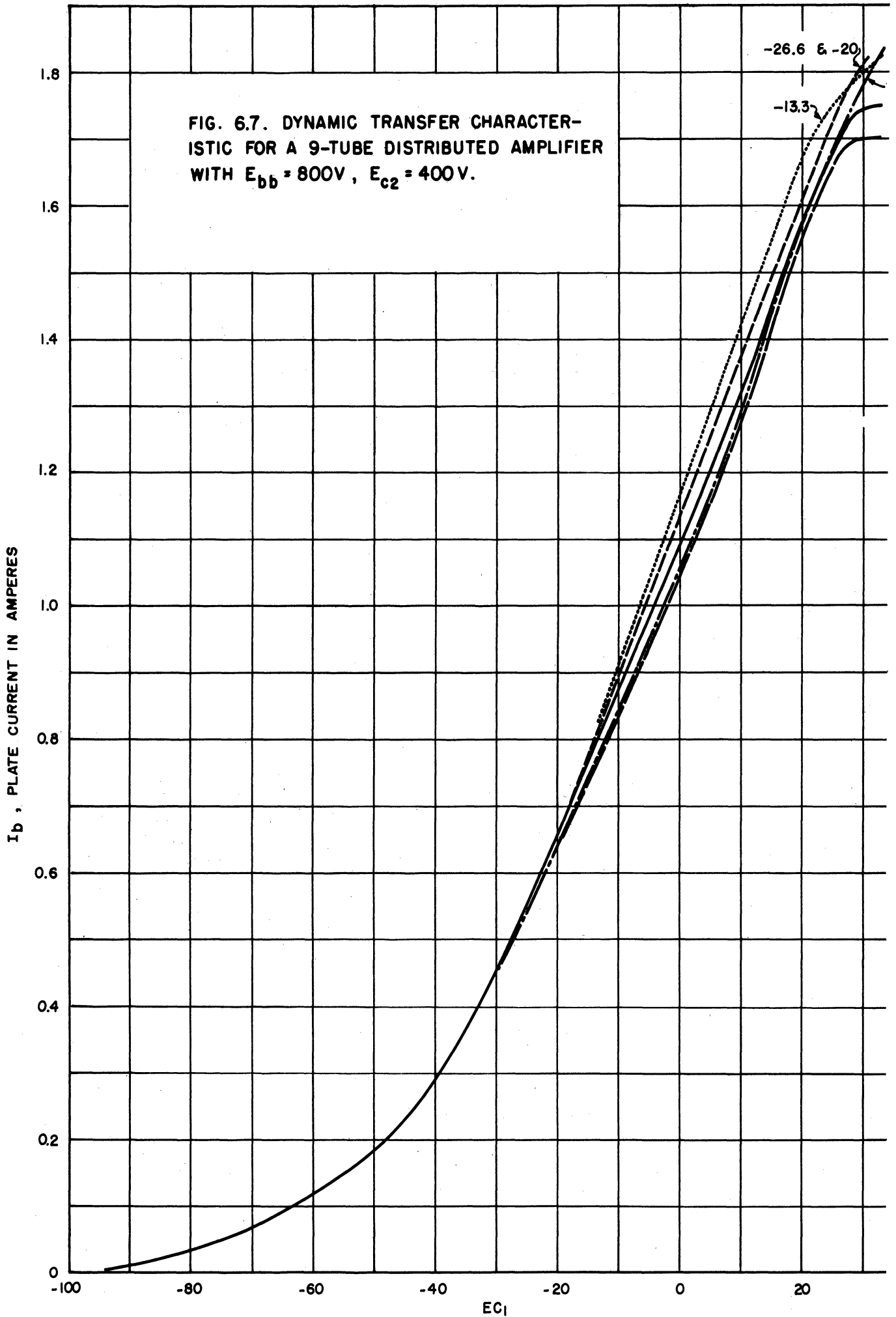


FIG. 6.6. PLATE CHARACTERISTICS FOR A 4X150A WITH $E_{c2} = 400$ VOLTS. LOAD LINES DRAWN FOR A 9-TUBE DISTRIBUTED AMPLIFIER AT LOW FREQUENCIES FOR VARIOUS Q-POINTS CONSIDERED IN GRAPHICAL ANALYSIS.



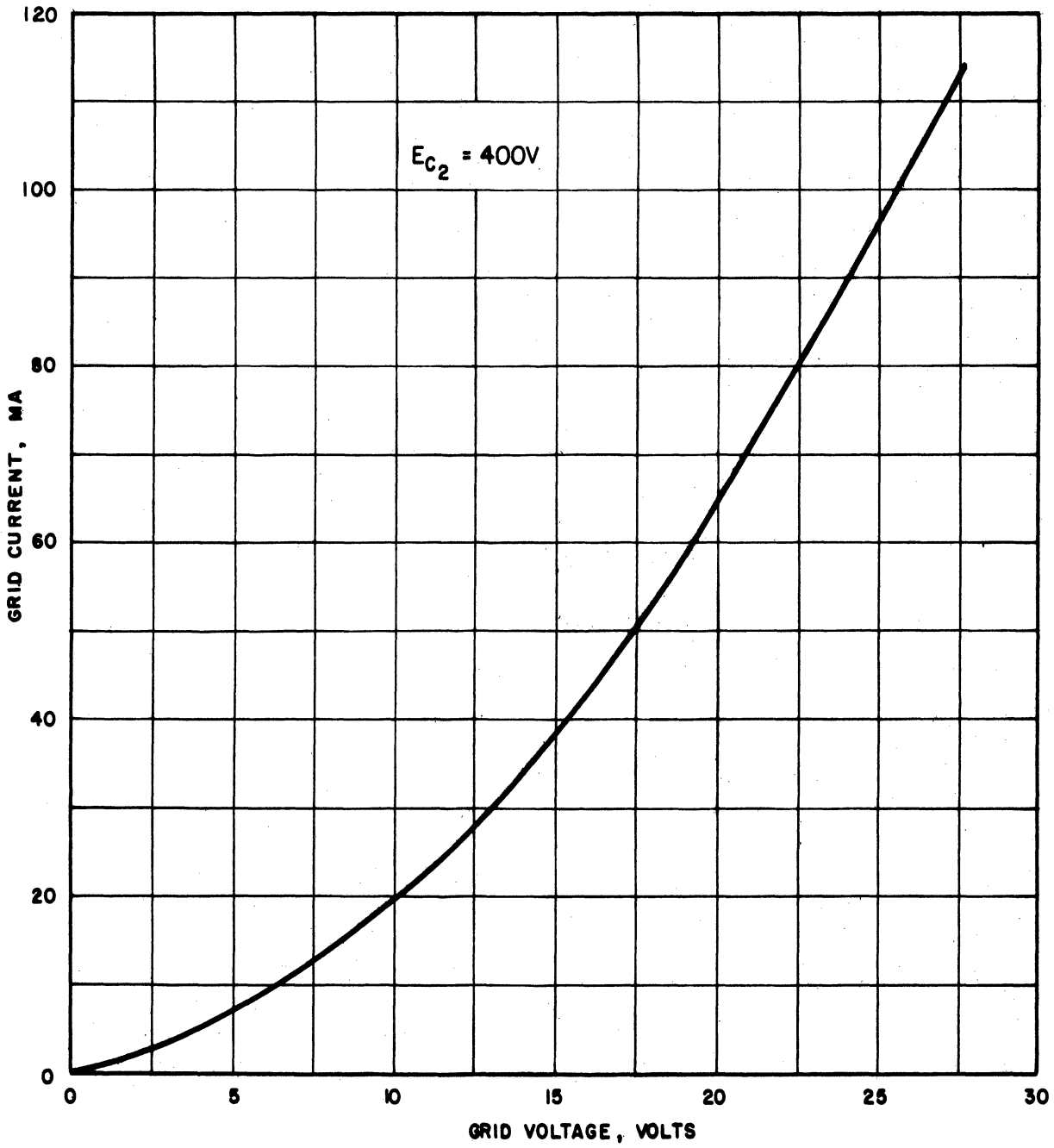


FIG. 6.8. GRID CURRENT AS A FUNCTION OF GRID VOLTAGE FOR A 4 X 150 A .

TABLE 6.1

Instantaneous Values of Plate Current and Grid Current
 $E_{bq} = 800 \text{ v}$; $E_{c2} = 400\text{v}$; $E_{c1} = -13.3 \text{ volts}$; $E_{sig} = 33.3 \text{ volts peak}$

ωt	$33.3 \cos \omega t$ -13.3	i_b	$i_b \cos \omega t$	$i_b \cos 2\omega t$	$i_c \text{ (ma)}$	$i_c \cos \omega t$
0	20	1.68	1.68	1.68	64.7	64.7
15	18.9	1.64	1.58	1.42	57.5	55.6
30	15.5	1.56	1.35	0.78	40.5	35.1
45	10.2	1.42	1.0	0.0	20	14.1
60	3.4	1.25	0.63	-0.63	4	2
75	-4.7	1.06	0.27	-0.92	0	0
90	-13.3	.82	0	-0.82	0	0
105	-21.9	.62	-0.16	-0.54	0	0
120	-30.0	.45	-0.23	-0.23	0	0
135	-36.8	.34	-0.24	0.0	0	0
150	-42.1	.26	-0.23	0.13	0	0
165	-45.5	.22	-0.21	0.19	0	0
180	-46.6	.21	-0.21	0.21	0	0

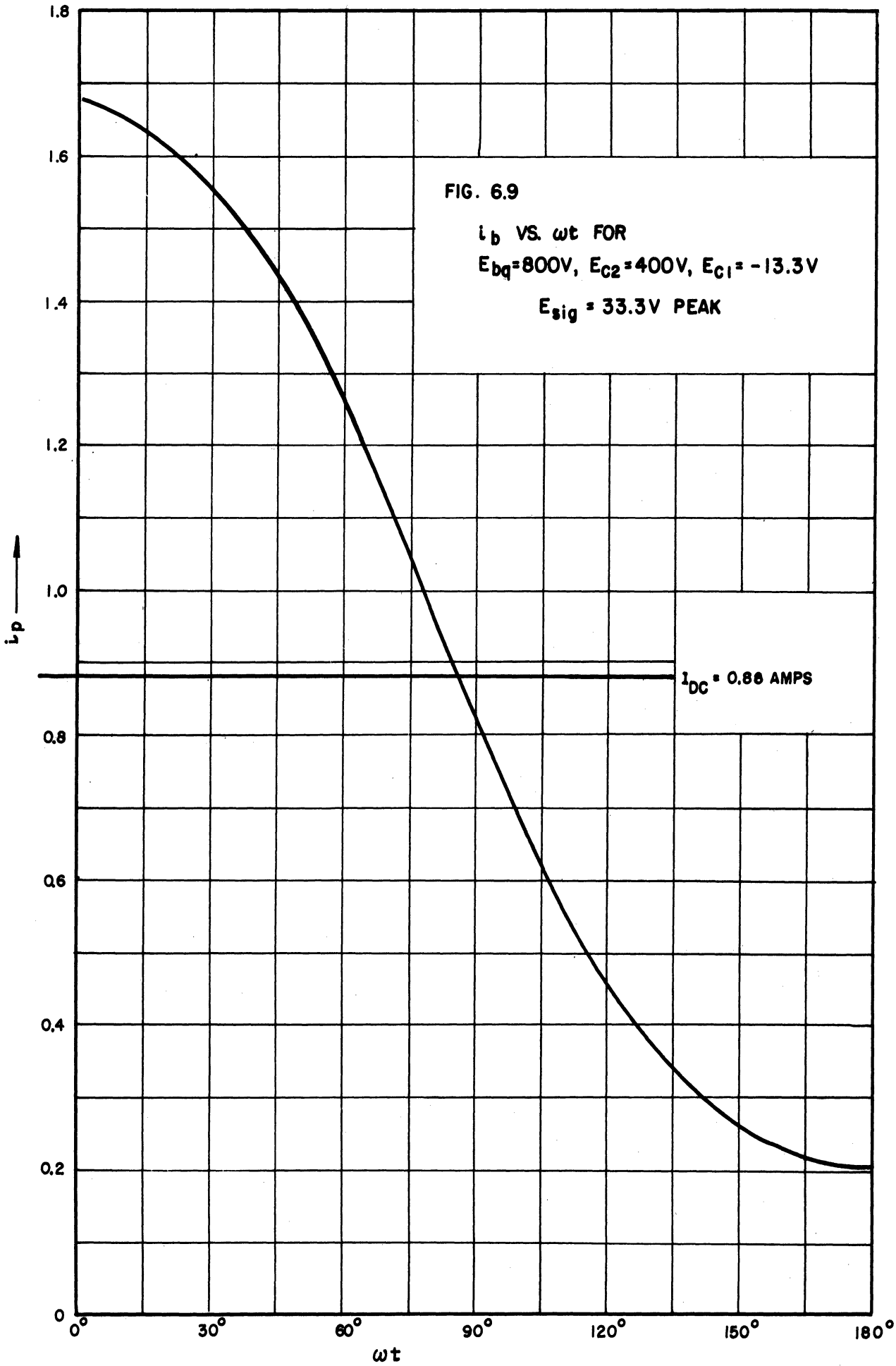


FIG. 6.9

i_p VS. ωt FOR

$E_{bq} = 800V$, $E_{c2} = 400V$, $E_{c1} = -13.3V$

$E_{sig} = 33.3V \text{ PEAK}$

$I_{DC} = 0.86 \text{ AMPS}$

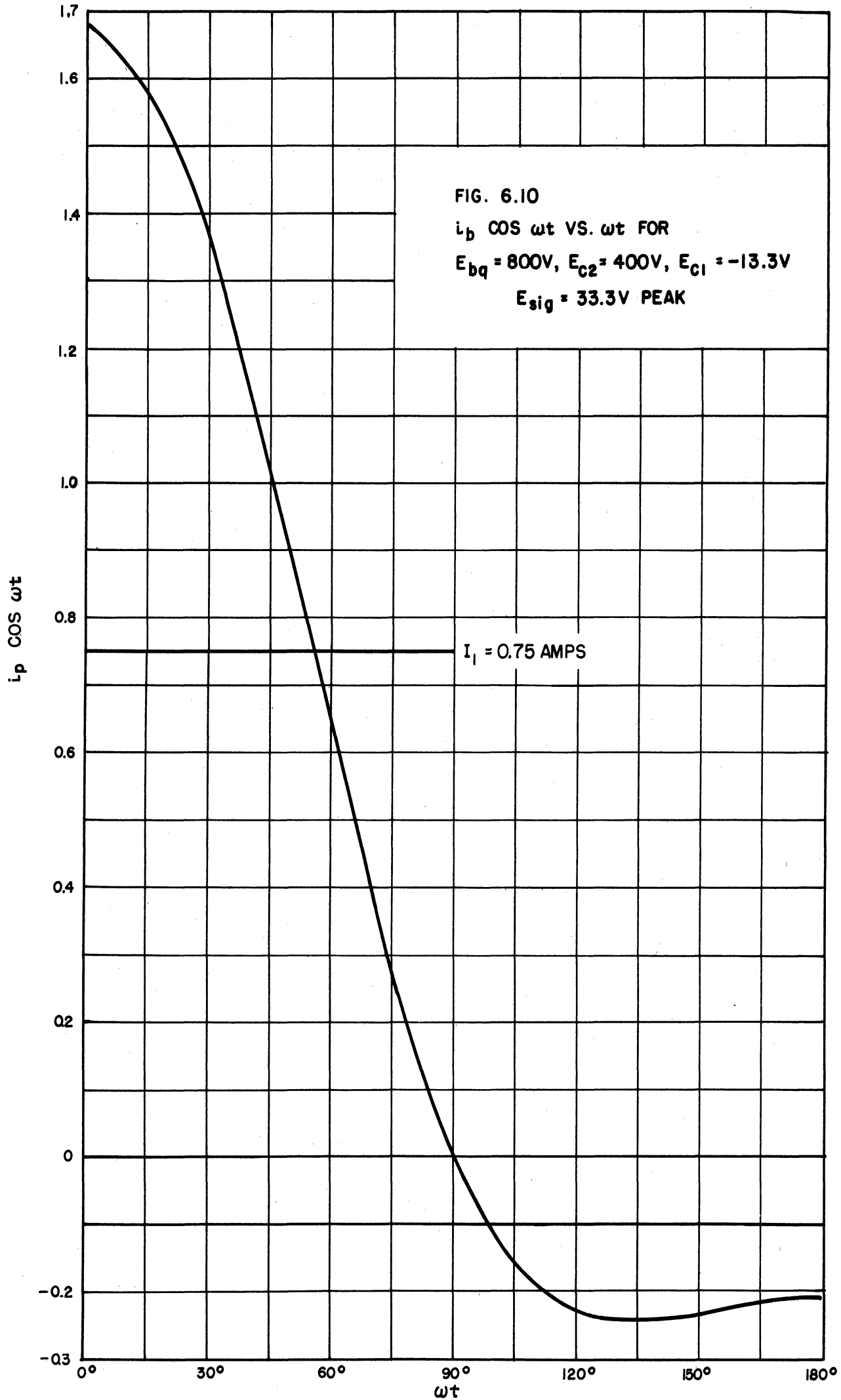


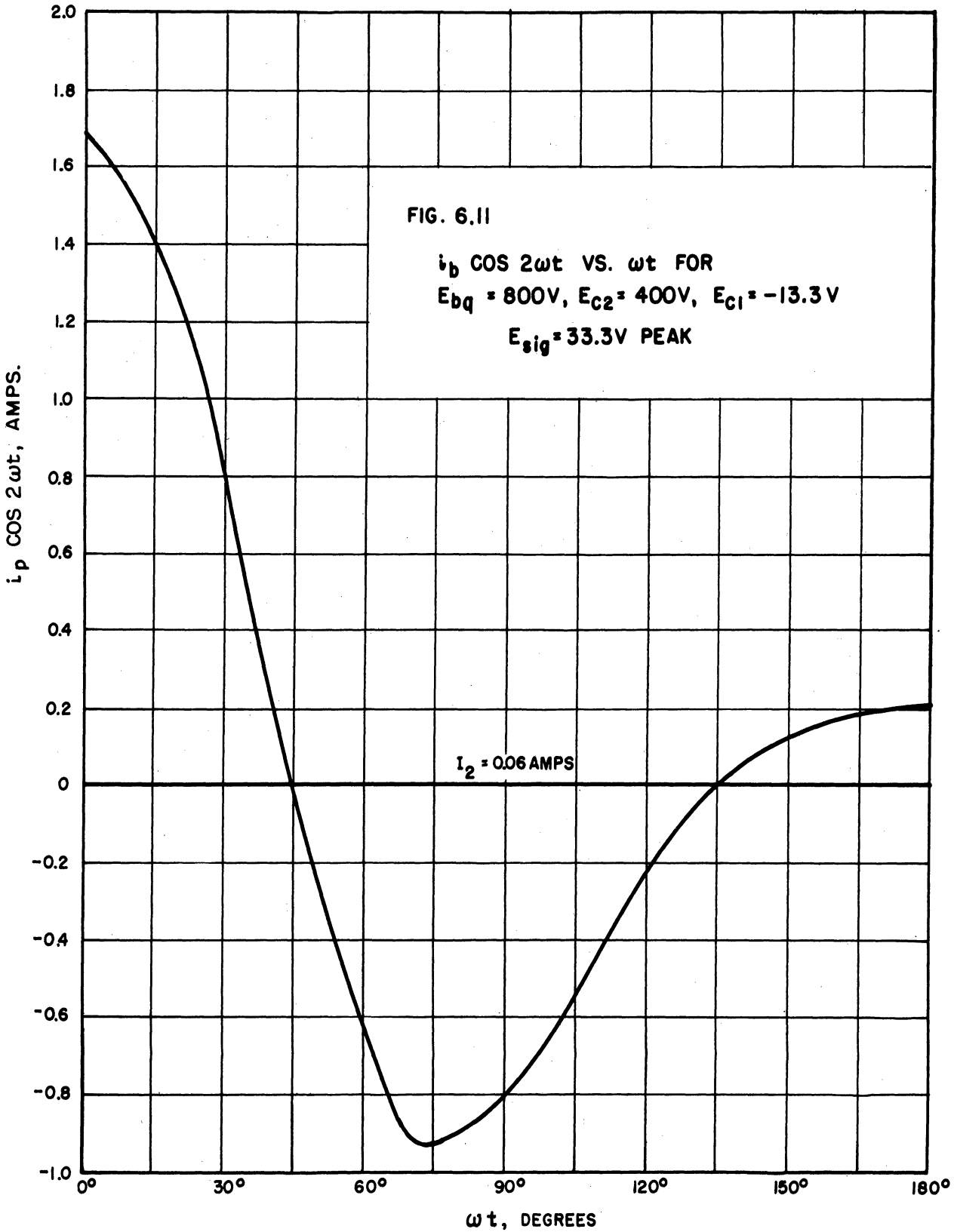
FIG. 6.10

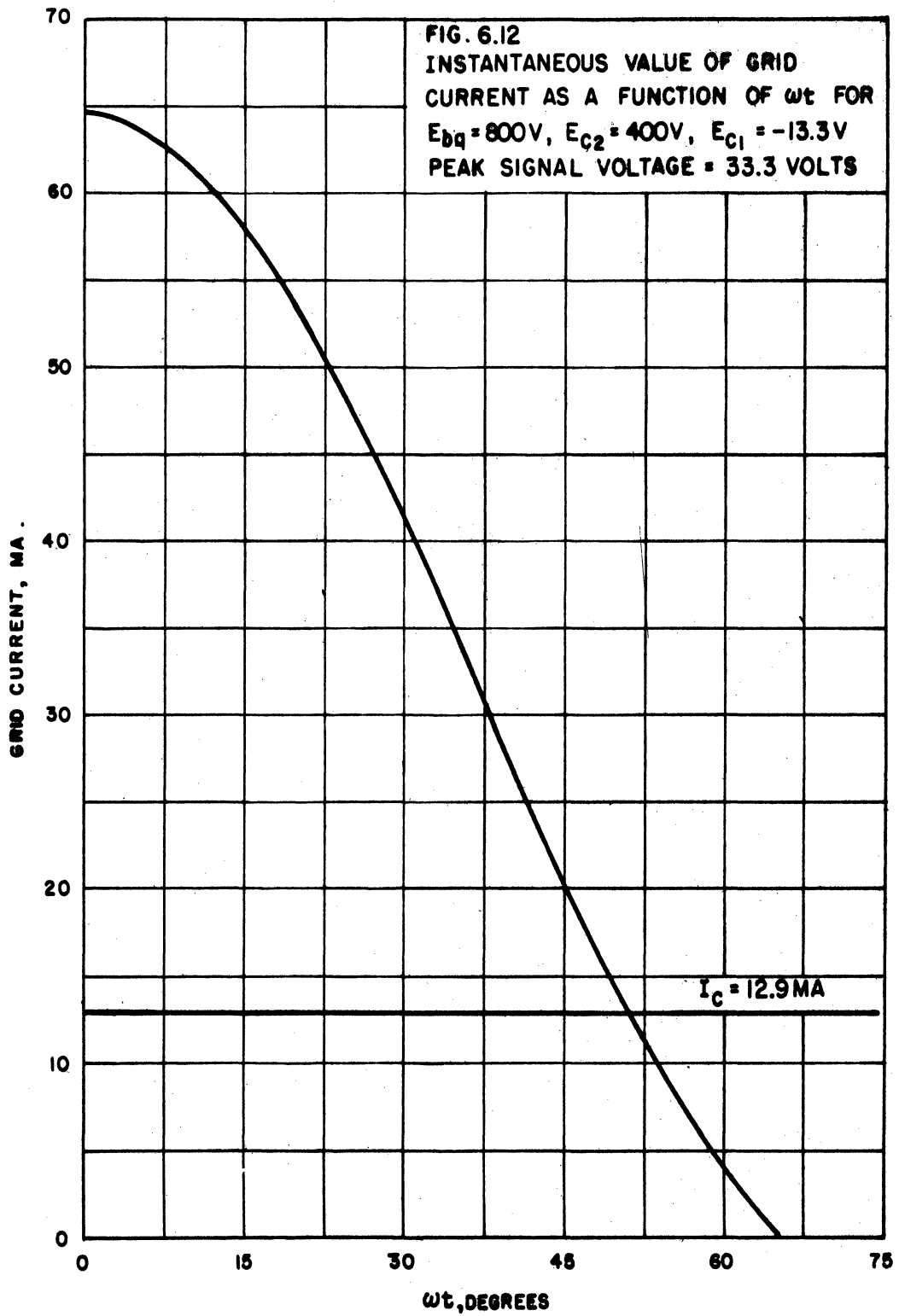
$i_p \cos \omega t$ VS. ωt FOR

$E_{bq} = 800V, E_{c2} = 400V, E_{c1} = -13.3V$

$E_{sig} = 33.3V$ PEAK

$I_1 = 0.75$ AMPS





instantaneous value of grid current. The dc grid current is the average value of this curve. Figure 6.13 is a plot of the instantaneous value of grid current multiplied by the $\cos \omega t$. Twice the average value of this curve is the peak value of the fundamental component of grid current.

Due to the non-linearity of the dynamic transfer characteristic of the 6X150A, the load line will shift from the small-signal operating point. Each of the load lines drawn on Figure 6.6 is drawn for a voltage at the Q-point of 800 volts. The actual dc supply voltage, E_{bb} , will in general be less than the plate voltage at the Q-point. E_{bb} is easily determined from the load line as the voltage across the tube when the plate current has its average value. This is shown in Figure 6.6.

Table 6.2 summarizes the calculations and results for the 9-tube distributed amplifier operating under the conditions stated above.

The graphical calculations for the other operating points shown in Figure 6.6 are given in Appendix F.

Figure 6.14 is a compilation of the calculated results for a 9-tube distributed amplifier operating with a plate voltage at the Q-point of 800 volts, a screen voltage of 400 volts, and a peak signal voltage adjusted so that the grids are driven 20 volts positive. It will be noted from these curves that the dc input power is in excess of the plate dissipation rating of the tubes. In order to realize these operating conditions in a distributed amplifier it is necessary to operate the amplifier intermittently so that the tubes remain in a safe operating region as far as heat dissipation is concerned. The maximum duty cycle for safe operation of the tubes is indicated in Figure 6.14.

The compromises which are involved in the final selection of the operating point may be seen from Figure 6.14. For the particular plate voltage at the Q-point

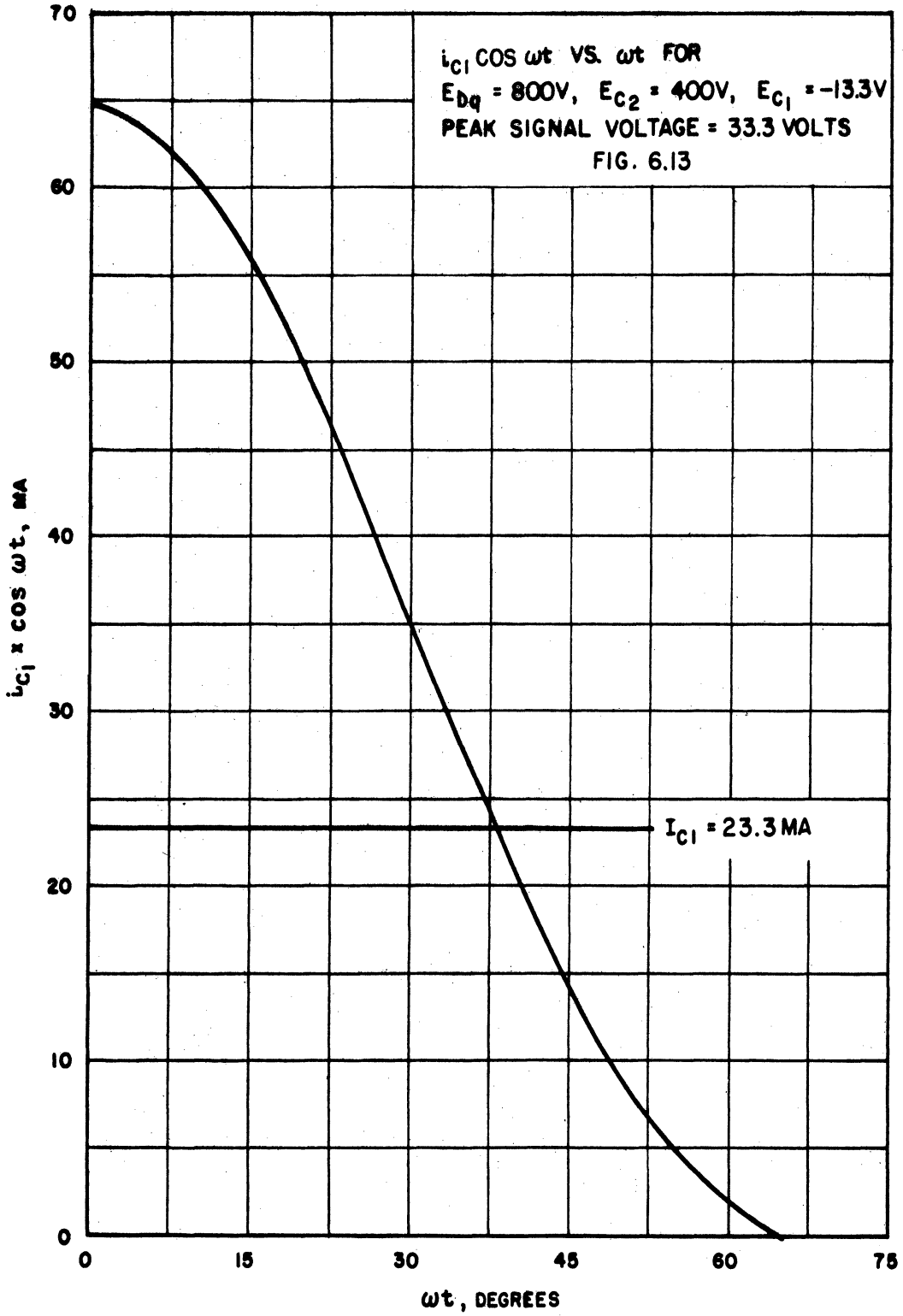


TABLE 6.2

RESULTS AND COMPUTATIONS

$$E_{bq} = 800v, E_{c2} = 400v, E_{c1} = -13.3, E_{sig} = 33.3 \text{ volts peak}$$

$$I_b = 0.88 \text{ Amps.}$$

$$I_1 = 0.75 \text{ Amps.}$$

$$I_2 = 0.06 \text{ Amps.}$$

$$I_c = 12.9 \text{ Ma.}$$

$$I_{c1} = \mathbf{23.3 \text{ Ma.}}$$

$$R_{geq} = 1.43 \text{ K}\Omega$$

$$\alpha_{odr} = 0.0175 \text{ nepers/section}$$

$$\frac{\alpha_{odr}}{\alpha_o} = 0.175$$

$$E_{bb} = 770 \text{ volts}$$

$$\text{Power Output} = 437 \text{ watts}$$

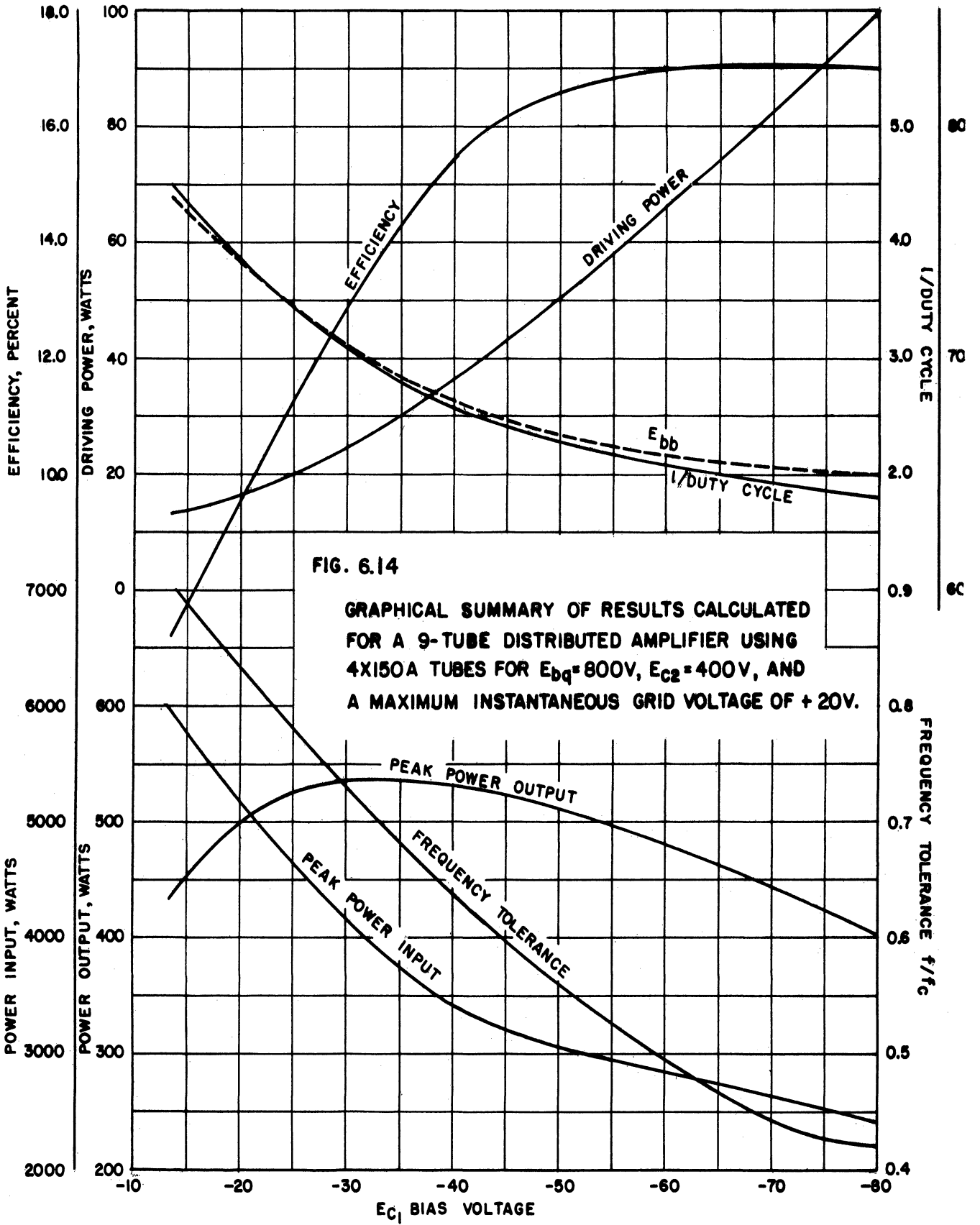
$$\text{Power Input} = 6090$$

$$\eta = 7.18\%$$

$$\text{Driving Power} = 11.1 \text{ watts}$$

$$\text{Frequency Tolerance} = 0.9$$

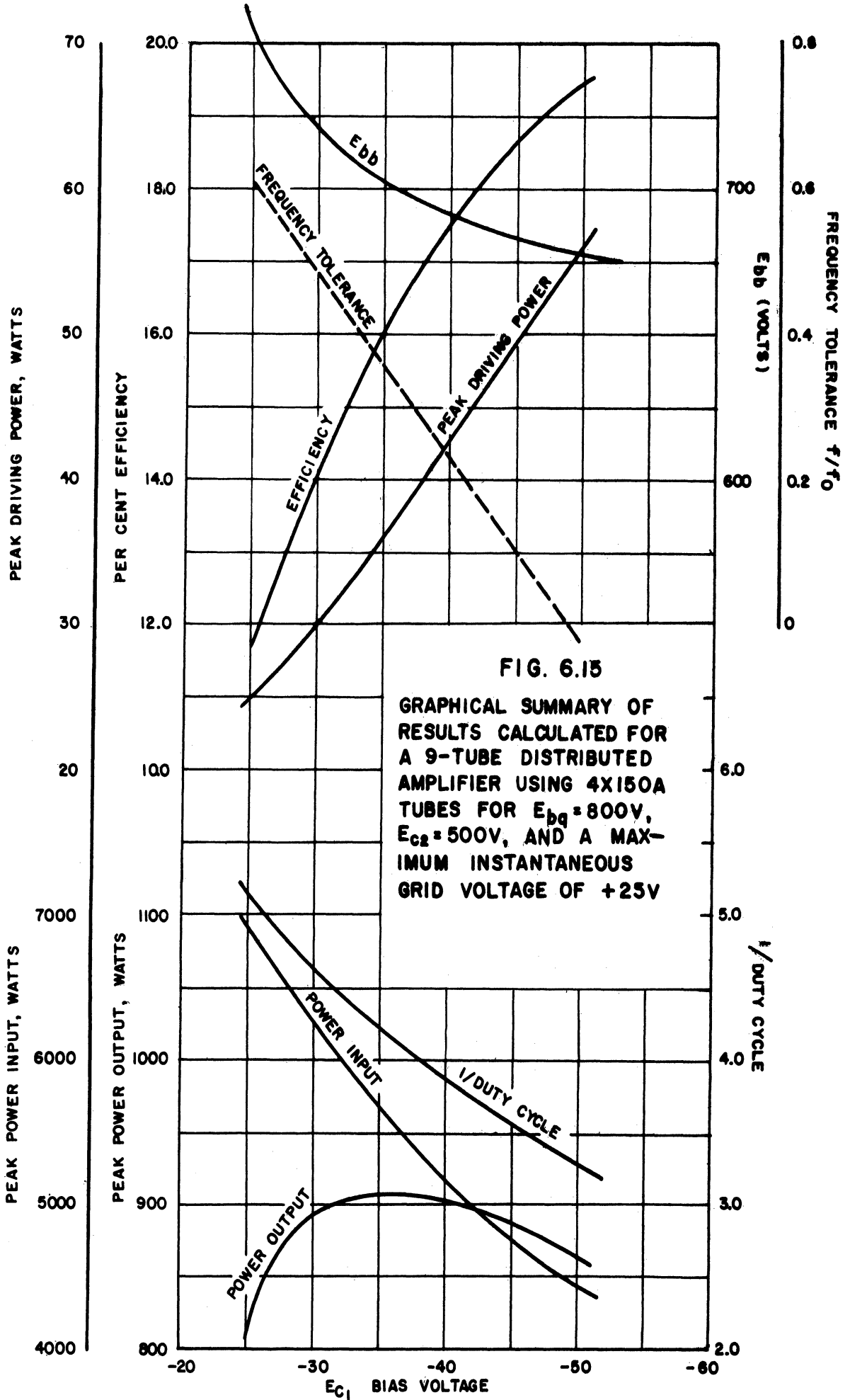
$$\text{Power Out } 2^{\text{nd}} \text{ Harmonic} = 3.3 \text{ watts}$$



and screen voltage assumed, the output power peaks at a bias voltage of about -35 volts; however, the efficiency reaches a maximum value in the neighborhood of -60 volts bias. The cost of this increase in efficiency comes from a larger driving power requirement and a decreased frequency tolerance.

Figures 6.15 through 6.19 show a graphical summary of the results of calculations for a 9-tube distributed amplifier using 4X150A tubes for several values of plate voltage at the Q-point and screen voltage. It can be seen from these figures that the peaks in the power output curves tend to increase with screen voltage; however, the efficiency reaches a maximum and decreases as the screen voltage is further increased. If curves were drawn for a constant input power, one would expect to find an optimum value of screen voltage from the standpoint of power output and efficiency. In general, the frequency tolerance decreases as the operating bias increases. The driving power increases as the bias increases.

The general trends mentioned in the preceding paragraph are useful in determining the proper direction in which to move in assuming new operating voltages on distributed amplifier tubes after an unsatisfactory design has been completed.



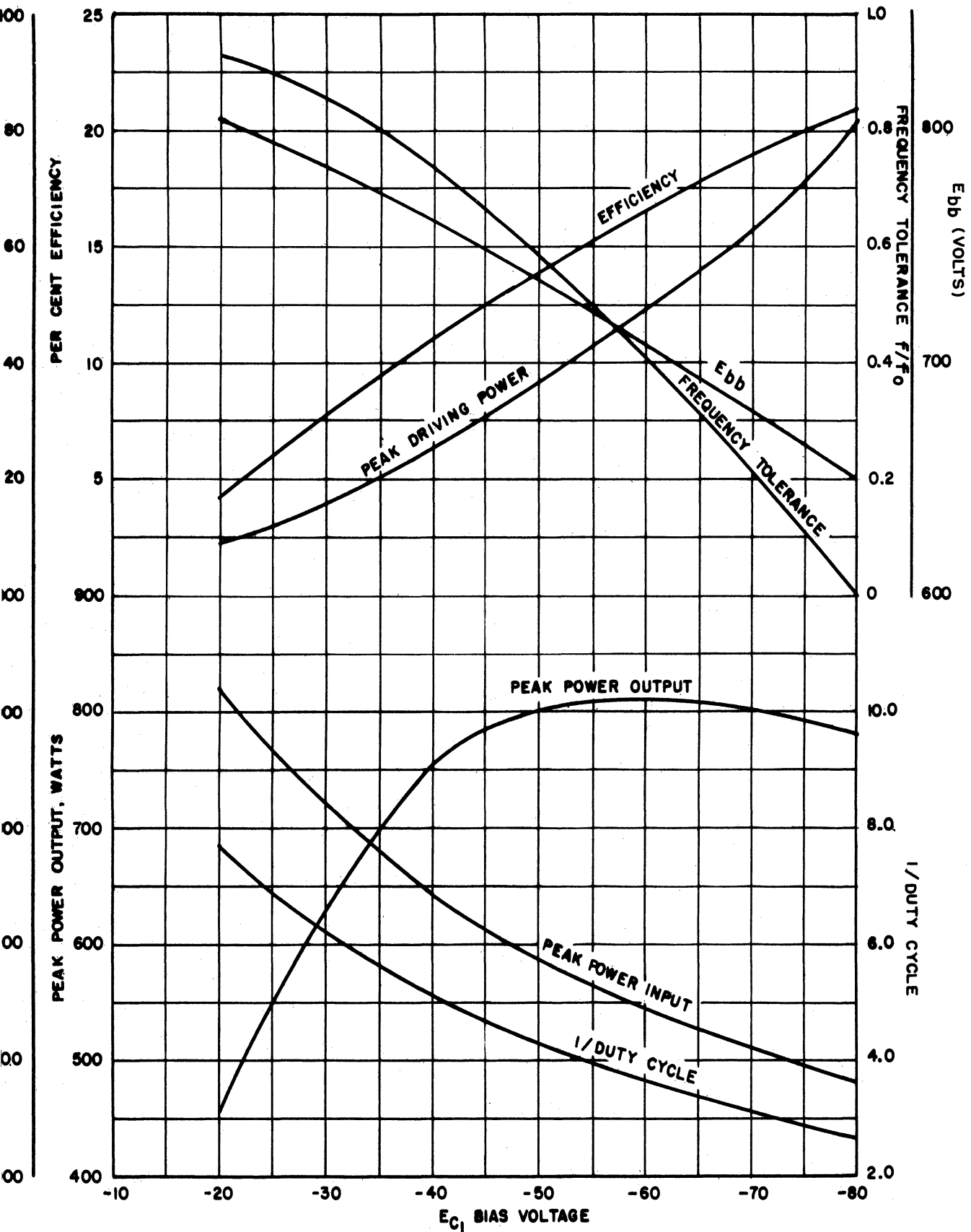


FIG 6.16
GRAPHICAL SUMMARY OF RESULTS CALCULATED
FOR A 9-TUBE DISTRIBUTED AMPLIFIER USING
4X150A TUBES FOR $E_{bq} = 800V$, $E_{c2} = 600V$, AND
A MAXIMUM INSTANTANEOUS GRID VOLTAGE OF +10V

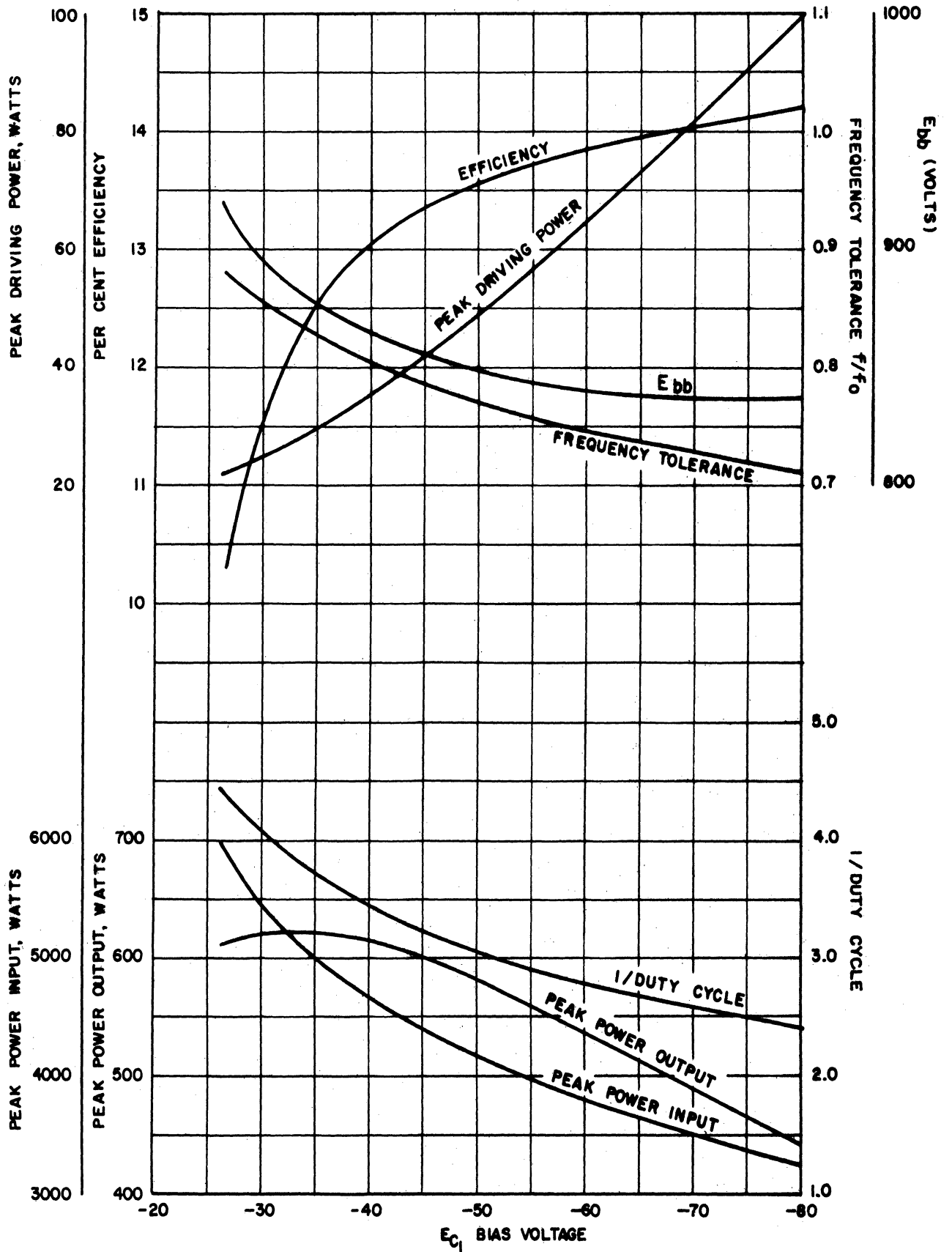


FIG. 6.17
 GRAPHICAL SUMMARY OF RESULTS CALCULATED FOR A 9-TUBE DISTRIBUTED AMPLIFIER USING 4X150A TUBES FOR $E_{bb} = 1000$ VOLTS, $E_{c2} = 400$ VOLTS, AND A MAXIMUM INSTANTANEOUS GRID VOLTAGE OF +20 VOLTS

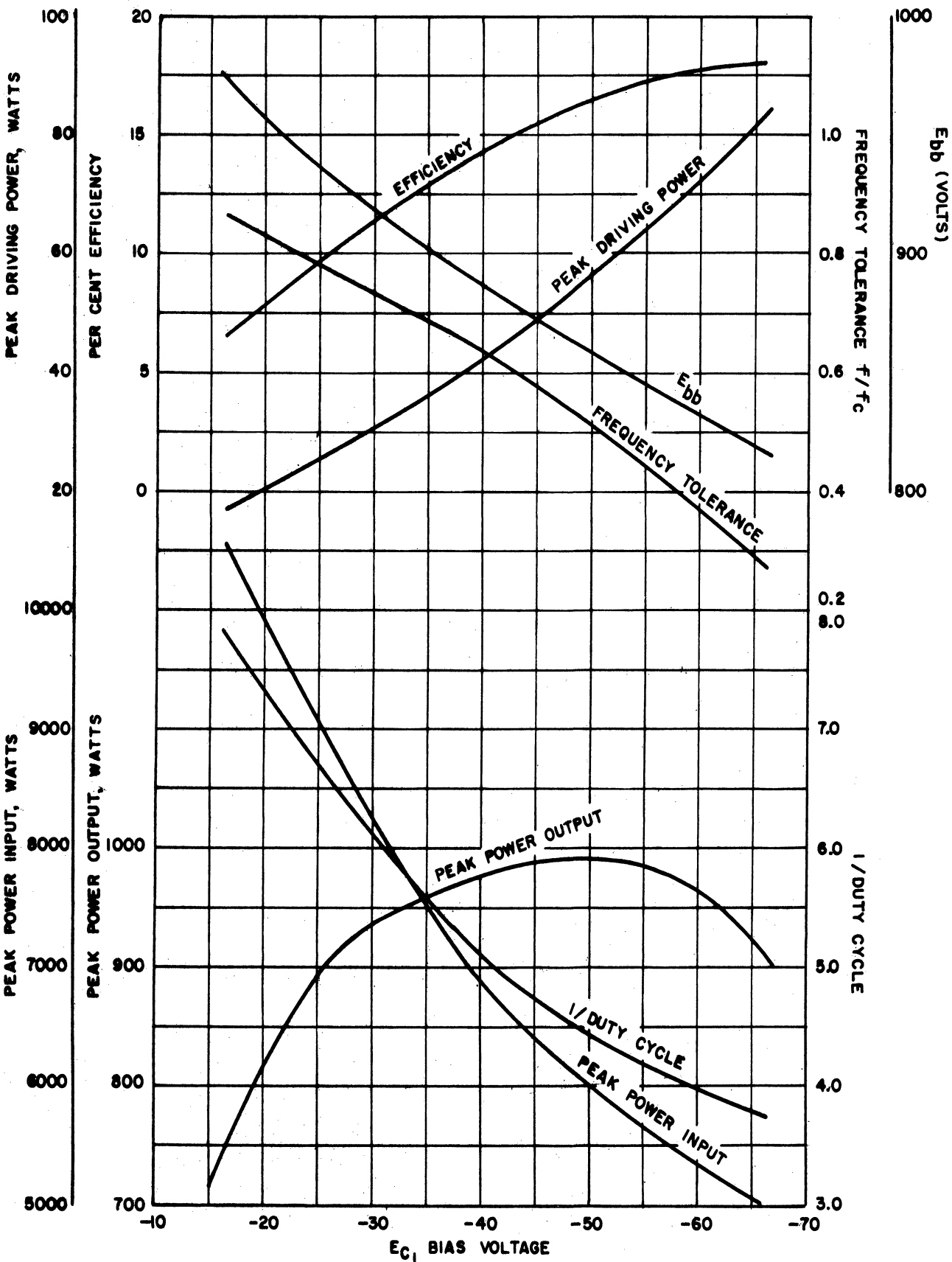


FIG. 6.18
 GRAPHICAL SUMMARY OF RESULTS CALCULATED
 FOR A 9-TUBE DISTRIBUTED AMPLIFIER USING
 4X150A TUBES FOR $E_{bq} = 1000V$, $E_{c2} = 500V$, AND
 A MAXIMUM INSTANTANEOUS GRID VOLTAGE OF +25V

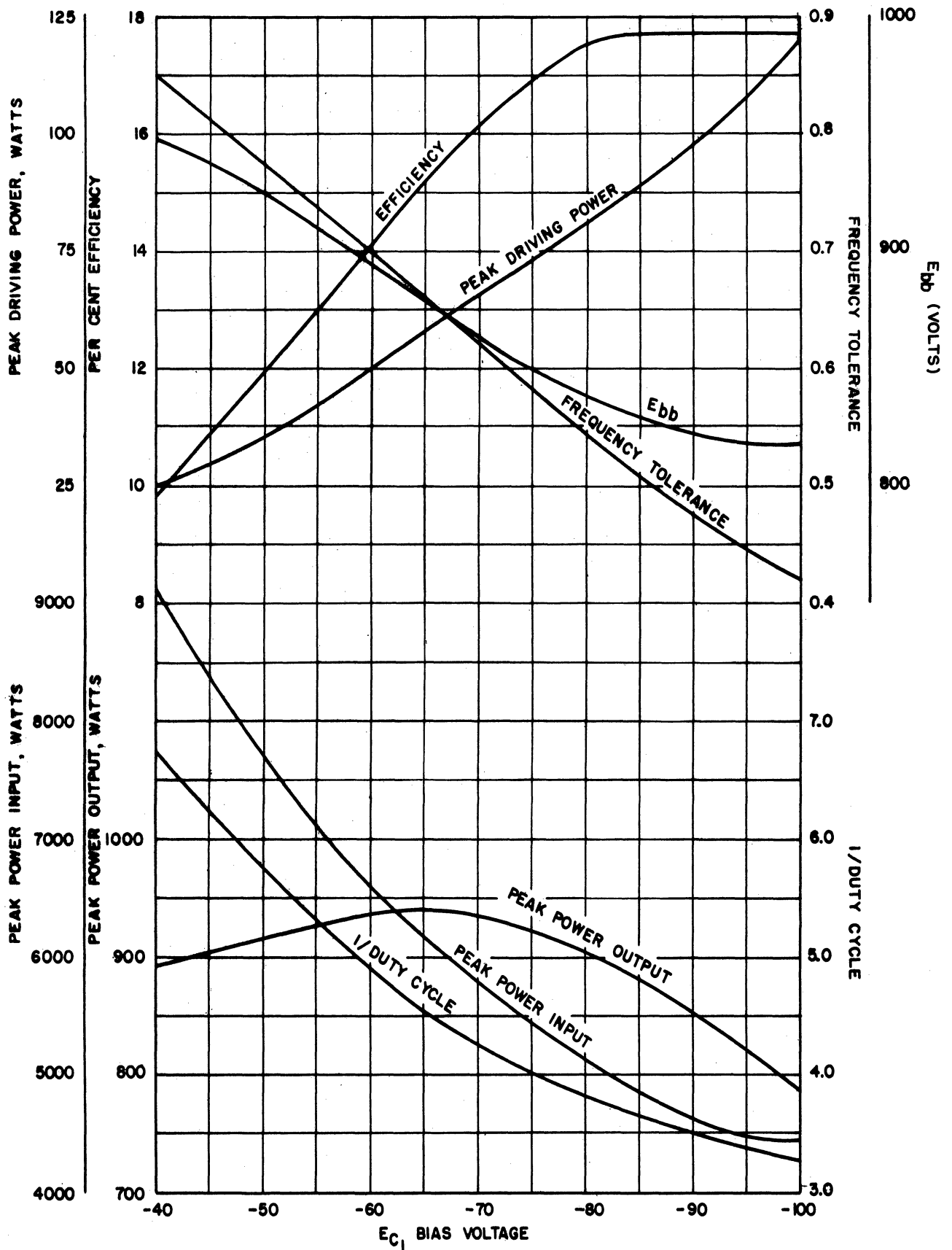


FIG. 6.19

GRAPHICAL SUMMARY OF RESULTS CALCULATED FOR A 9-TUBE DISTRIBUTED AMPLIFIER USING 4X150A TUBES FOR $E_{bq}=1000V$, $E_{c2}=600V$, AND A MAXIMUM INSTANTANEOUS GRID VOLTAGE OF +10V

CHAPTER VII. CONCLUSIONS

7.1 Introduction

In the preceding chapters the small-signal distributed amplifier equations have been modified to account for the additional complications encountered in large-signal operation. A graphical procedure for analysis of power distributed amplifiers operating in a non-linear region was also presented.

7.2 Summary of Results

1. It was shown in Chapter VI that an exact graphical analysis is possible. However, this method of analysis involves a cut-and-try procedure, which is long and tedious. If certain assumptions are made, it is possible to use an approximate graphical analysis for distributed amplifier operation.

2. It was shown in Chapter V that the maximum theoretical efficiency of a distributed amplifier operating at low frequencies is 30 percent. It was also pointed out in Chapter IV that it should be possible to increase the actual efficiency of a distributed amplifier by about 30 percent if the low-frequency operation is limited so that the plate load impedance remains low over the operating frequency range. This increase in efficiency is accomplished by operating the first few tubes at a reduced plate supply voltage.

3. The equations for a flat frequency response for a small-signal distributed amplifier are modified to account for the loss due to the positive operation of the grids. Curves showing the frequency response of a distributed amplifier for several values of $\frac{\alpha_{odr}}{\alpha_0}$ are presented in Chapter IV.

4. The frequency limitations are pointed out in Chapter III. The inductance of the grid lead is found to be the most serious limiting factor on the upper cut-off frequency as far as the small-signal response is concerned. A serious limitation on the large-signal frequency response is incurred by the on-set of clipping in the plate circuit of the last few tubes in a distributed amplifier.

7.3 Suggestions for Further Research

During the course of this investigation several problems were encountered which seem worthy of investigation.

1. Power tubes designed to operate in the VHF-UHF region are not designed for grounded cathode operation. The frequency limitation imposed by the grid lead inductance and the plate lead inductance could be essentially removed if tubes were built with two grid leads and two plate leads. One of the important parameters in the determination of the proper number of tubes to be used in a distributed amplifier is the input conductance. If the transit time and the cathode lead inductance were decreased, it would be possible to use more tubes in a distributed amplifier and, therefore, present the possibility of achieving greater output power and increased efficiency.

2. The plate circuit of a distributed amplifier is only 50 percent efficient. If a more efficient plate circuit for a distributed amplifier could be synthesized without incurring other serious defects, a large increase in the efficiency should be possible.

3. Triodes operating in a grounded-grid distributed amplifier circuit in which the impedance of the cathode line is changed at each tube in order to match all the tubes to the input seems worthy of consideration when bandwidths of the order of 500 mc are contemplated.

APPENDIX A

SERIES FOR PLATE-CATHODE VOLTAGE ON KTH TUBE OF AN N-TUBE DISTRIBUTED AMPLIFIER

From Equation 2.3 Chapter II the voltage on the plate of the kth tube

is given by

$$e_k = \sum_{j=1}^n e_{kj} \quad (A.1)$$

where:

$$e_{k1} = G_m E_{gm} \frac{Z_0}{2} \sin[\omega t - (k-1)\varphi]$$

$$\vdots$$

$$e_{kk} = G_m E_{gm} \frac{Z_0}{2} \sin[\omega t - (k-1)\varphi]$$

$$e_{k(k+1)} = G_m E_{gm} \frac{Z_0}{2} \sin[\omega t - (k-1)\varphi - 2\varphi]$$

$$\vdots$$

$$e_{kn} = G_m E_{gm} \frac{Z_0}{2} \sin[\omega t - (k-1)\varphi - 2(n-k)\varphi] \quad .$$

Therefore

$$e_k = G_m E_{gm} \frac{Z_0}{2} \left\{ k \sin[\omega t - (k-1)\varphi] \right. \\
+ \sin[\omega t - (k-1)\varphi - 2\varphi] + \sin[\omega t - (k-1)\varphi - 4\varphi] \\
+ \dots + \sin[\omega t - (k-1)\varphi - 2(n-1-k)\varphi] \\
\left. + \sin[\omega t - (k-1)\varphi - 2(n-k)\varphi] \right\} \quad (A.2)$$

Consider the series

$$S = \sin(A - 2\varphi) + \sin(A - 4\varphi) + \dots \\
+ \sin[A - 2(m-1)\varphi] + \sin[A - 2m\varphi] \quad (A.3)$$

$$\begin{aligned}
S &= \frac{e^{jA} \cdot e^{-j2\varphi} - e^{-jA} \cdot e^{j2\varphi}}{2j} + \frac{e^{jA} e^{-j4\varphi} - e^{-jA} \cdot e^{j4\varphi}}{2j} \\
&+ \dots + \frac{e^{jA} e^{-j2(m-1)\varphi} - e^{-jA} e^{j2(m-1)\varphi}}{2j} \\
&+ \frac{e^{jA} e^{-j2m\varphi} - e^{-jA} e^{j2m\varphi}}{2j} .
\end{aligned} \tag{A.4}$$

$$\begin{aligned}
&= \frac{1}{2j} \left[e^{jA} \left\{ e^{-j2\varphi} + e^{-j4\varphi} + \dots + e^{-j2(m-1)\varphi} + e^{-j2m\varphi} \right\} \right. \\
&\quad \left. - e^{-jA} \left\{ e^{j2\varphi} + e^{j4\varphi} + \dots + e^{j2(m-1)\varphi} + e^{j2m\varphi} \right\} \right]
\end{aligned} \tag{A.5}$$

$$\text{Let } S_1 = e^{-j2\varphi} + e^{-j4\varphi} + \dots + e^{-j2(m-1)\varphi} + e^{-j2m\varphi} \tag{A.6}$$

$$S_1 e^{-j2\varphi} = e^{-j4\varphi} + e^{-j6\varphi} + \dots + e^{-j2m\varphi} + e^{-j2(m+1)\varphi} \tag{A.7}$$

Subtracting Equation A.7 from A.6

$$S_1(1 - e^{-j2\varphi}) = e^{-j2\varphi} - e^{-j2(m+1)\varphi} \tag{A.8}$$

or

$$S_1 = e^{-j2\varphi} \frac{1 - e^{-j2m\varphi}}{1 - e^{-j2\varphi}} \tag{A.9}$$

Similarly if

$$S_2 = e^{j2\varphi} + e^{j4\varphi} + \dots + e^{j2(m-1)\varphi} + e^{j2m\varphi} , \tag{A.10}$$

then

$$S_2 = e^{j2\varphi} \frac{1 - e^{j2m\varphi}}{1 - e^{j2\varphi}} . \tag{A.11}$$

Equation A.5 can be written as

$$\begin{aligned}
S &= \frac{1}{2j} \left[e^{jA} e^{-j2\varphi} \frac{1 - e^{-j2m\varphi}}{1 - e^{-j2\varphi}} \right. \\
&\quad \left. - e^{-jA} e^{j2\varphi} \frac{1 - e^{j2m\varphi}}{1 - e^{j2\varphi}} \right]
\end{aligned} \tag{A.12}$$

$$\frac{1 - e^{-j2m\varphi}}{1 - e^{-j2\varphi}} \text{ can be written as}$$

$$\frac{e^{-jm\varphi} (e^{jm\varphi} - e^{-jm\varphi})}{e^{-j\varphi} (e^{j\varphi} - e^{-j\varphi})} = e^{-j(m-1)\varphi} \frac{\sin m\varphi}{\sin \varphi} \quad (\text{A.13})$$

Similarly

$$\frac{1 - e^{j2m\varphi}}{1 - e^{j2\varphi}} = \frac{e^{jm\varphi} (e^{-jm\varphi} - e^{jm\varphi})}{e^{j\varphi} (e^{-j\varphi} - e^{j\varphi})} \quad (\text{A.14})$$

$$= e^{j(m-1)\varphi} \frac{\sin m\varphi}{\sin \varphi}$$

So that Equation A.12 can be written as

$$S = \frac{1}{2j} \left[e^{j[A - 2\varphi - (m-1)\varphi]} \frac{\sin m\varphi}{\sin \varphi} - e^{-j[A - 2\varphi - (m-1)\varphi]} \frac{\sin m\varphi}{\sin \varphi} \right] \quad (\text{A.15})$$

Now S can be written as

$$S = \frac{\sin m\varphi}{\sin \varphi} \sin[A - 2\varphi - (m-1)\varphi]$$

$$= \frac{\sin m\varphi}{\sin \varphi} \sin[A - (m+1)\varphi] \quad (\text{A.16})$$

Identifying the terms of this series with those in Equation A.2, A.2 can be written as

$$e_k = G_m E_{gm} \frac{Z_0}{2} \left\{ k \sin[\omega t - (k-1)\varphi] \right.$$

$$\left. + \frac{\sin(n-k)\varphi}{\sin \varphi} \sin[\omega t - (k-1)\varphi - (n-k+1)\varphi] \right\} \quad (\text{A.17})$$

APPENDIX B

LOW-FREQUENCY DISTRIBUTED AMPLIFIER USING 807 TUBES

The following values were picked for convenience.

$$n = 6$$

$$f_c = 15 \text{ kc}$$

$$C_p = .04 \text{ } \mu\text{f}$$

$$C_g = .044 \text{ } \mu\text{f}$$

$$R_p = \frac{2}{\omega_c C_p} = \frac{2}{2\pi \times 15 \times 10^3 \times .044 \times 10^{-6}} = 530 \text{ } \Omega$$

$$L_p = 2 \frac{R_p}{\omega_c} = 2 \times \frac{530}{2\pi \times 15 \times 10^3} = 11.25 \text{ mh}$$

$$R_g = \frac{2}{\omega_c C_g} = \frac{2}{2\pi \times 15 \times 10^3 \times .044 \times 10^{-6}} = 482 \text{ } \Omega$$

$$L_g = 2 \frac{R_g}{\omega_c} = 2 \times \frac{482}{2\pi \times 15 \times 10^3} = 10.25 \text{ mh.}$$

The schematic diagram is shown in Figure B.1. The 10 ohm resistors in the plate of each tube are used in order to be able to measure the plate current on an oscilloscope.

Table B.1 shows the experimental data obtained for the plate load impedance for the first tube in the amplifier. The method of data reduction is also shown in Table B.1. The absolute value of the plate load impedance of the first tube is normalized to one-half the mid-shunt impedance of the constant-k plate line. In order to plot the experimental points on Figure 2.2, the phase shift per section of the artificial transmission lines was calculated from the ratio of f/f_c .

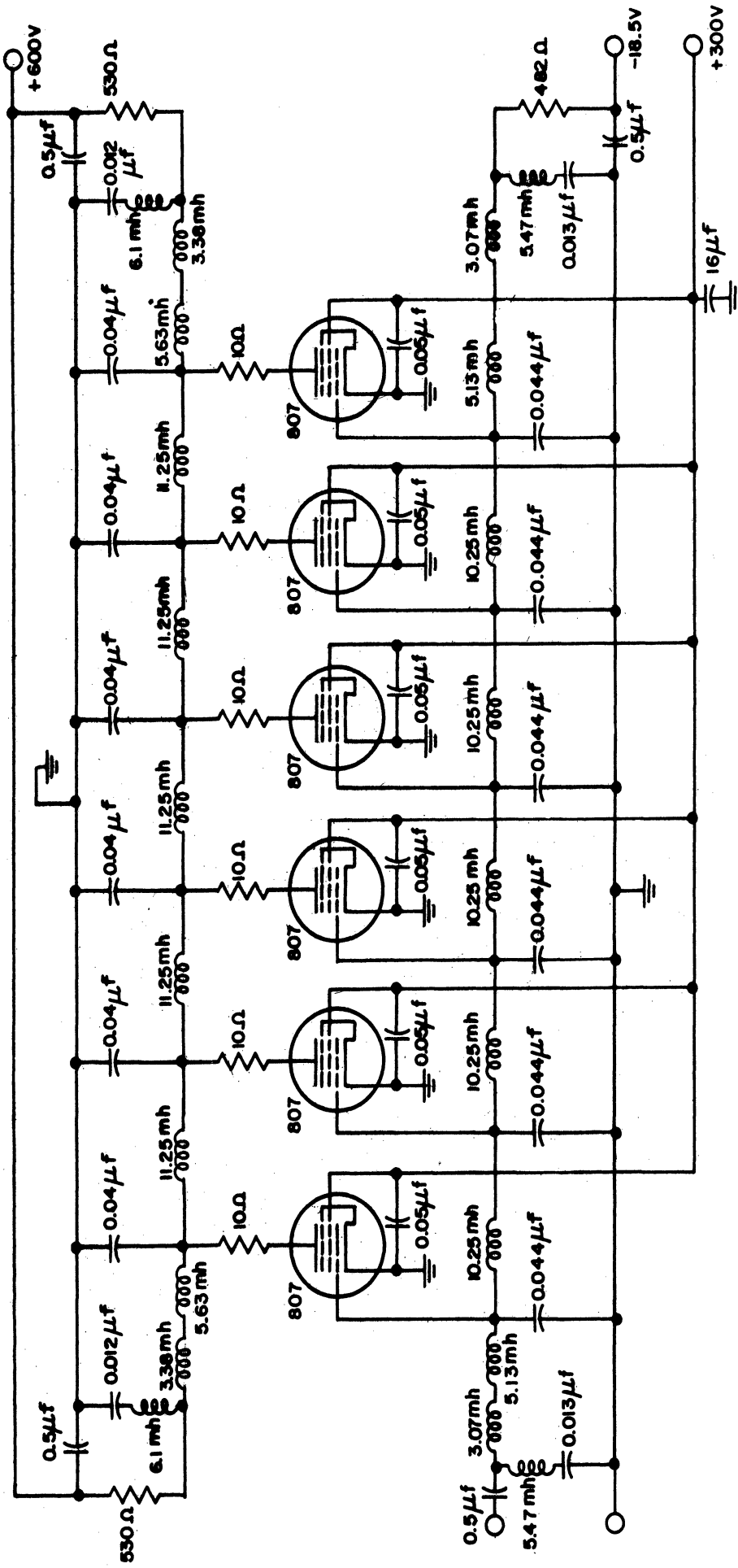


FIG. B.1.1. SCHEMATIC DIAGRAM FOR 15kc DISTRIBUTED AMPLIFIER.

TABLE B.1MEASUREMENTS ON TUBE NUMBER 1 OF 15 KC DISTRIBUTED AMPLIFIER

freq.(kc)	E(VOLTS)	I ₁ (ma)	Z	f/fc	∅ DEGREES	Z π/R	Z/R/2	Z/R/2 × R/Zπ
1	13	8.5	1530	.0667	7.5	1.002	5.74	5.73
2	11	9	1220	.1335	13.5	1.004	4.57	4.54
3	5.5	9.5	580	.2	23	1.02	2.17	2.13
3.9	0.5	9.5	52	.26	30	1.028	.195	.19
4	1	10	100	.266	30.5	1.03	.375	.364
5	5.5	10	550	.333	38.5	1.06	2.06	1.945
5.5	5.5	9.5	580	.367	43	1.075	2.17	2.02
6	5.5	10	550	.4	47	1.09	2.06	1.89
7	2.7	9.5	284	.467	55.5	1.125	1.065	.947
7.5	1	9.5	105	.5	60	1.15	.394	.343
8	2.5	10	250	.533	64	1.175	.938	.798
8.5	4	10	400	.566	69	1.21	1.5	1.24
9	5	10.7	467	.6	74	1.25	1.75	1.4
10	4.5	10.5	428	.667	83.5	1.35	1.605	1.19
10.7	0	10.5	0	-----	-----	-----	0	0
11	2.5	11.5	217	.734	94	1.49	.815	.547
11.5	5.5	12	458	.767	100	1.515	1.72	1.08
12	8	12	666	.8	106	1.67	2.5	1.5
12.5	8	11.5	695	.834	113.5	1.82	2.6	1.43
13	4	11.5	348	.867	121	1.99	1.305	.657
13.2	1.8	11.5	156	.88	123	2.07	.585	.282
13.5	3	12.5	240	.9	128.5	2.3	.9	.39
14	12	13	924	.934	134	2.77	3.46	1.25
14.5	5	13	385	.967	152	3.75	1.445	.386

APPENDIX C

PLATE LOAD IMPEDANCE FOR PAIRED-PLATE

The circuit for paired-plate connection is shown in Figure C.1.

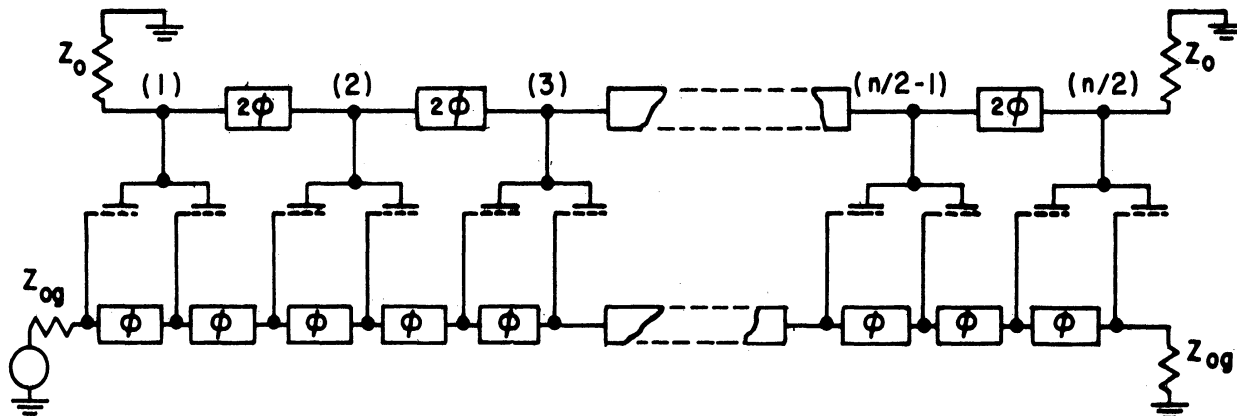


FIG. C.1. BLOCK DIAGRAM OF PAIRED-PLATE DISTRIBUTED AMPLIFIER.

The current supplied to the line by any pair of tubes is composed of

components which are equal in magnitude but differ in phase by φ .

$$\begin{aligned}
 I_1 &= 2|I_p| \cos \frac{\varphi}{2} \left[-\frac{\varphi}{2} \right] \\
 I_2 &= 2|I_p| \cos \frac{\varphi}{2} \left[-\frac{\varphi}{2} - 2\varphi \right] \\
 I_3 &= 2|I_p| \cos \frac{\varphi}{2} \left[-\frac{\varphi}{2} - 4\varphi \right] \\
 &\vdots \\
 I_k &= 2|I_p| \cos \frac{\varphi}{2} \left[-\frac{\varphi}{2} - (2k-2)\varphi \right] \\
 &\vdots \\
 I_{\frac{n}{2}} &= 2|I_p| \cos \frac{\varphi}{2} \left[-\frac{\varphi}{2} - (n-2)\varphi \right]
 \end{aligned}$$

Voltage on kth Pair Plates

$$\begin{aligned}
 E_{k1} &= |I_p| \cos \frac{\phi}{2} Z_0 \left[-\frac{\phi}{2} - (2k-2)\phi \right] \\
 E_{kk} &= |I_p| \cos \frac{\phi}{2} Z_0 \left[-\frac{\phi}{2} - (2k-2)\phi \right] \\
 E_{k(k+1)} &= |I_p| \cos \frac{\phi}{2} Z_0 \left[-\frac{\phi}{2} - (2k)\phi - 2\phi \right] \\
 E_{k(k+2)} &= |I_p| \cos \frac{\phi}{2} Z_0 \left[-\frac{\phi}{2} - (2k+2)\phi - 4\phi \right] \\
 E_{kn} &= |I_p| \cos \frac{\phi}{2} Z_0 \left[-\frac{\phi}{2} - (n-2)\phi - \left(\frac{n}{2} - k\right)2\phi \right]
 \end{aligned}$$

Now

$$\begin{aligned}
 E_k &= \sum_{i=1}^{n/2} E_{ki} \\
 &= k |I_p| \cos \frac{\phi}{2} Z_0 \left[-\frac{\phi}{2} - (2k-2)\phi \right] \\
 &\quad + |I_p| \cos \frac{\phi}{2} Z_0 \left\{ 1 \left[-\frac{\phi}{2} - (2k+2)\phi \right] \right. \\
 &\quad + 1 \left[-\frac{\phi}{2} - (2k+6)\phi \right] \\
 &\quad \quad \quad \vdots \\
 &\quad \left. + 1 \left[-\frac{\phi}{2} - (n-2)\phi - (n-2k)\phi \right] \right\}
 \end{aligned}$$

Consider the series in brackets.

$$\begin{aligned}
 &1 \left[-\frac{\phi}{2} - (2k-2)\phi - 4\phi \right] \\
 &+ 1 \left[-\frac{\phi}{2} - (2k-2)\phi - 8\phi \right] \\
 &\quad \quad \quad \vdots \\
 &+ 1 \left[-\frac{\phi}{2} - (2k-2)\phi - 2(n-2k)\phi \right] \\
 &= e^{-j\left[\frac{\phi}{2} + (2k-2)\phi\right]} \left[e^{-j4\phi} + e^{-j8\phi} + \dots + e^{-j2(n-2k)\phi} \right]
 \end{aligned}$$

Let

$$S = e^{-j4\phi} + e^{-j8\phi} + \dots + e^{-j2(n-2k)\phi},$$

hen

$$S e^{-j4\varphi} = -j8\varphi + \dots + e^{-j2(n-2k)\varphi} + e^{-j[2(n-2k)\varphi+4\varphi]} .$$

$$\begin{aligned} S &= \frac{e^{-j4\varphi} - e^{-j[2(n-2k)\varphi+4\varphi]}}{1 - e^{-j4\varphi}} \\ &= \frac{e^{-j4\varphi} e^{-j(n-2k)\varphi} [\sin (n-2k)\varphi]}{e^{-j2\varphi} [\sin 2\varphi]} \\ &= e^{-j(n-2k+2)\varphi} \frac{\sin [(n-2k)\varphi]}{\sin 2\varphi} \end{aligned}$$

$$S e^{-j\left[\frac{\varphi}{2} + (2k-2)\varphi\right]} = e^{-j\left(n\varphi + \frac{\varphi}{2}\right)} \frac{\sin [(n-2k)\varphi]}{\sin 2\varphi}$$

$$\begin{aligned} E_k &= |I_p| \cos \frac{\varphi}{2} Z_o \left[k e^{-j\left[\frac{\varphi}{2} + (2k-2)\varphi\right]} \right. \\ &\quad \left. + \frac{\sin [(n-2k)\varphi]}{\sin 2\varphi} e^{-j\left(n\varphi + \frac{\varphi}{2}\right)} \right] \end{aligned}$$

$$I_k = 2|I_p| \cos \frac{\varphi}{2} \left[-\frac{\varphi}{2} - (2k-2)\varphi \right]$$

$$Z_k = \frac{E_k}{I_k} = \frac{Z_o}{2} \left[k + \frac{\sin [(n-2k)\varphi]}{\sin 2\varphi} e^{-j[n-2k+2]\varphi} \right] .$$

INPUT RESISTANCE OF A VACUUM TUBE DUE TO CATHODE LEAD INDUCTANCE

Figure D.1 shows the equivalent circuit used for the determination of input resistance.

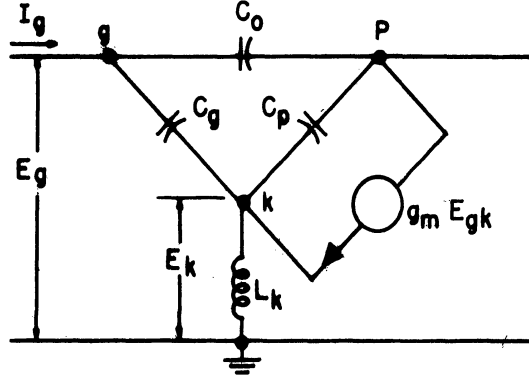


FIG. D. 1. EQUIVALENT CIRCUIT OF A TUBE USED FOR THE DETERMINATION OF INPUT CONDUCTANCE.

The node equations for this circuit are shown in Equation D.1 and D.2

$$I_g = E_g [j\omega(C_o + C_g)] - E_k [j\omega C_g] \quad (D.1)$$

$$g_m E_{gk} = -E_g [j\omega C_g] + E_k \left[j\omega(C_g + C_p) + \frac{1}{j\omega L_k} \right]. \quad (D.2)$$

But $E_{gk} = E_g - E_k$. Equation D.2 can be written as shown in Equation D.3.

$$0 = -E_g \left[g_m + j\omega C_g \right] + E_k \left[g_m + j\omega(C_g + C_p) + \frac{1}{j\omega L_k} \right] \quad (D.3)$$

Equations D.1 and D.3 can be solved for E_g as shown in Equation D.4

$$E_g = \frac{I_g \left[g_m + j\omega(C_g + C_p) + \frac{1}{j\omega L_k} \right]}{\left[j\omega(C_o + C_g) \right] \left[g_m + j\omega(C_g + C_p) + \frac{1}{j\omega L_k} \right] - \left[j\omega C_g \right] \left[g_m + j\omega C_g \right]} \quad (D.4)$$

The input admittance is given by the ratio of I_g to E_g or

$$Y_{in} = \frac{[j\omega(C_o + C_g)] \left[g_m + j\omega(C_g + C_p) + \frac{1}{j\omega L_k} \right] - [j\omega C_g] [g_m + j\omega C_g]}{g_m + j\omega(C_g + C_p) + \frac{1}{j\omega L_k}}$$

The real part of Equation D.5 can be written as shown in Equation D.6

$$G_{in} = g_m \omega^2 L_k C_g \frac{[1 - \omega^2 L_k C_p]}{g_m^2 \omega^2 L_k^2 + [\omega^2 (C_g + C_p) L_k - 1]^2} \quad (D.6)$$

APPENDIX E

DETERMINATION OF PLATE LOAD IMPEDANCE WITH ATTENUATION IN THE GRID LINE

The grid voltages on the various tubes are assumed to be of the form

$$\begin{aligned}
 E_1 &= E_g \angle 0^\circ \\
 E_2 &= E_g e^{-\alpha} \angle -\phi \\
 E_3 &= E_g e^{-2\alpha} \angle -2\phi \\
 &\vdots \\
 &\vdots \\
 E_n &= E_g e^{-(n-1)\alpha} \angle -(n-1)\phi
 \end{aligned}
 \tag{E.1}$$

These grid voltages will result in the following fundamental component of plate current

$$\begin{aligned}
 I_1 &= E_g G_m \angle 0^\circ \\
 I_2 &= E_g e^{-\alpha} G_m \angle -\phi \\
 &\vdots \\
 &\vdots \\
 I_n &= E_g e^{-(n-1)\alpha} G_m \angle -(n-1)\phi
 \end{aligned}
 \tag{E.2}$$

The voltage on the plate of the k^{th} tube can be written as

$$E_k = \sum_{j=1}^n E_{k_j}
 \tag{E.3}$$

where E_{k_j} = the voltage that appears on the plate of the k^{th} tube with only the j^{th} tube operating.

These voltages may be written as shown in Equation E.4.

$$\begin{aligned}
E_{k1} &= G_m \frac{Z_o}{2} E_g \left| \underline{-(k-1)\varphi} \right. \\
E_{k2} &= G_m \frac{Z_o}{2} E_g e^{-\alpha} \left| \underline{-(k-1)\varphi} \right. \\
&\vdots \\
&\vdots \\
E_{kk} &= G_m \frac{Z_o}{2} E_g e^{-(k-1)\alpha} \left| \underline{-(k-1)\varphi} \right. \\
&\vdots \\
E_{k(k+1)} &= G_m \frac{Z_o}{2} E_g e^{-k\alpha} \left| \underline{-(k-1)\varphi-2\varphi} \right. \\
&\vdots \\
&\vdots \\
E_{kn} &= G_m \frac{Z_o}{2} E_g e^{-(n-1)\alpha} \left| \underline{-(k-1)\varphi-2(n-k)\varphi} \right.
\end{aligned} \tag{E.4}$$

Substituting Equation E.4 into E.3 the voltage on the k^{th} tube is

$$\begin{aligned}
E_k &= G_m \frac{Z_o}{2} E_g e^{-j(k-1)\varphi} \left[1 + e^{-\alpha} + \dots + e^{-(k-1)\alpha} \right. \\
&\quad \left. + e^{-k\alpha} e^{-j2\varphi} + e^{-(k+1)\alpha} e^{-j4\varphi} + \dots \right. \\
&\quad \left. + e^{-(n-1)\alpha} e^{-j2(n-k)\varphi} \right]
\end{aligned} \tag{E.5}$$

Let S_1 indicate the series

$$S_1 = 1 + e^{-\alpha} + \dots + e^{-(k-1)\alpha} \tag{E.6}$$

$$S_1 e^{-\alpha} = e^{-\alpha} + e^{-2\alpha} + \dots + e^{-(k-1)\alpha} + e^{-k\alpha} \tag{E.7}$$

If Equation E.7 is subtracted from Equation E.6 the result is

$$S_1(1 - e^{-\alpha}) = 1 - e^{-k\alpha} \tag{E.8}$$

or

$$\begin{aligned}
S_1 &= \frac{1 - e^{-k\alpha}}{1 - e^{-\alpha}} = \frac{e^{-k\frac{\alpha}{2}}}{e^{-\frac{\alpha}{2}}} \frac{e^{+\frac{k\alpha}{2}} - e^{-\frac{k\alpha}{2}}}{e^{+\frac{\alpha}{2}} - e^{-\frac{\alpha}{2}}} \\
&= e^{-(k-1)\frac{\alpha}{2}} \frac{\sinh \frac{k\alpha}{2}}{\sinh \frac{\alpha}{2}}
\end{aligned} \tag{E.9}$$

Let S_2 indicate the series

$$S_2 = e^{-k\alpha} e^{-j2\varphi} \left[1 + e^{-\alpha} e^{-j2\varphi} + \dots + e^{-(n-k-1)\alpha} e^{-j2(n-k-1)\varphi} \right] \tag{E.10}$$

$$S_2 e^{-\alpha} e^{-j2\varphi} = e^{-k\alpha} e^{-j2\varphi} \left[e^{-\alpha} e^{-j2\varphi} + \dots + e^{-(n-k-1)\alpha} e^{-j2(n-k-1)\varphi} + e^{-(n-k)\alpha} e^{-j2(n-k)\varphi} \right] \quad (\text{E.11})$$

Subtracting Equation E.11 from Equation E.10 we have

$$S_2 (1 - e^{-\alpha} e^{-j2\varphi}) = e^{-k\alpha} e^{-j2\varphi} \left[1 - e^{-(n-k)\alpha} e^{-j2(n-k)\varphi} \right] \quad (\text{E.12})$$

or

$$S_2 = e^{-k\alpha - j2\varphi} \frac{1 - e^{-(n-k)\alpha - j2(n-k)\varphi}}{1 - e^{-\alpha - j2\varphi}} \quad (\text{E.13})$$

$$= \frac{e^{-k\alpha - j2\varphi} e^{-(n-k)\frac{\alpha}{2} - j(n-k)\varphi}}{e^{-\frac{\alpha}{2} - j\varphi}} \frac{\sinh \left[(n-k)\frac{\alpha}{2} + j(n-k)\varphi \right]}{\sinh \left[\frac{\alpha}{2} + j\varphi \right]}$$

$$= e^{-(n+k-1)\frac{\alpha}{2} - j(n+1)\varphi} \frac{\sinh \left[(n-k)\frac{\alpha}{2} + j(n-k)\varphi \right]}{\sinh \left[\frac{\alpha}{2} + j\varphi \right]} \quad (\text{E.14})$$

Substituting Equations E.14 and E.9 into Equation E.5 the plate voltage on the k^{th} tube becomes

$$E_k = G_m \frac{Z_0}{2} E_g e^{-j(k-1)\varphi} \times$$

$$\left[e^{-(k-1)\frac{\alpha}{2}} \frac{\sinh \frac{k\alpha}{2}}{\sinh \frac{\alpha}{2}} + e^{-(n+k-1)\frac{\alpha}{2} - j(n-k+1)\varphi} \frac{\sinh \left[(n-k)\frac{\alpha}{2} + j(n-k)\varphi \right]}{\sinh \left[\frac{\alpha}{2} + j\varphi \right]} \right] \quad (\text{E.15})$$

The plate load impedance is given by the ratio of the plate voltage to

the plate current or

$$Z_k = \frac{E_k}{I_k} = \frac{Z_0}{2} e^{(k-1)\alpha} \left[e^{-(k-1)\frac{\alpha}{2}} \frac{\sinh \frac{k\alpha}{2}}{\sinh \frac{\alpha}{2}} + e^{-(n+k-1)\frac{\alpha}{2} - j(n-k+1)\varphi} \frac{\sinh \left[(n-k)\frac{\alpha}{2} + j(n-k)\varphi \right]}{\sinh \left[\frac{\alpha}{2} + j\varphi \right]} \right]$$

or

$$Z_k = \frac{Z_0}{2} \left[e^{(k-1)\frac{\alpha}{2}} \frac{\sinh \frac{k\alpha}{2}}{\sinh \frac{\alpha}{2}} + e^{-(n-k+1)\frac{\alpha}{2} - j(n-k+1)\varphi} \frac{\sinh \left[(n-k)\frac{\alpha}{2} + j(n-k)\varphi \right]}{\sinh \left[\frac{\alpha}{2} + j\varphi \right]} \right]$$

APPENDIX F

GRAPHICAL CALCULATION OF THE OPERATION OF A 9-TUBE DISTRIBUTED AMPLIFIER USING 4X150A TUBES

Figure F.1 shows the instantaneous value of plate current for a nine-tube distributed amplifier operating at a plate voltage at the Q point of 800 volts, a screen grid voltage of 400 volts, a control grid bias of -20 volts, and with a peak signal voltage of 40 volts. Figures F.2 through F.5 are for the same operating condition. Table F.1 summarizes the results of the distributed amplifier operating under the above conditions.

The rest of the figures in this appendix repeat the calculations mentioned above for several different operating conditions on the amplifier.

TABLE F.1

RESULTS AND COMPUTATIONS

$$E_{bq} = 800v, E_{c2} = 400v, E_{c1} = -20 v, E_{sig} = 40 v \text{ peak}$$

$$I_b = 0.76 \text{ amps.}$$

$$I_1 = 0.77 \text{ amps.}$$

$$I_2 = 0.10 \text{ amps.}$$

$$I_c = 11.7 \text{ ma.}$$

$$I_{c1} = 21.2 \text{ ma.}$$

$$R_{geq} = 1.89 \text{ K } \Omega$$

$$\alpha_{odr} = 0.01325 \text{ nepers/section}$$

$$\frac{\alpha_{odr}}{\alpha_o} = 0.133$$

$$\alpha_o$$

$$E_{bb} = 740 \text{ volts}$$

$$\text{Power Output} = 480 \text{ watts}$$

$$\text{Power Input} = 5060 \text{ watts}$$

$$\eta = 9.5\%$$

$$\text{Driving Power} = 16 \text{ watts}$$

$$\text{Frequency Tolerance} = 0.85$$

$$\text{Power Out } 2^{\text{nd}} \text{ Harmonic} = 9.1 \text{ watts}$$

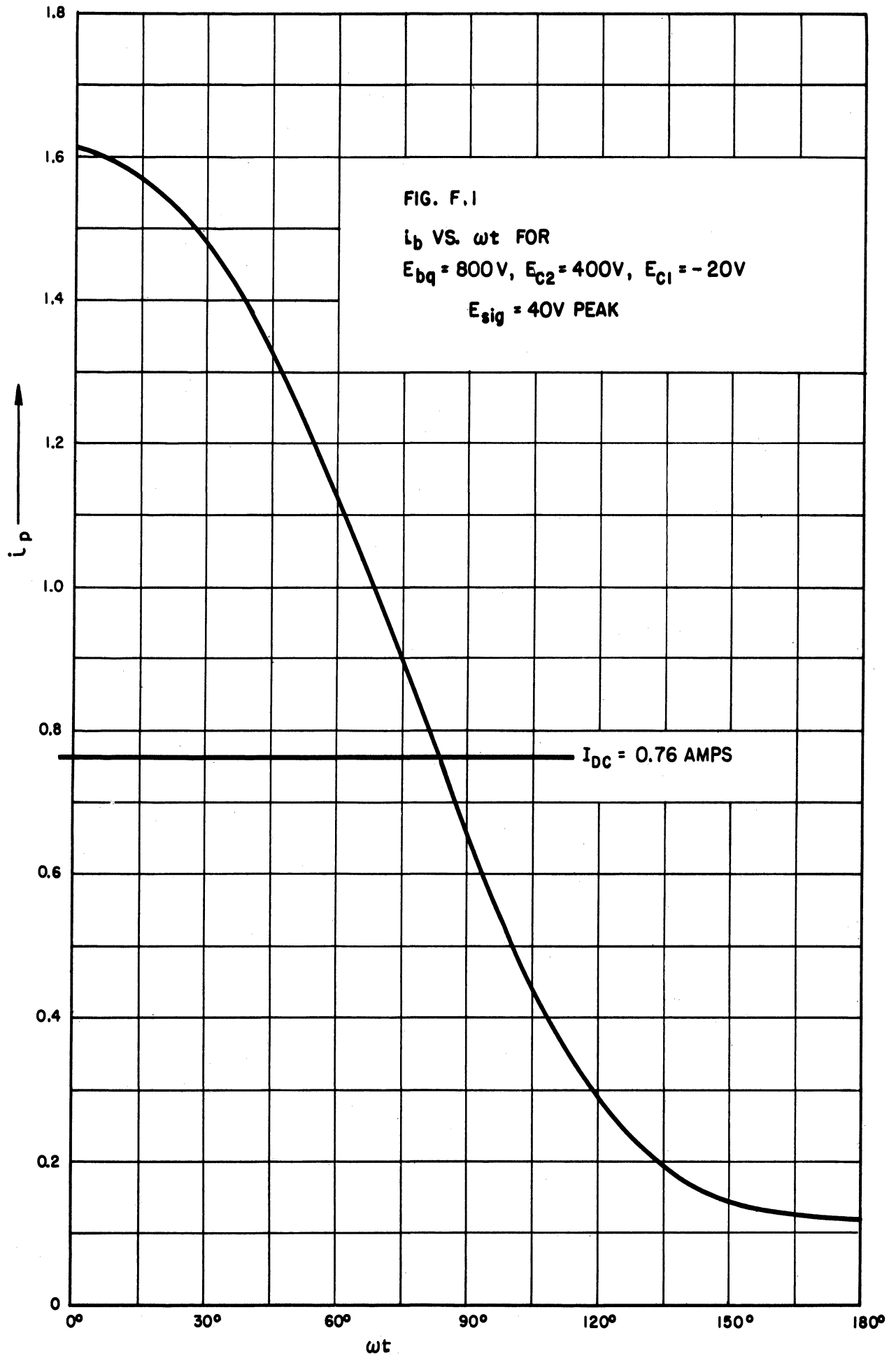
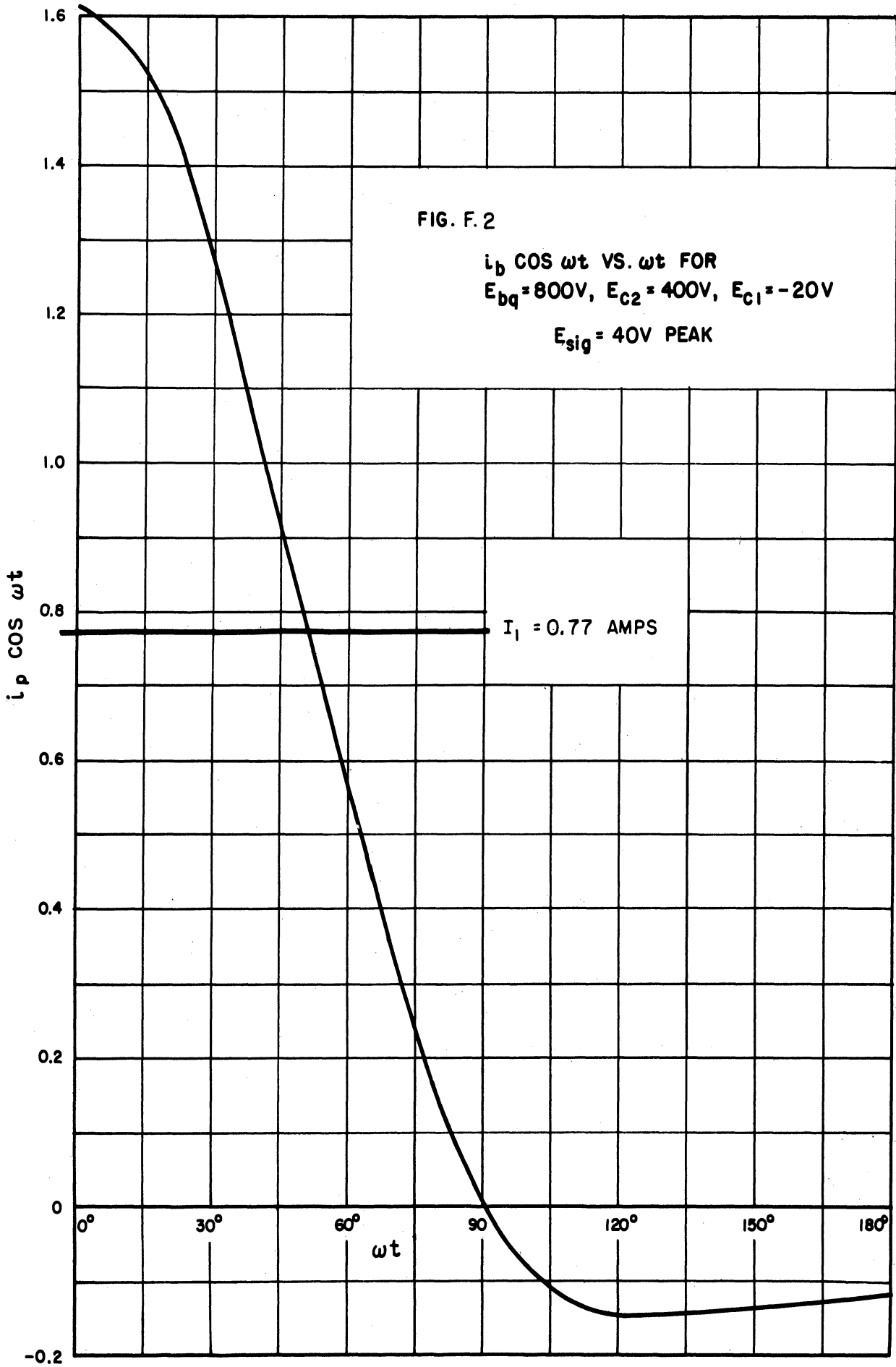


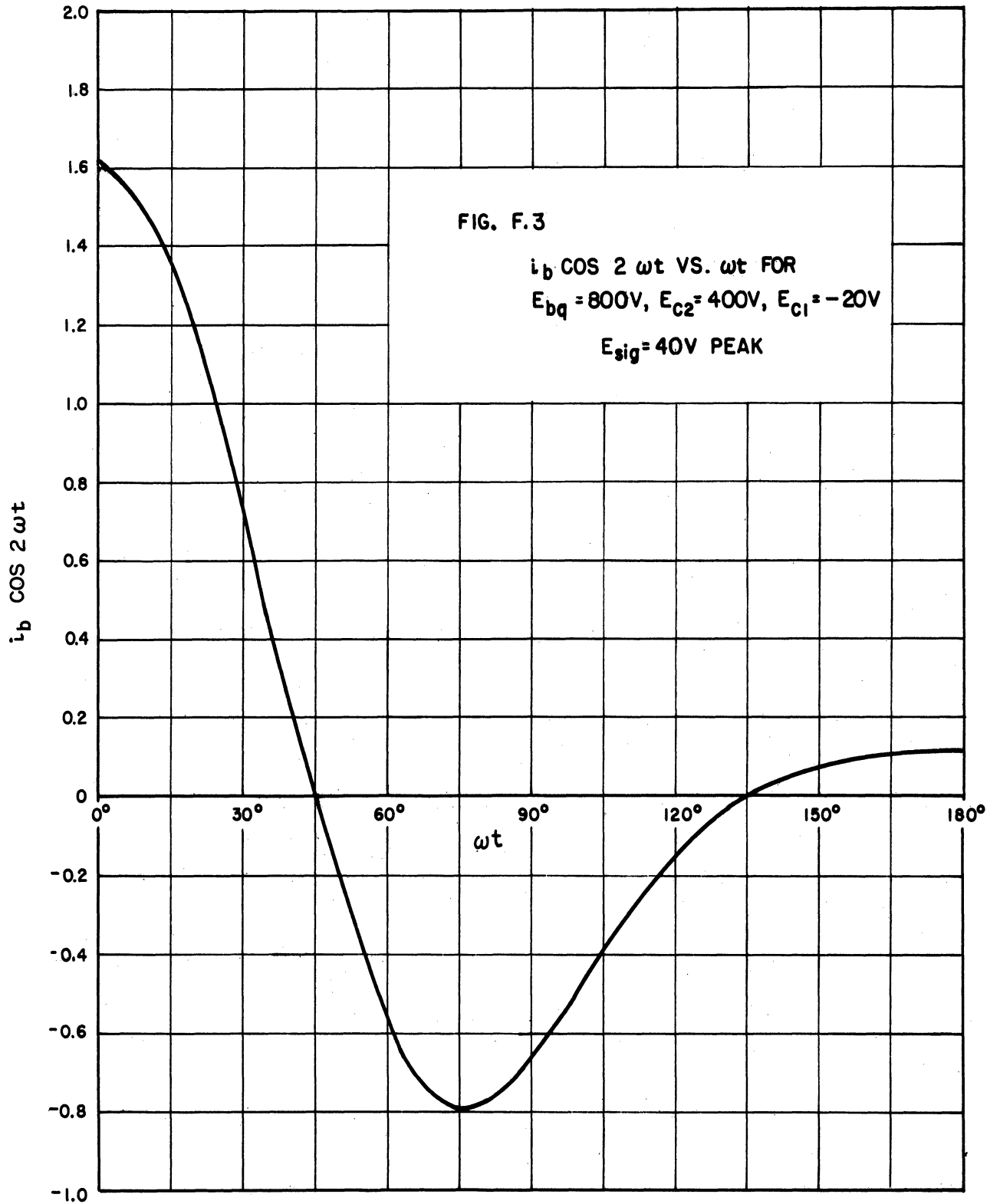
FIG. F.1

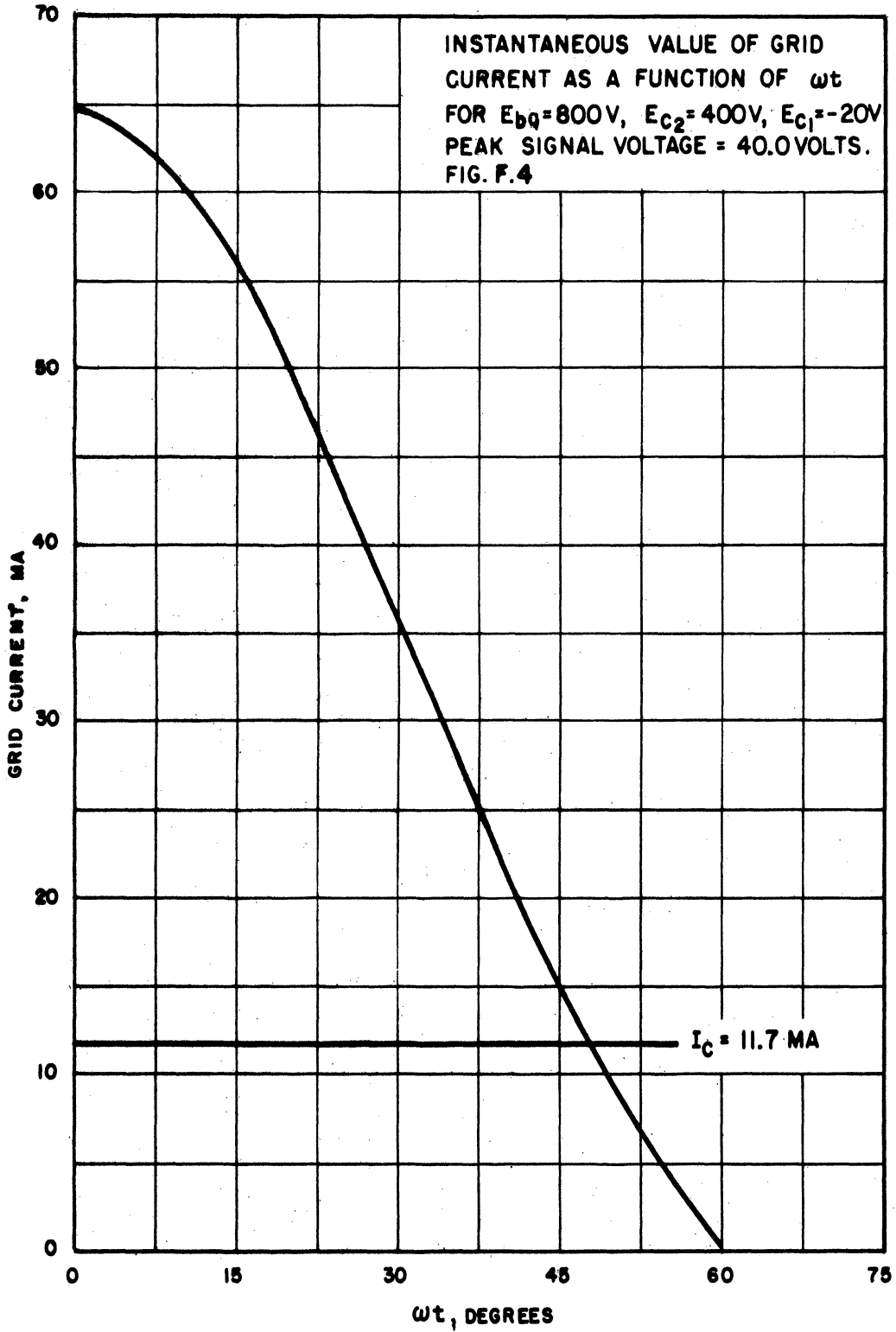
i_b VS. ωt FOR

$E_{bq} = 800V, E_{c2} = 400V, E_{c1} = -20V$

$E_{sig} = 40V$ PEAK







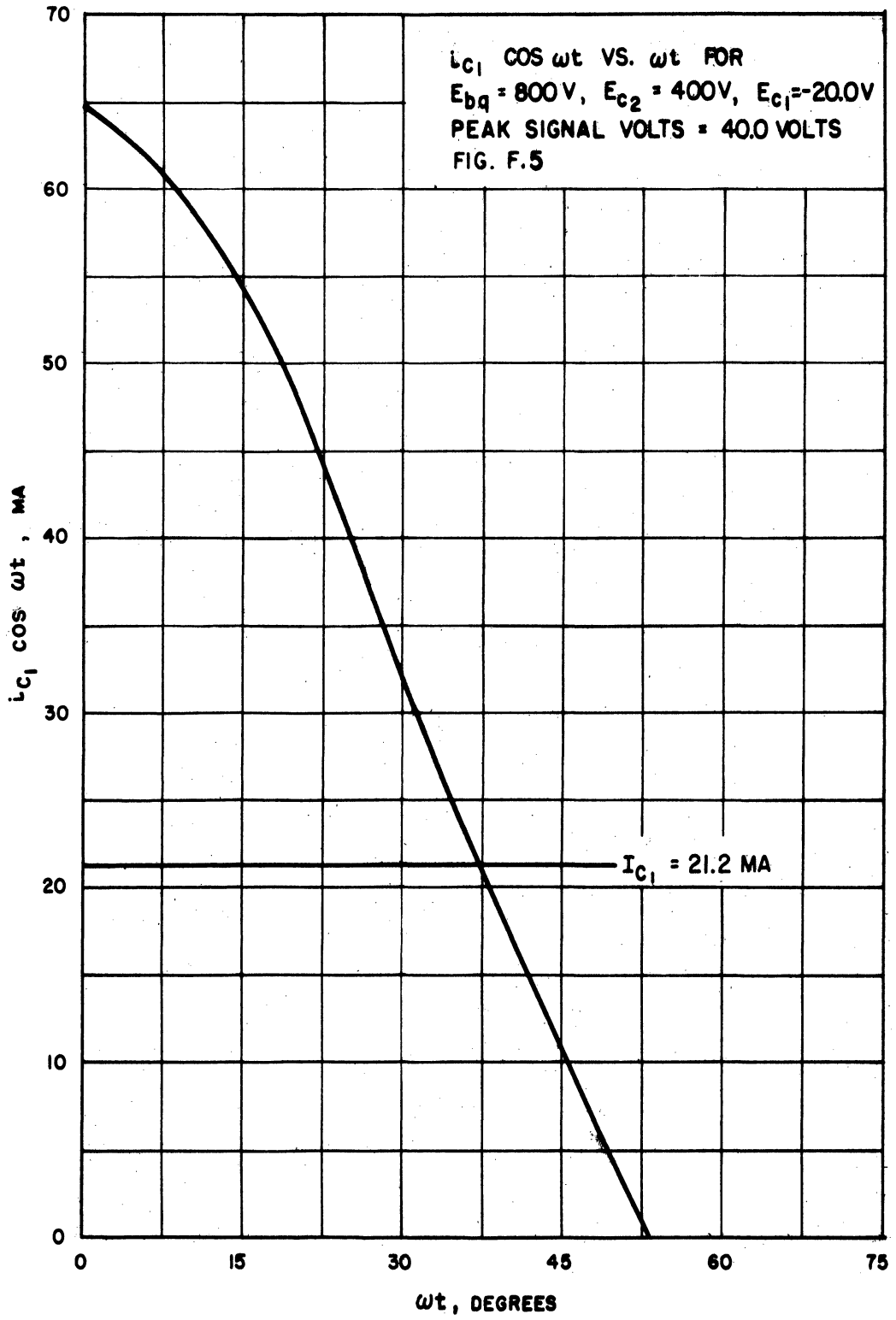


TABLE F.2

RESULTS AND COMPUTATIONS

$$E_{bq} = 800v, E_{c2} = 400v, E_{c1} = -26.6v, E_{sig} = 46.6v \text{ peak}$$

$$I_b = 0.685 \text{ amps}$$

$$I_1 = 0.806 \text{ amps}$$

$$I_2 = 0.14 \text{ amps}$$

$$I_c = 10.7 \text{ ma.}$$

$$I_{c1} = 21.7 \text{ ma.}$$

$$R_{geq} = 2.15 \text{ K } \Omega$$

$$\alpha_{odr} = .01165 \text{ nepers/section}$$

$$\frac{\alpha_{odr}}{\alpha_0} = 0.117$$

$$E_{bb} = 730 \text{ v.}$$

$$\text{Power Output} = 532 \text{ watts}$$

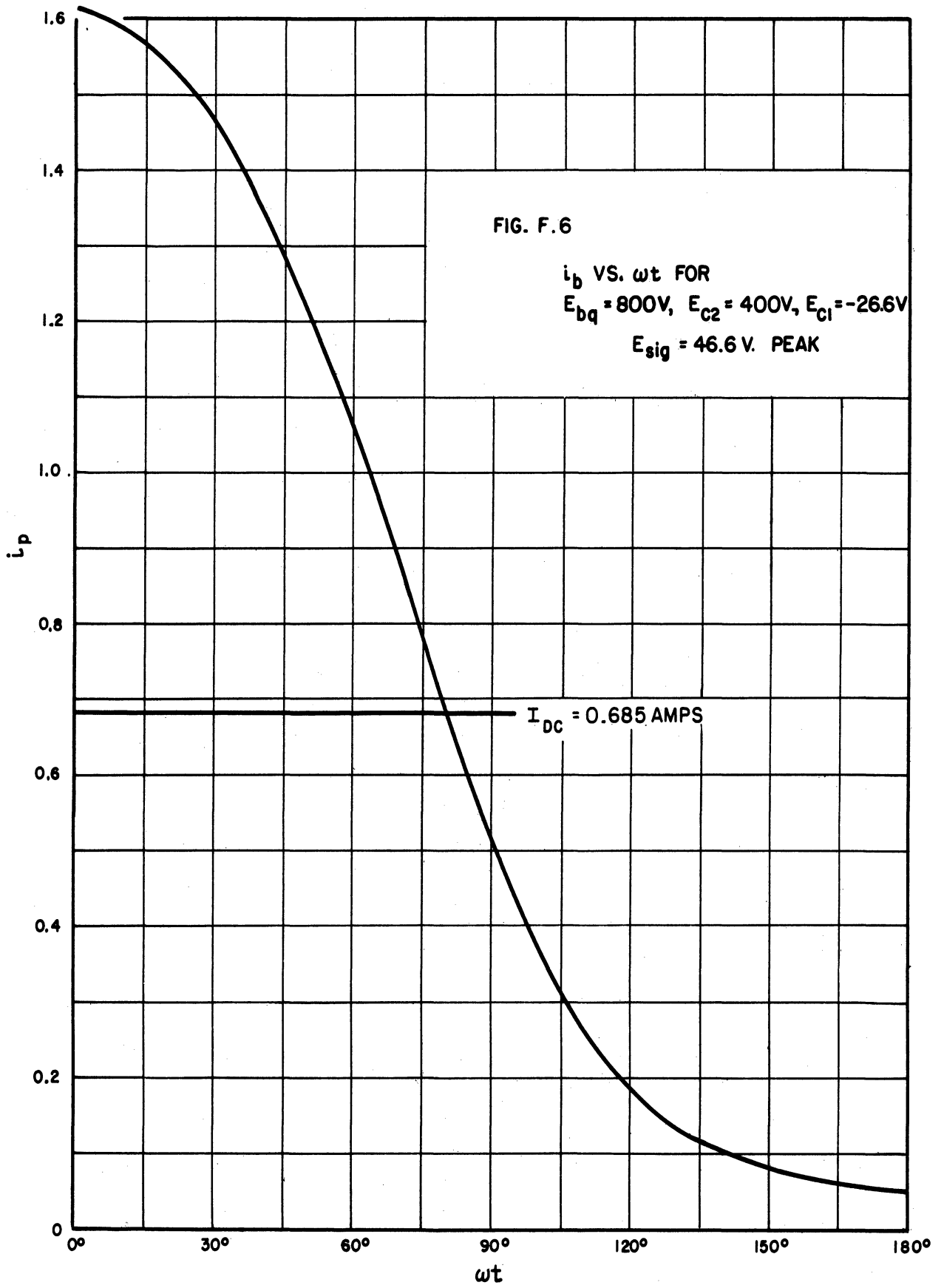
$$\text{Power Input} = 4500 \text{ watts}$$

$$\eta = 11.8\%$$

$$\text{Driving Power} = 21.7 \text{ watts}$$

$$\text{Frequency Tolerance} = 0.78$$

$$\text{Power Out } 2^{\text{nd}} \text{ Harmonic} = 17.9 \text{ watts}$$



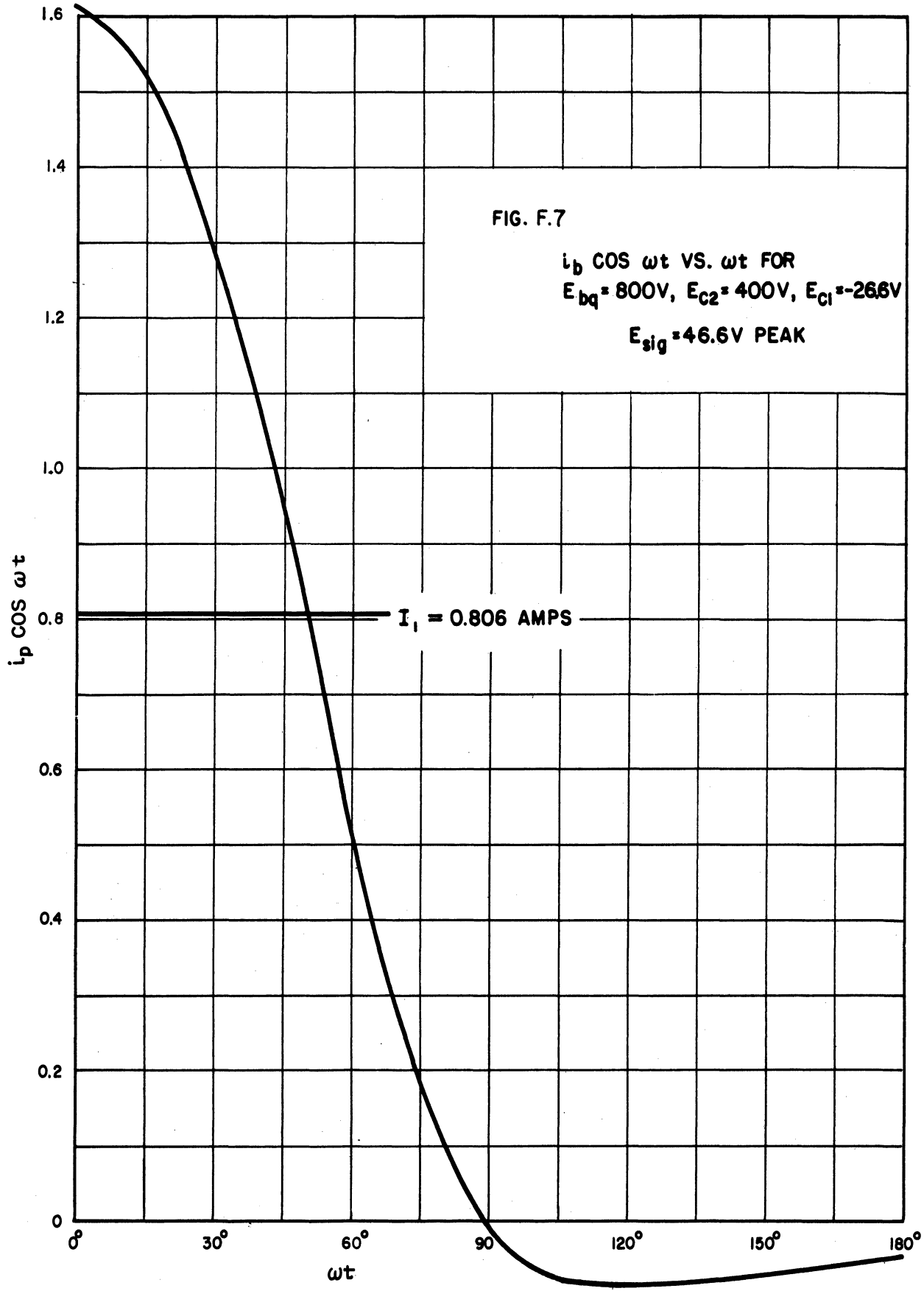
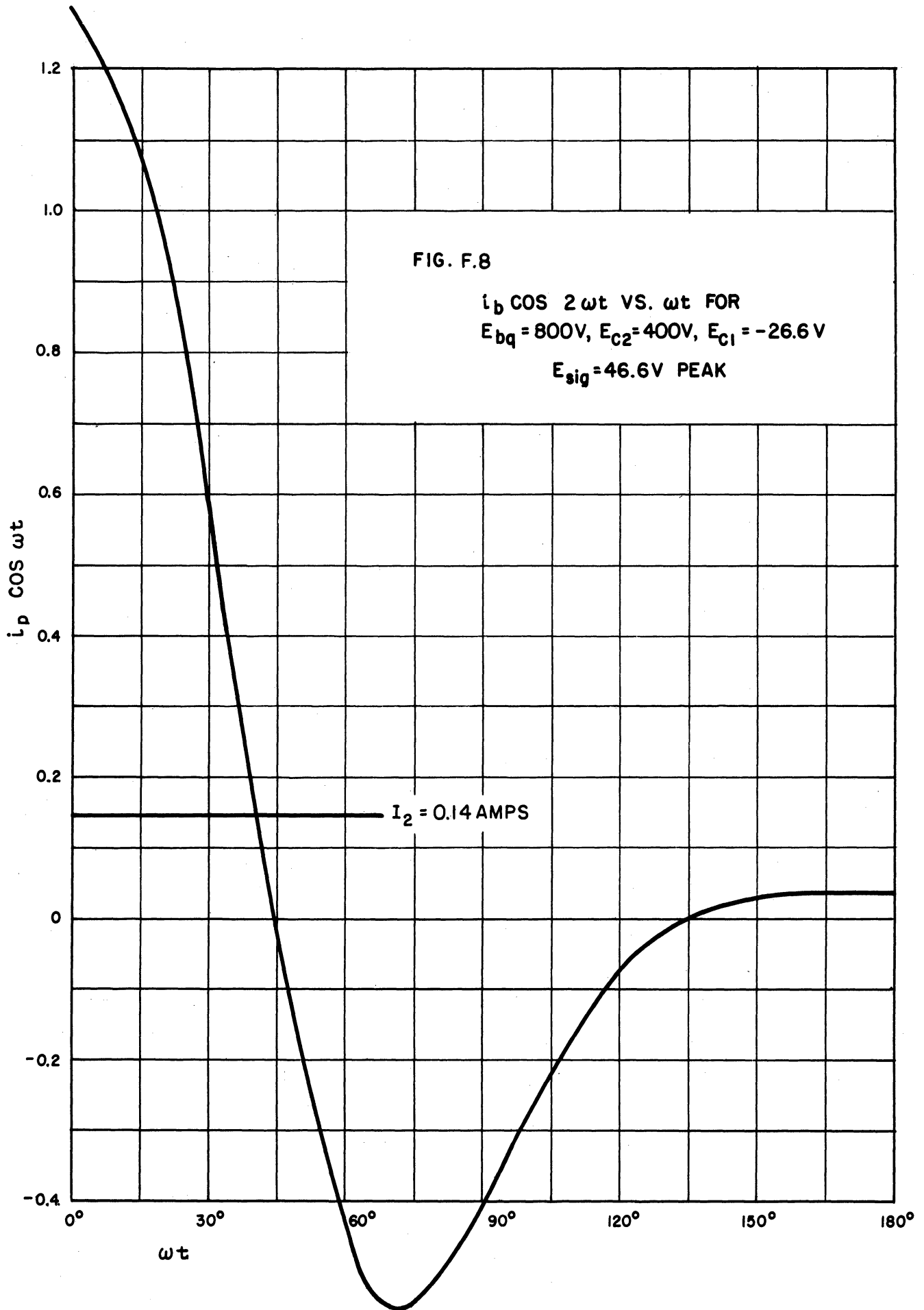


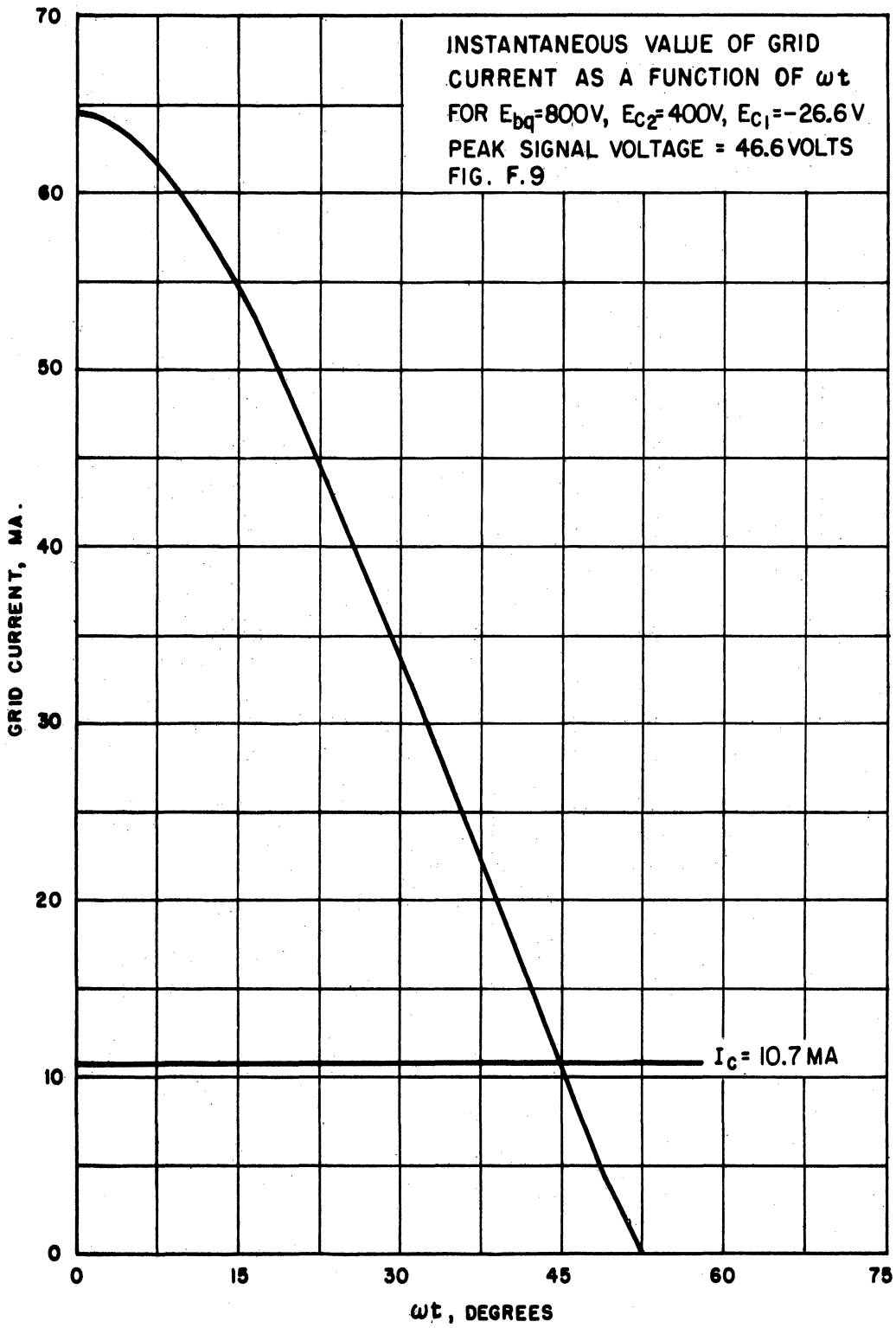
FIG. F.7

$i_b \cos \omega t$ VS. ωt FOR
 $E_{bq} = 800V$, $E_{c2} = 400V$, $E_{c1} = -266V$

$E_{sig} = 46.6V$ PEAK

$I_1 = 0.806$ AMPS





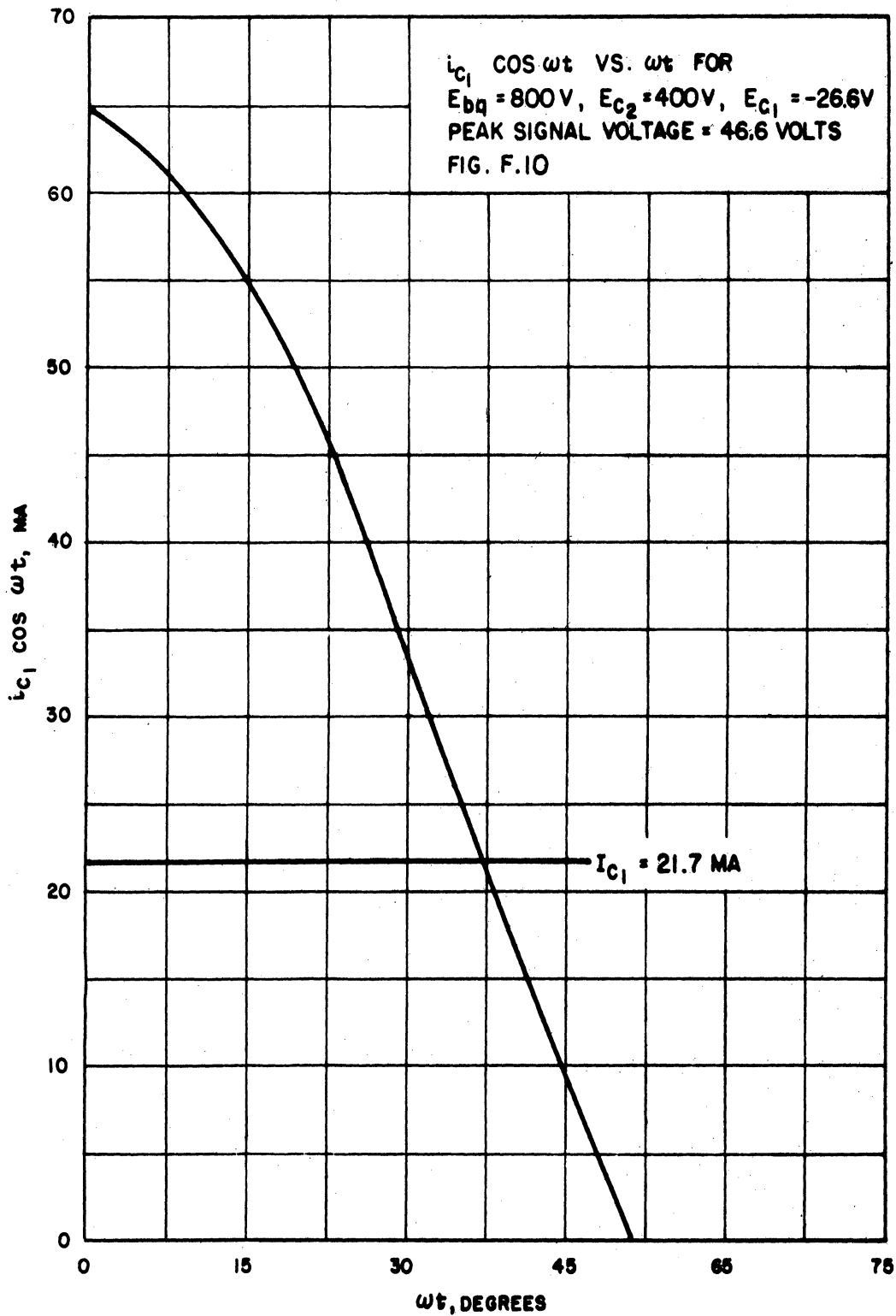


TABLE F.3

RESULTS AND COMPUTATIONS

$$E_{bq} = 800v, E_{c2} = 400v, E_{c1} = -40 \text{ volts}, E_{sig} = 60 \text{ v peak}$$

$$I_b = 0.56 \text{ amps.}$$

$$I_1 = 0.79 \text{ amps.}$$

$$I_2 = 0.24 \text{ amps.}$$

$$I_c = 9.6 \text{ ma.}$$

$$I_{c1} = 18.7 \text{ ma.}$$

$$R_{geq} = 3.2 \text{ K } \Omega$$

$$\alpha_{odr} = 0.0078 \text{ nepers/section}$$

$$\frac{\alpha_{odr}}{\alpha_o} = .0785$$

$$E_{bb} = 680 \text{ volts}$$

$$\text{Power Output} = 530 \text{ watts}$$

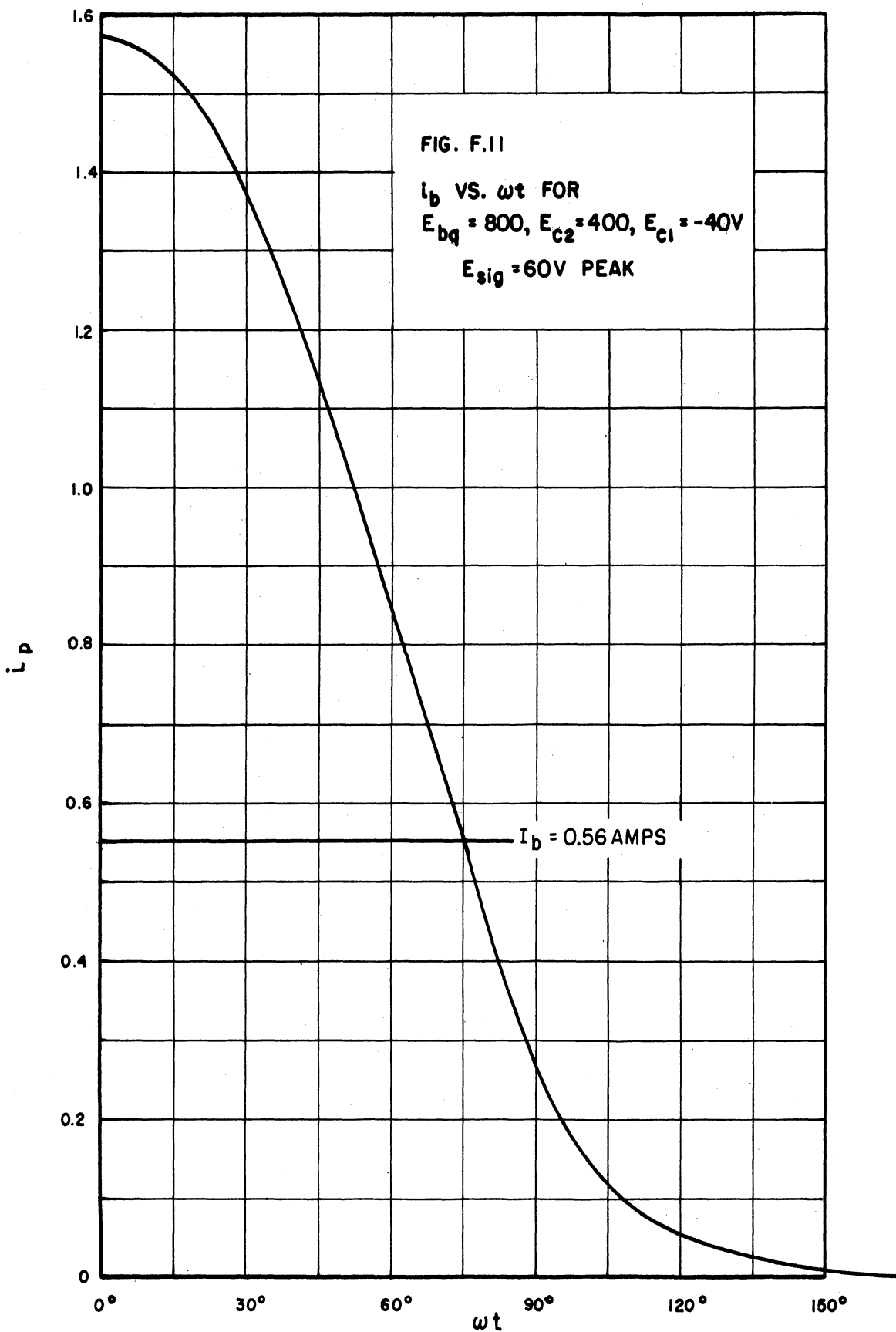
$$\text{Power Input} = 3425 \text{ watts}$$

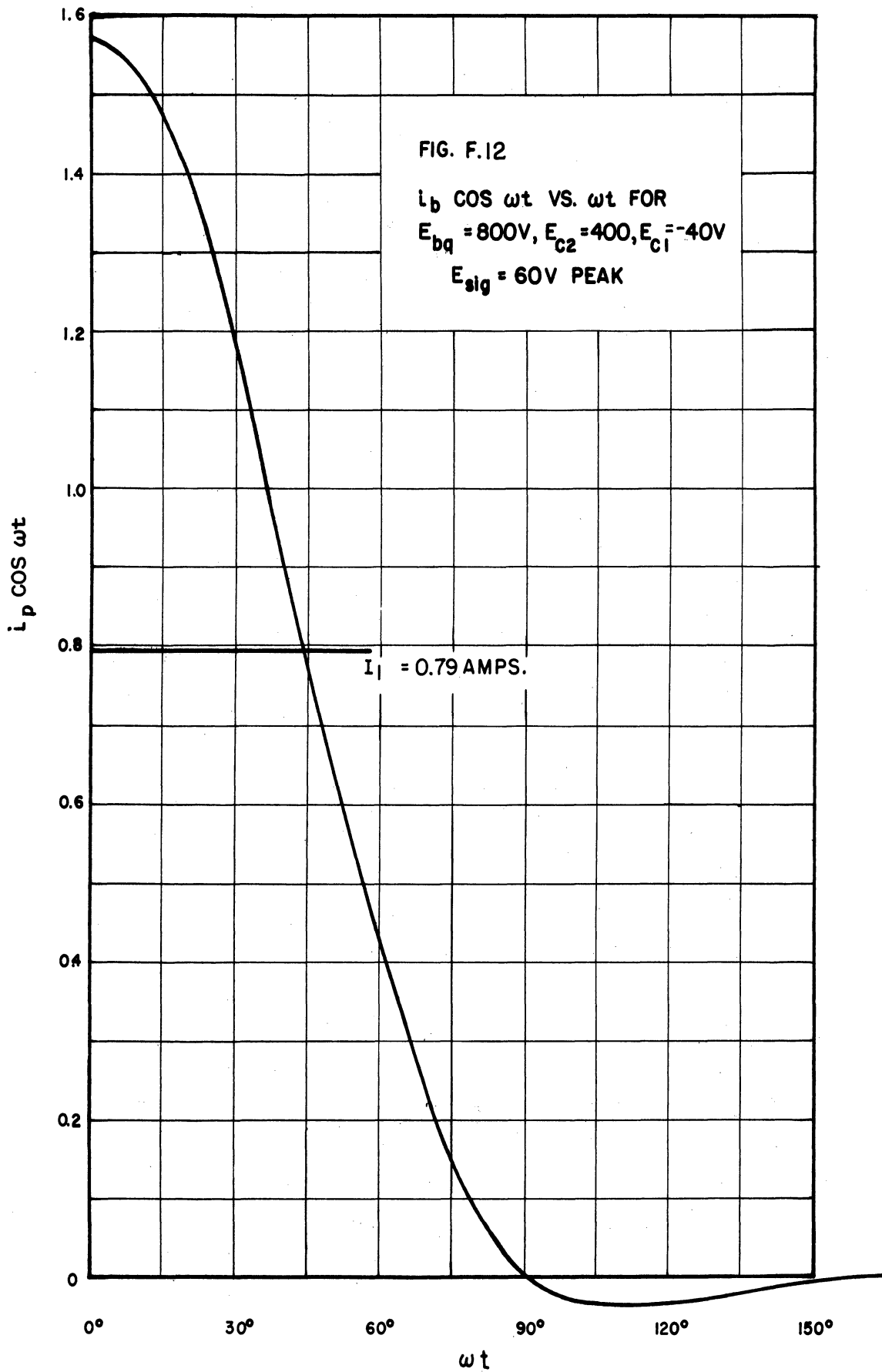
$$\eta = 15.5\%$$

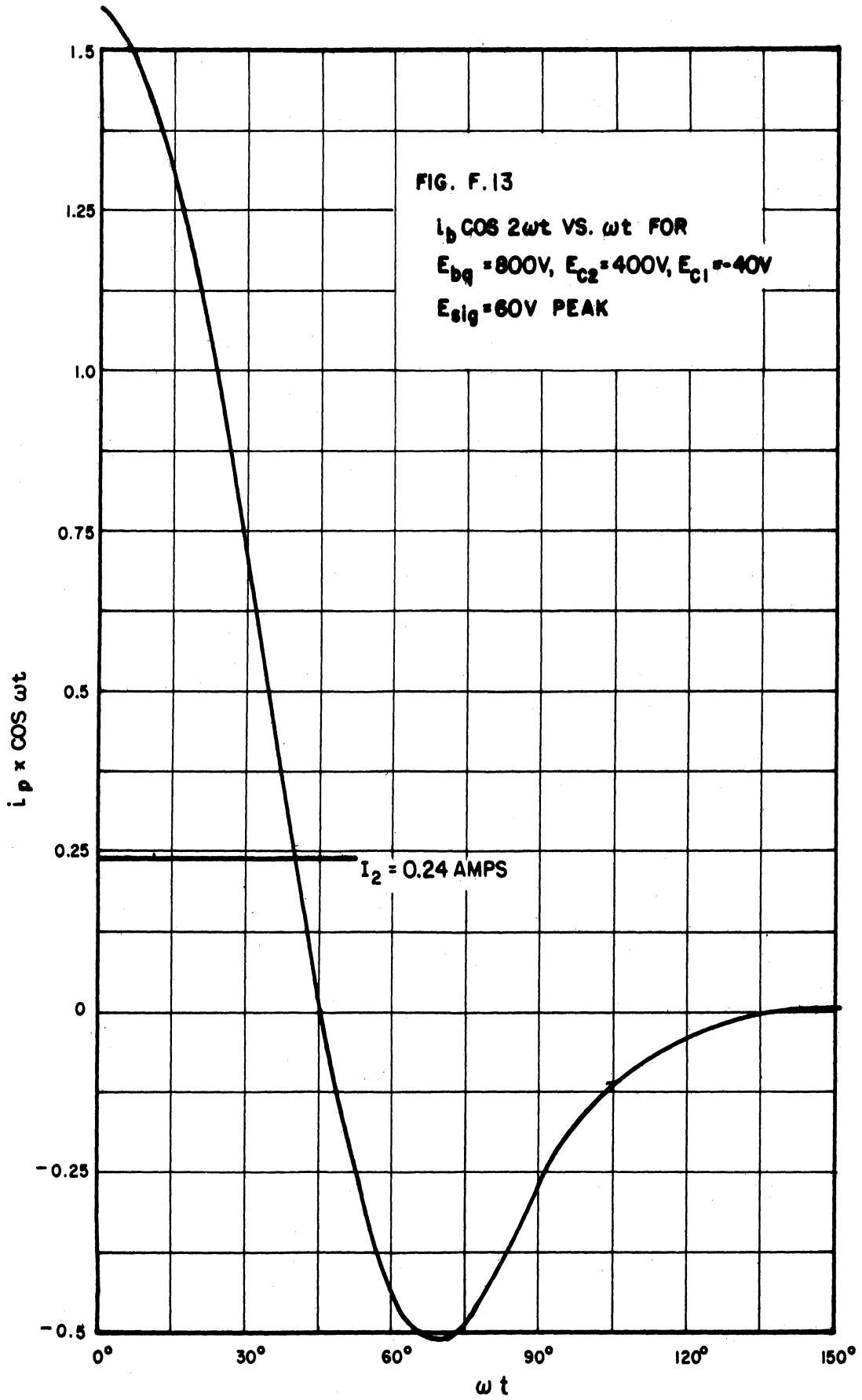
$$\text{Driving Power} = 36 \text{ watts}$$

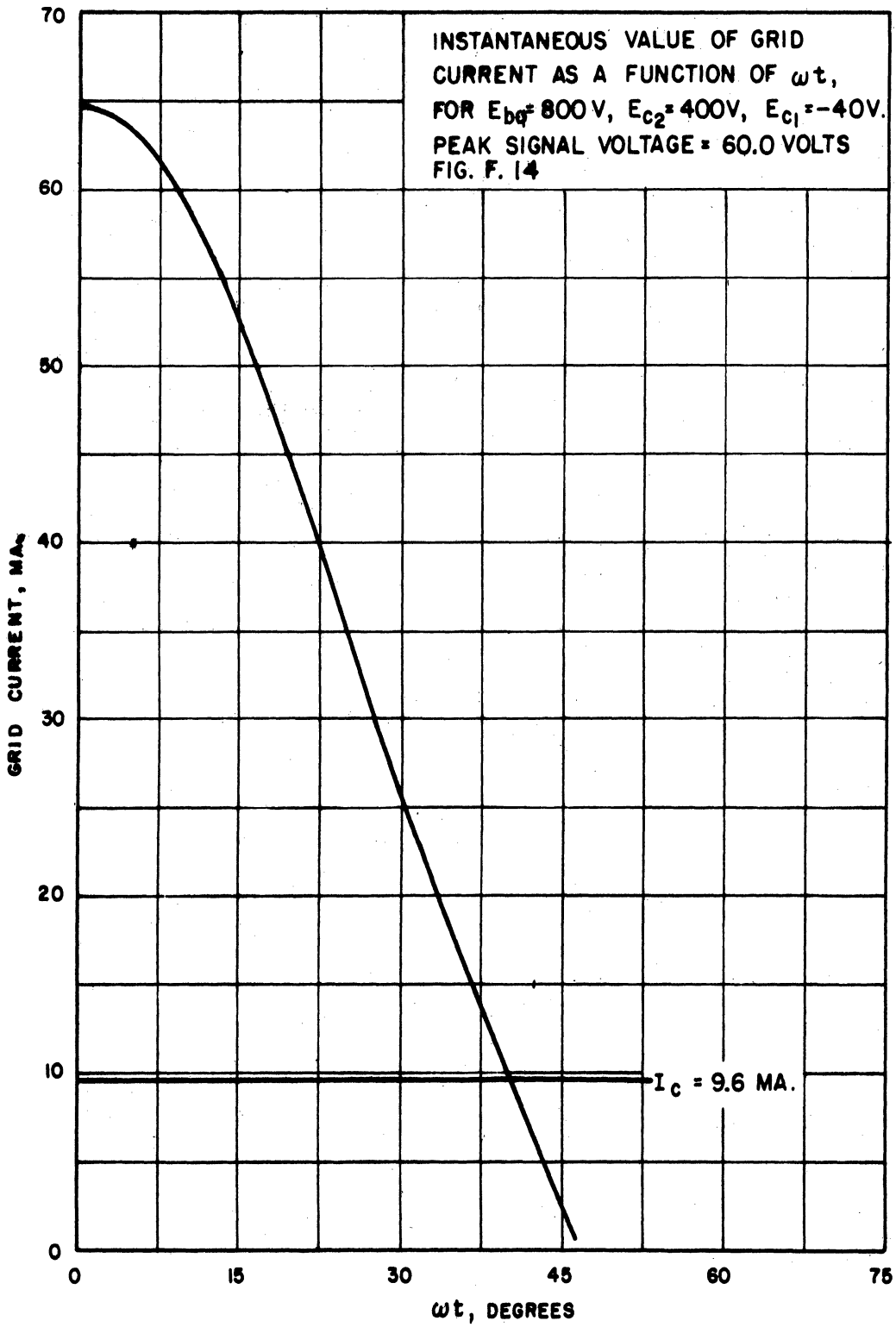
$$\text{Frequency Tolerance} = 0.63$$

$$\text{Power Out } 2^{\text{nd}} \text{ Harmonic} = 52.5 \text{ watts}$$









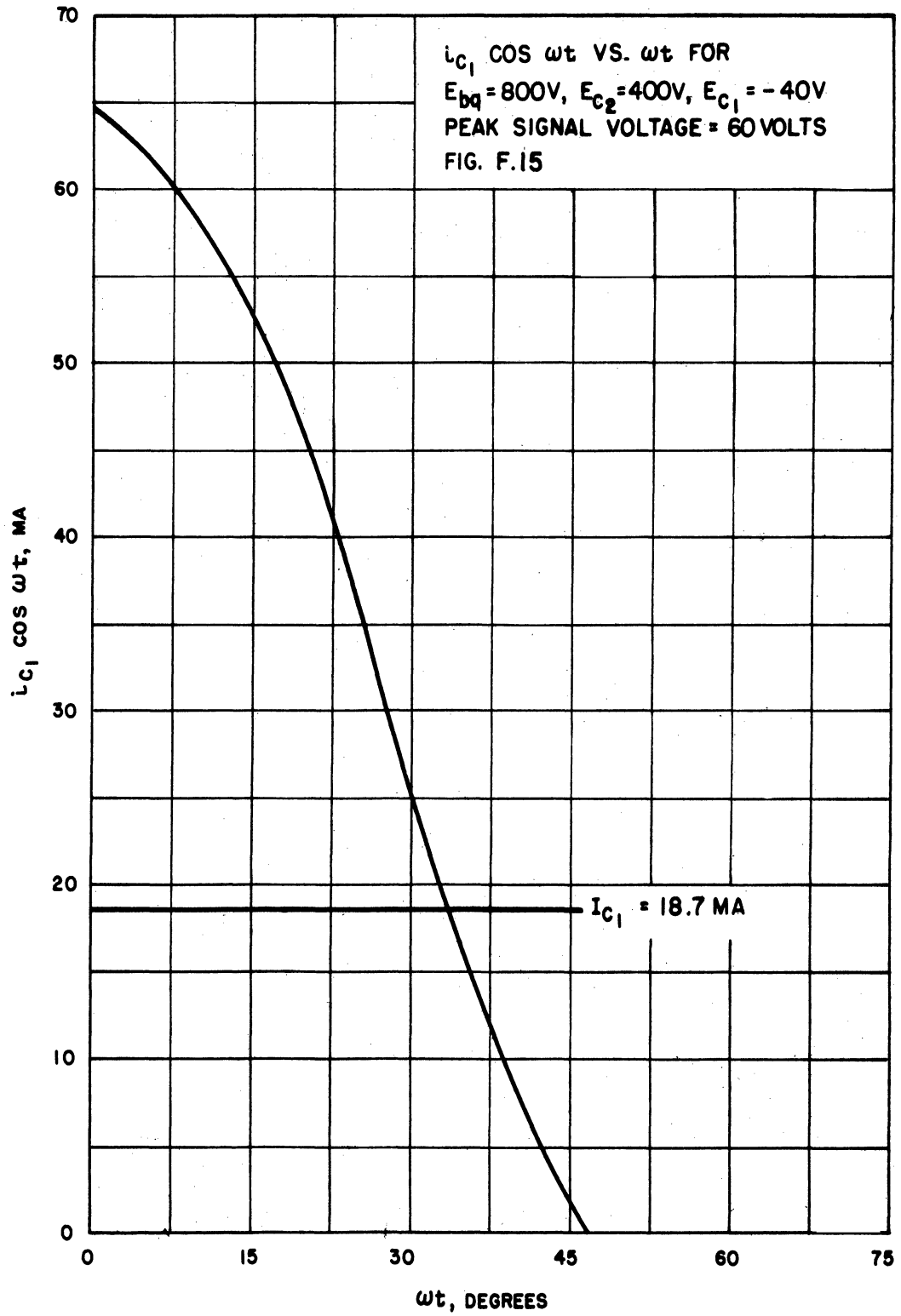


TABLE F.4

RESULTS AND COMPUTATIONS

$$E_{bq} = 800v, E_{c2} = 400v, E_{c1} = -53.3v, E_{sig} = 73.3v \text{ peak}$$

$$I_b = 0.5 \text{ amps.}$$

$$I_1 = 0.76 \text{ amps.}$$

$$I_2 = 0.325 \text{ amps.}$$

$$I_c = 8.8 \text{ ma.}$$

$$I_{c1} = 16.6 \text{ ma.}$$

$$R_{geq} = 4.4 \text{ K } \Omega$$

$$\alpha_{odr} = 0.00567 \text{ nepers/section}$$

$$\frac{\alpha_{odr}}{\alpha_o} = 0.057$$

$$E_{bb} = 663 \text{ volts}$$

$$\text{Power Output} = 501 \text{ watts}$$

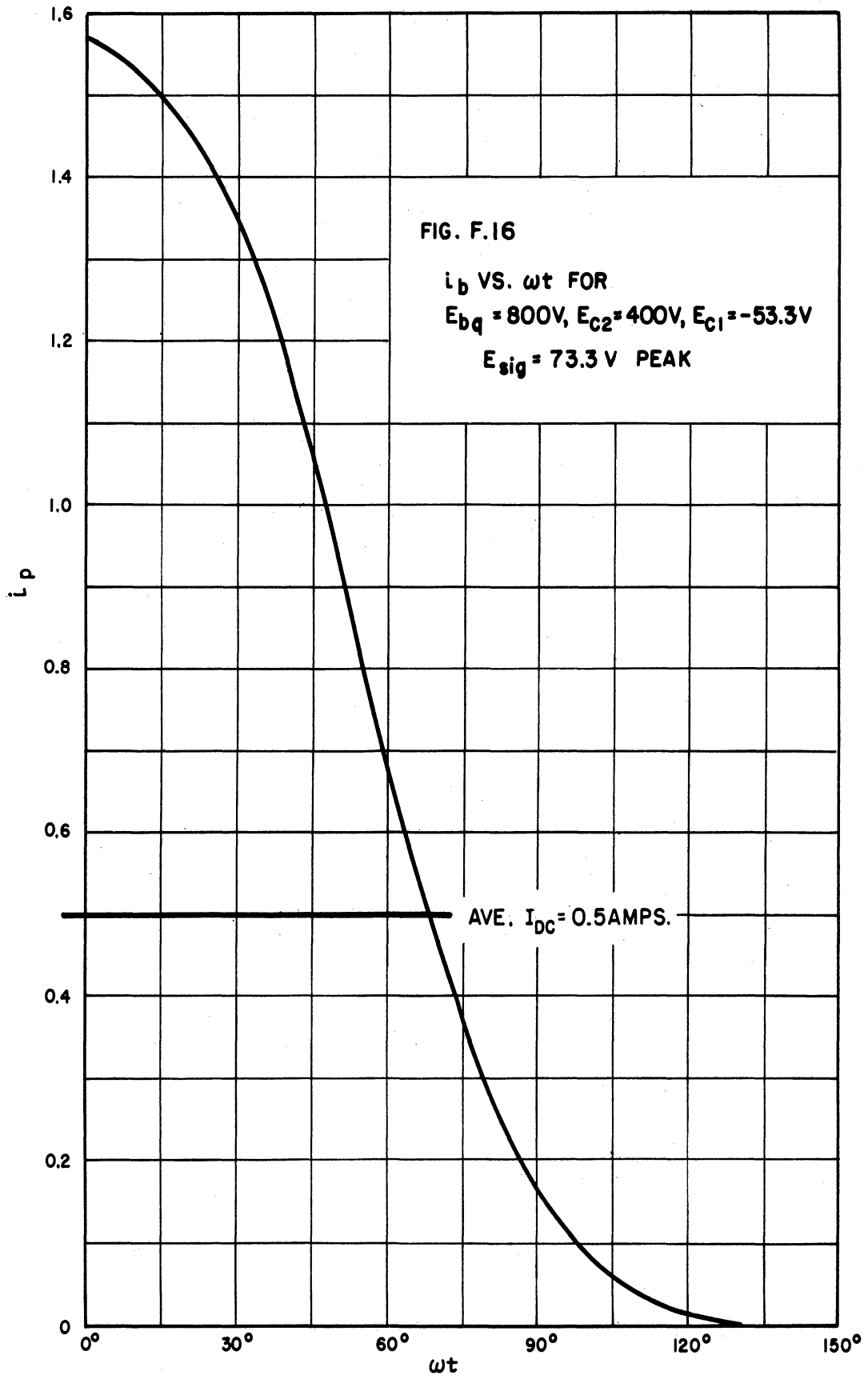
$$\text{Power Input} = 2980 \text{ watts}$$

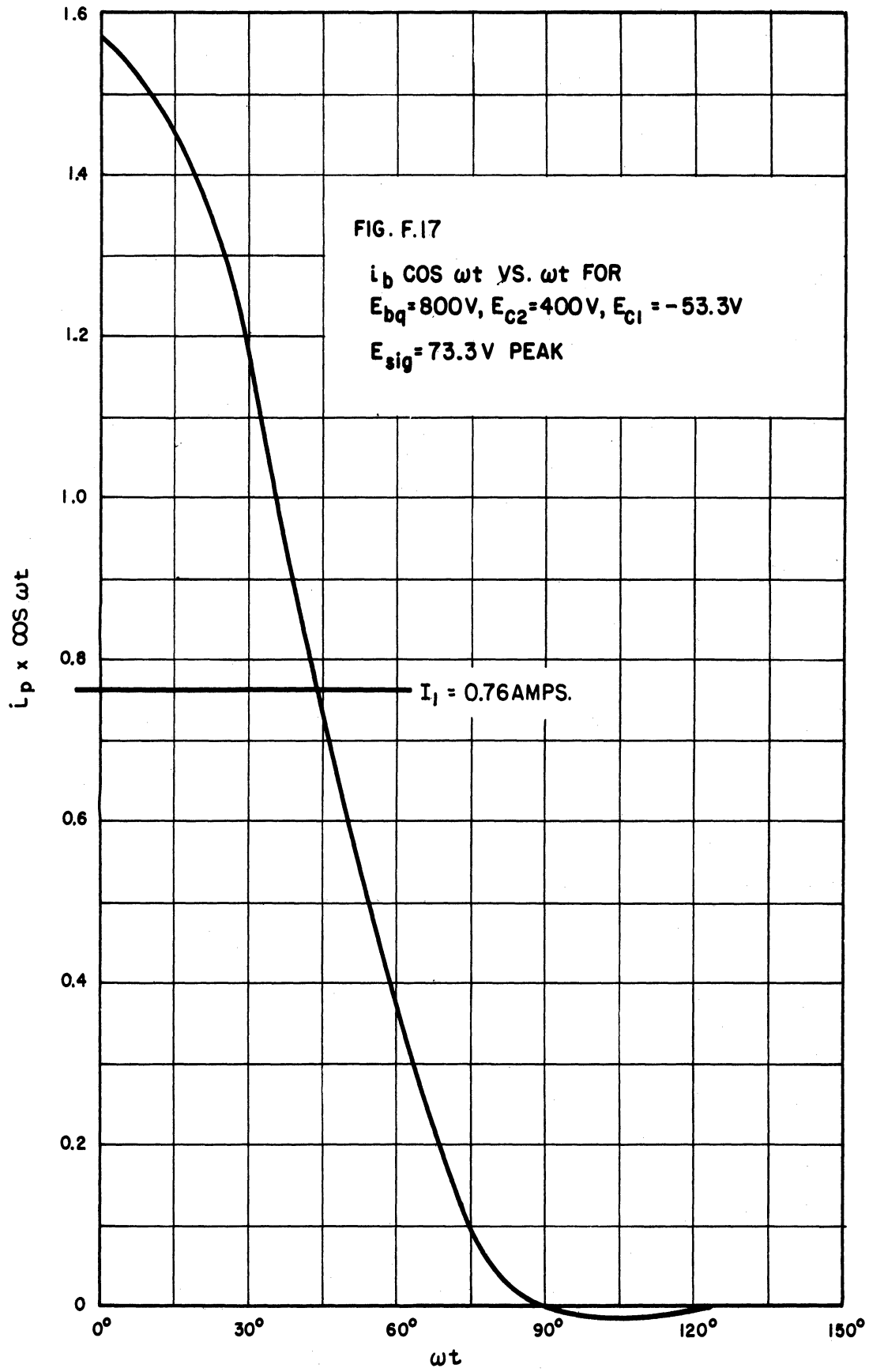
$$\eta = 16.8\%$$

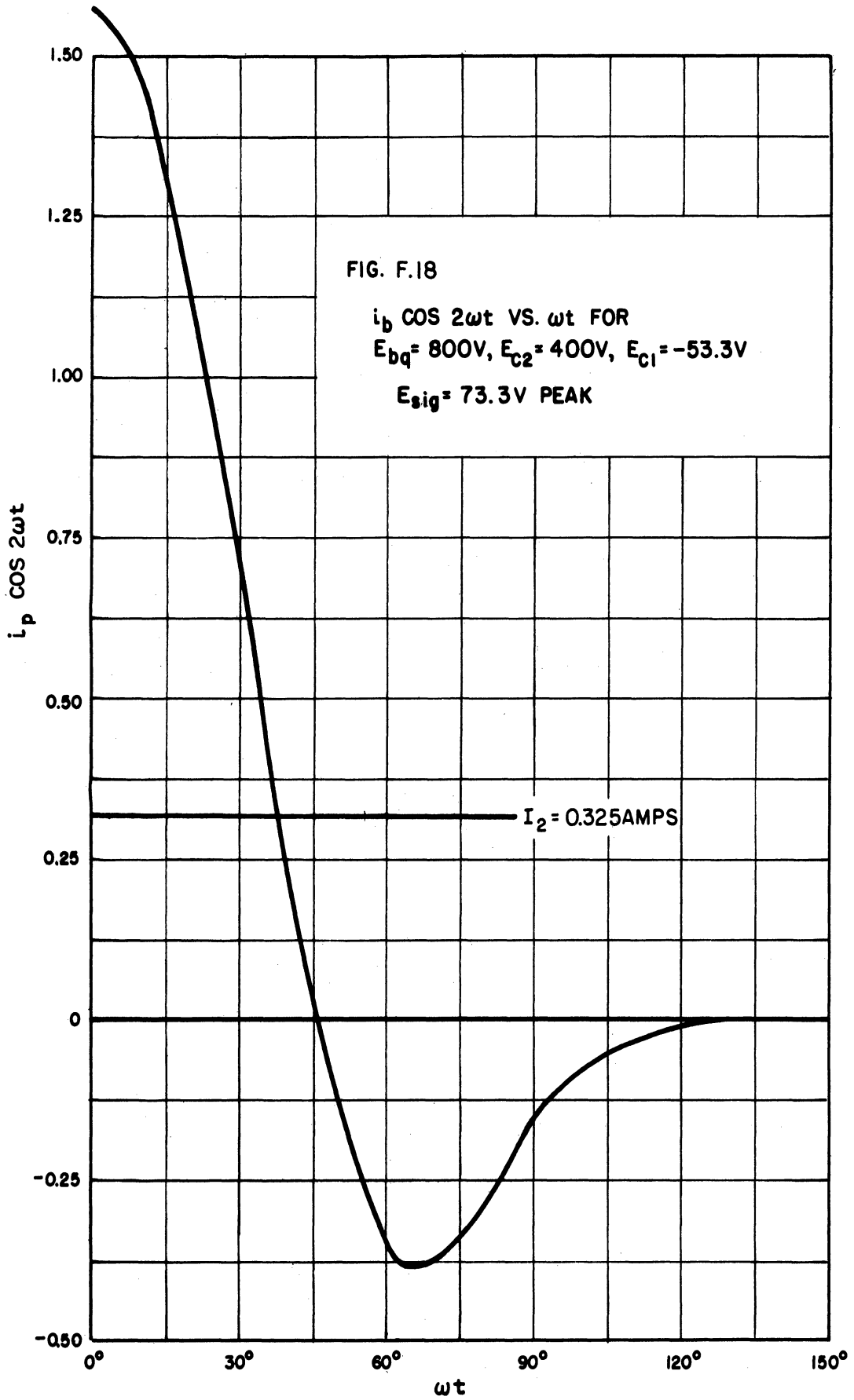
$$\text{Driving Power} = 53.7 \text{ watts}$$

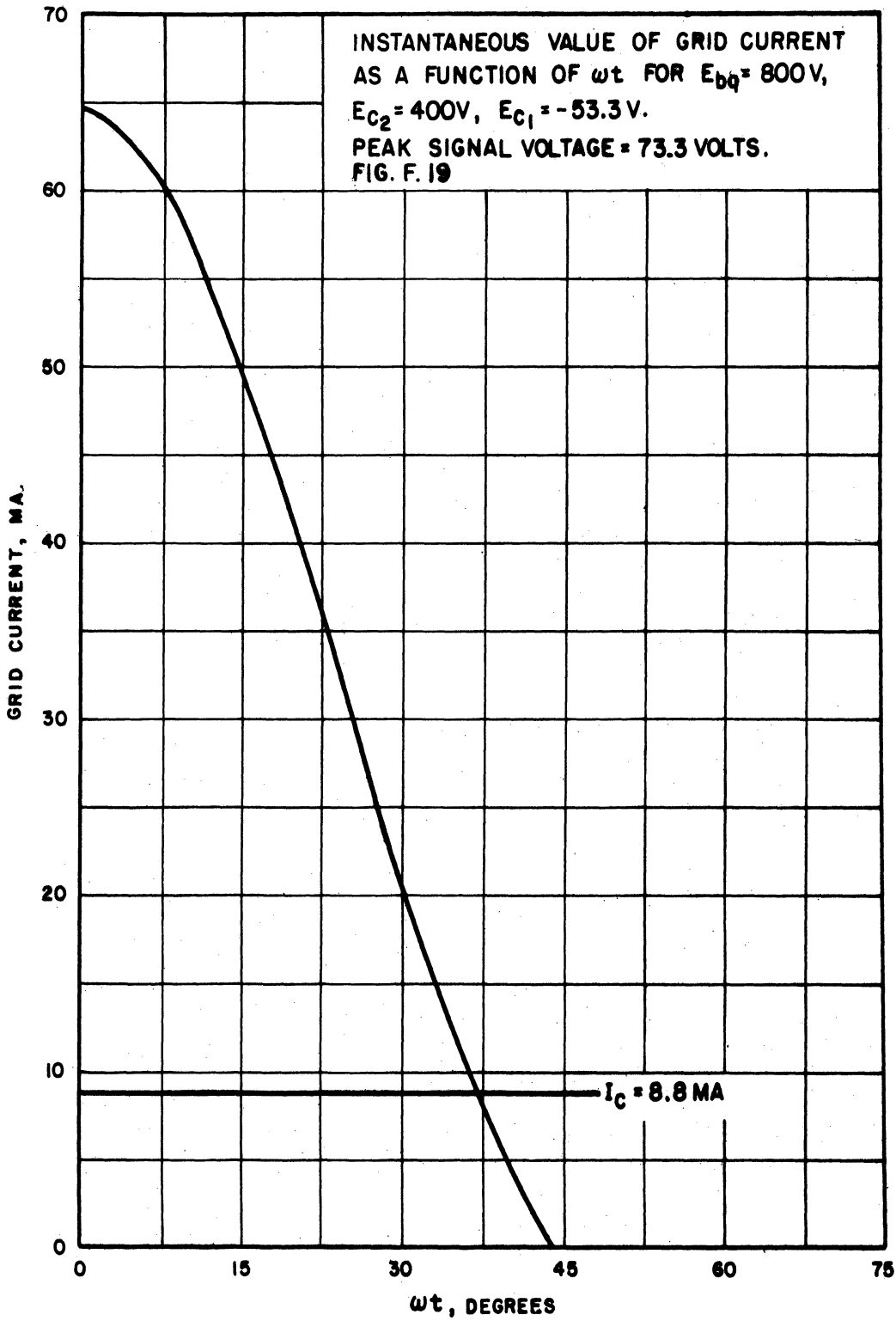
$$\text{Frequency Tolerance} = 0.55$$

$$\text{Power Out } 2^{\text{nd}} \text{ Harmonic} = 96.3 \text{ watts}$$









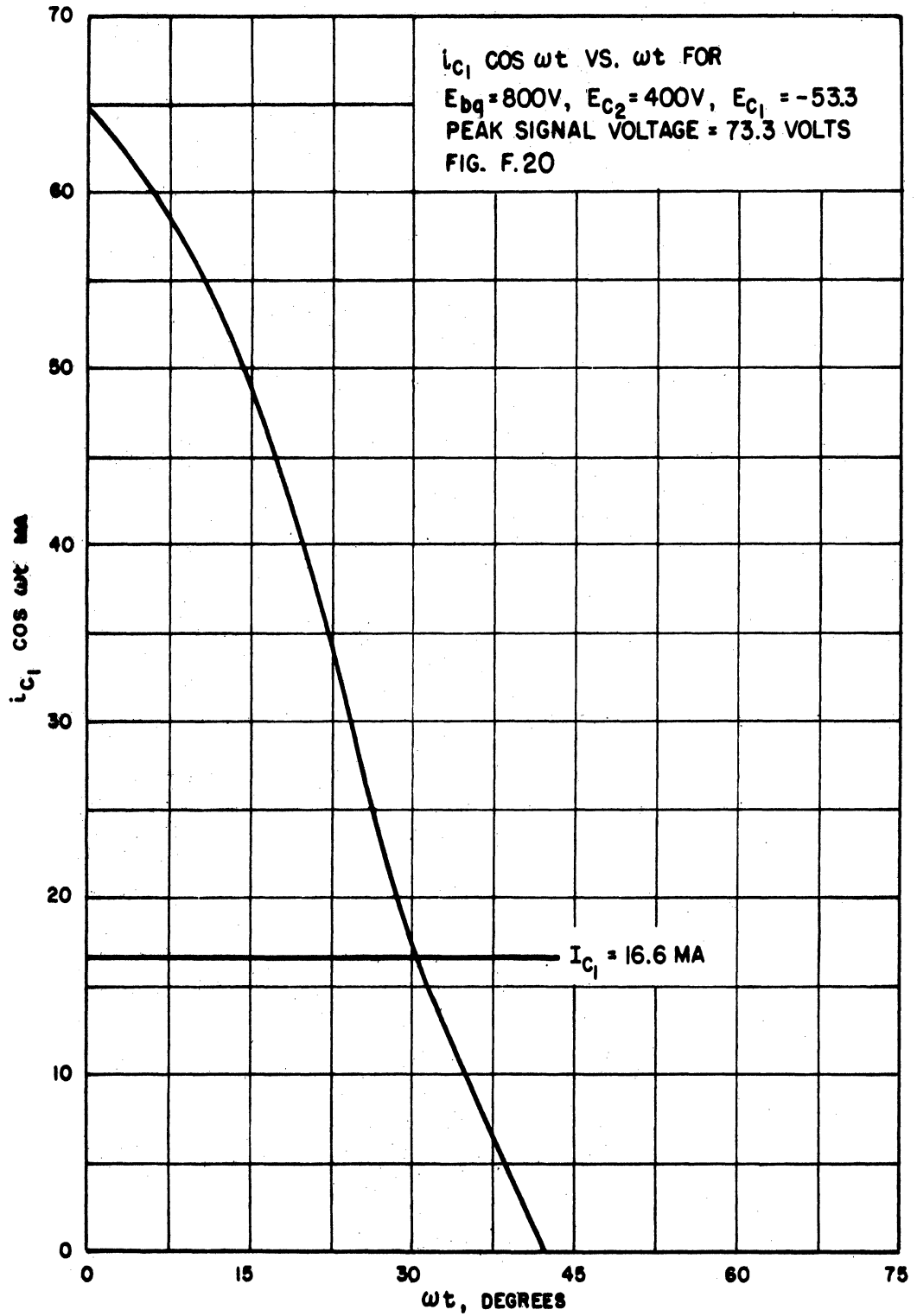


TABLE F.5

RESULTS AND COMPUTATIONS

$$E_{bq} = 800v, E_{c2} = 400v, E_{c1} = -66.6v, E_{sig} = 86.6 v \text{ peak}$$

$$I_b = 0.44 \text{ amps.}$$

$$I_1 = 0.701 \text{ amps.}$$

$$I_2 = 0.36 \text{ amps.}$$

$$I_c = 8.3 \text{ ma.}$$

$$I_{c1} = 15.4 \text{ ma.}$$

$$R_{geq} = 5.6 \text{ K } \Omega$$

$$\alpha_{odr} = .00445 \text{ nepers/section}$$

$$\frac{\alpha_{odr}}{\alpha_o} = .0447$$

$$E_{bb} = 655 \text{ volts}$$

$$\text{Power Output} = 430 \text{ watts}$$

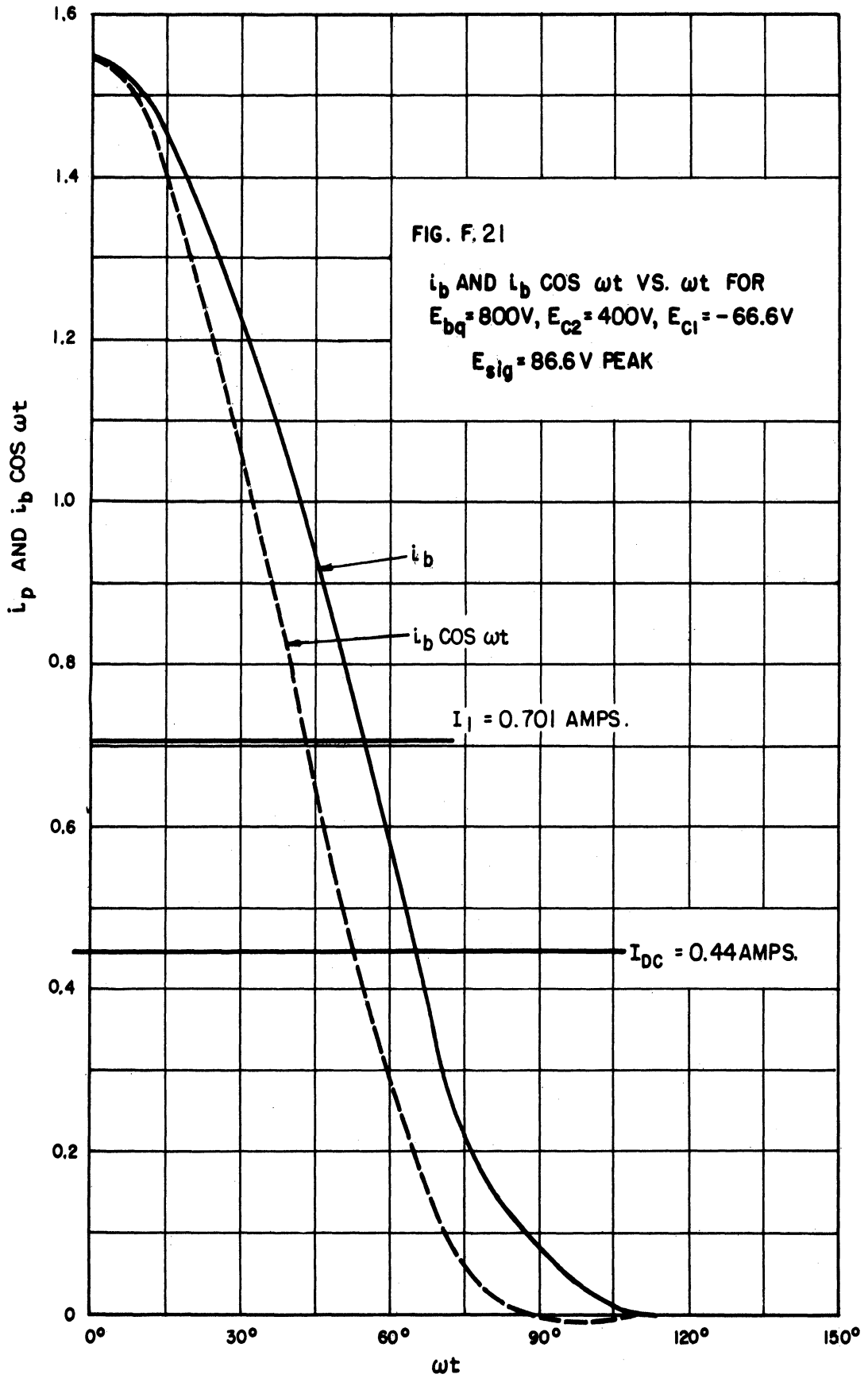
$$\text{Power Input} = 2685 \text{ watts}$$

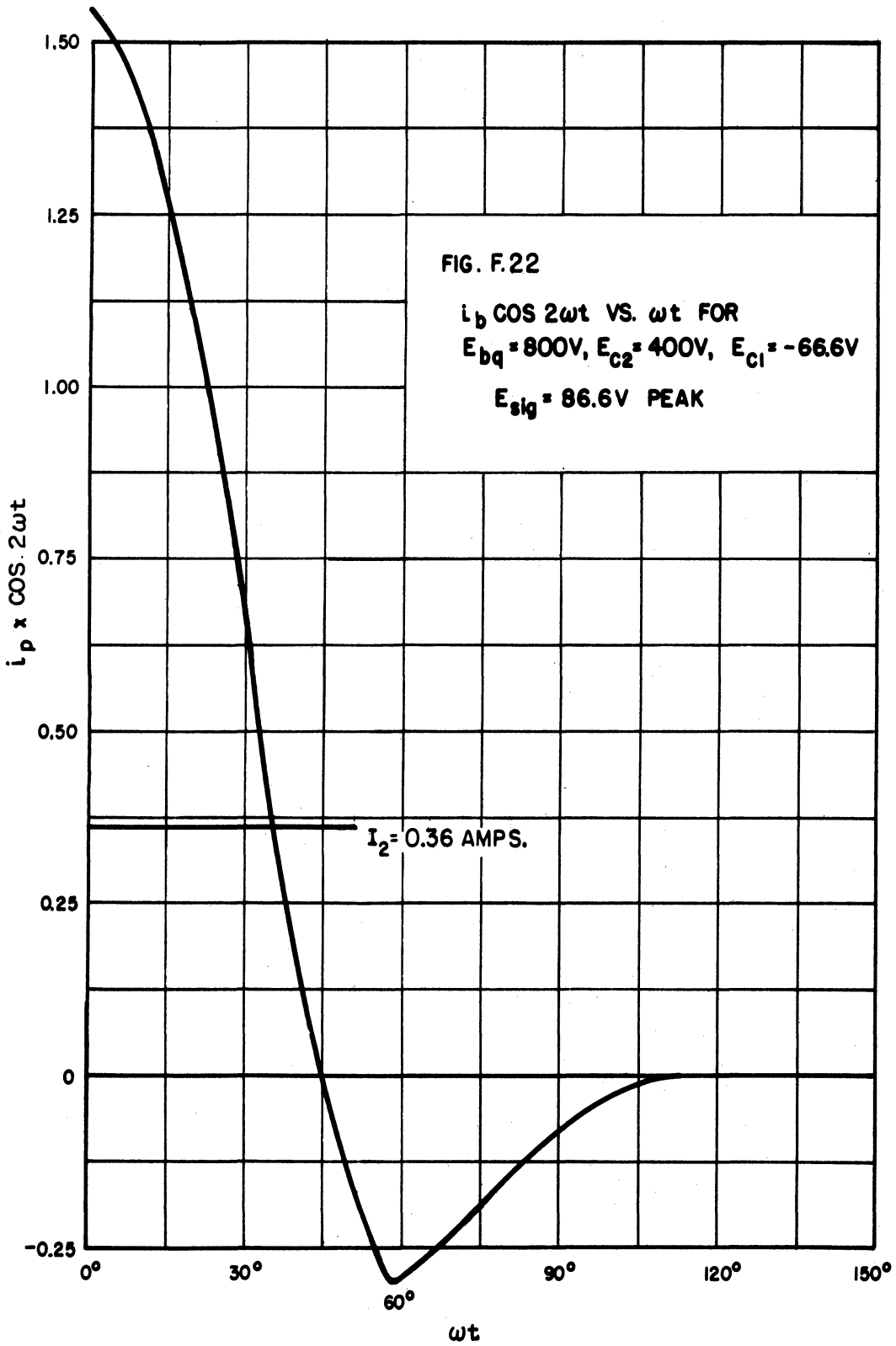
$$\eta = 16.0\%$$

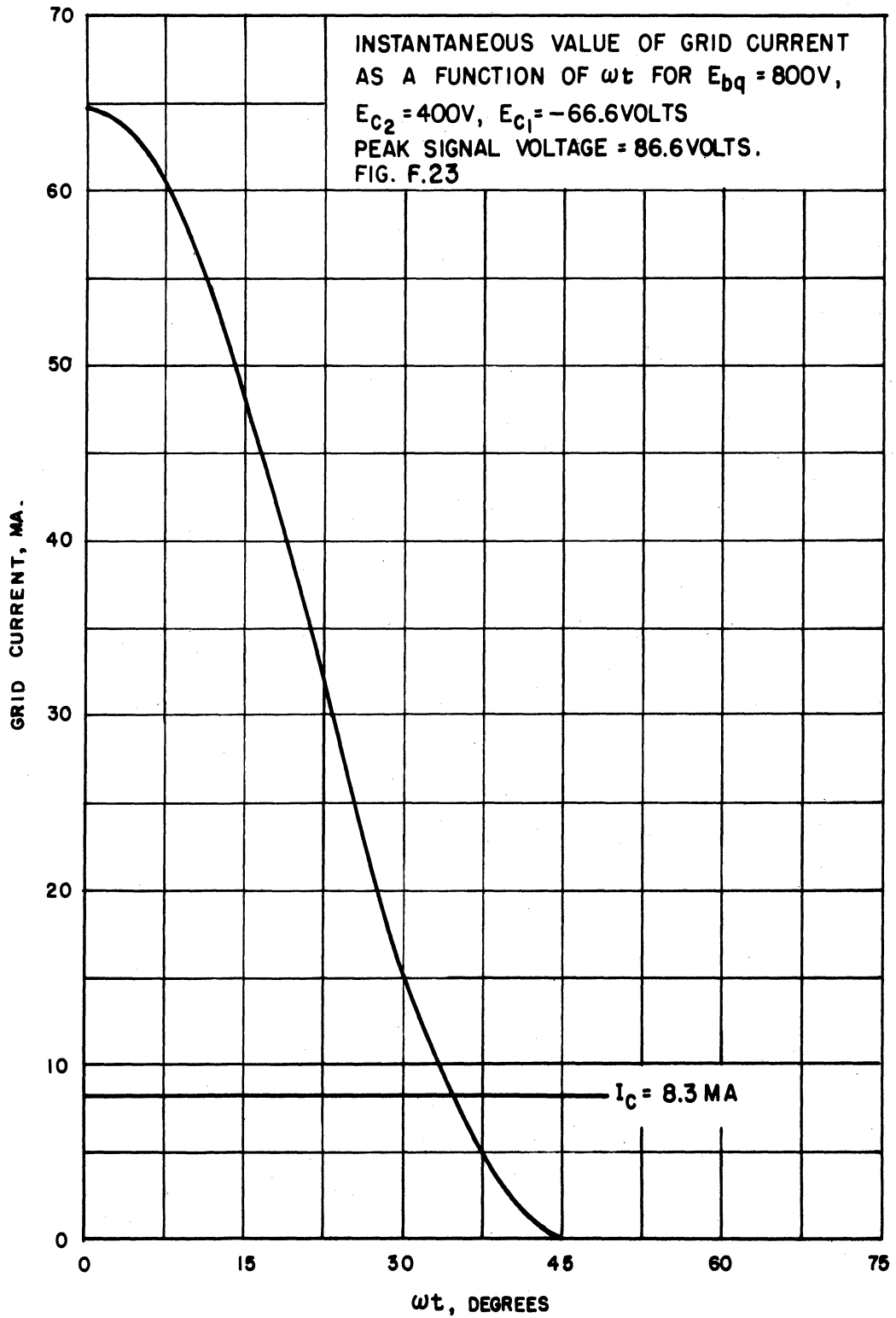
$$\text{Driving Power} = 75 \text{ watts}$$

$$\text{Frequency Tolerance} = 0.46$$

$$\text{Power Out 2}^{\text{nd}} \text{ Harmonic} = 118.1 \text{ watts}$$







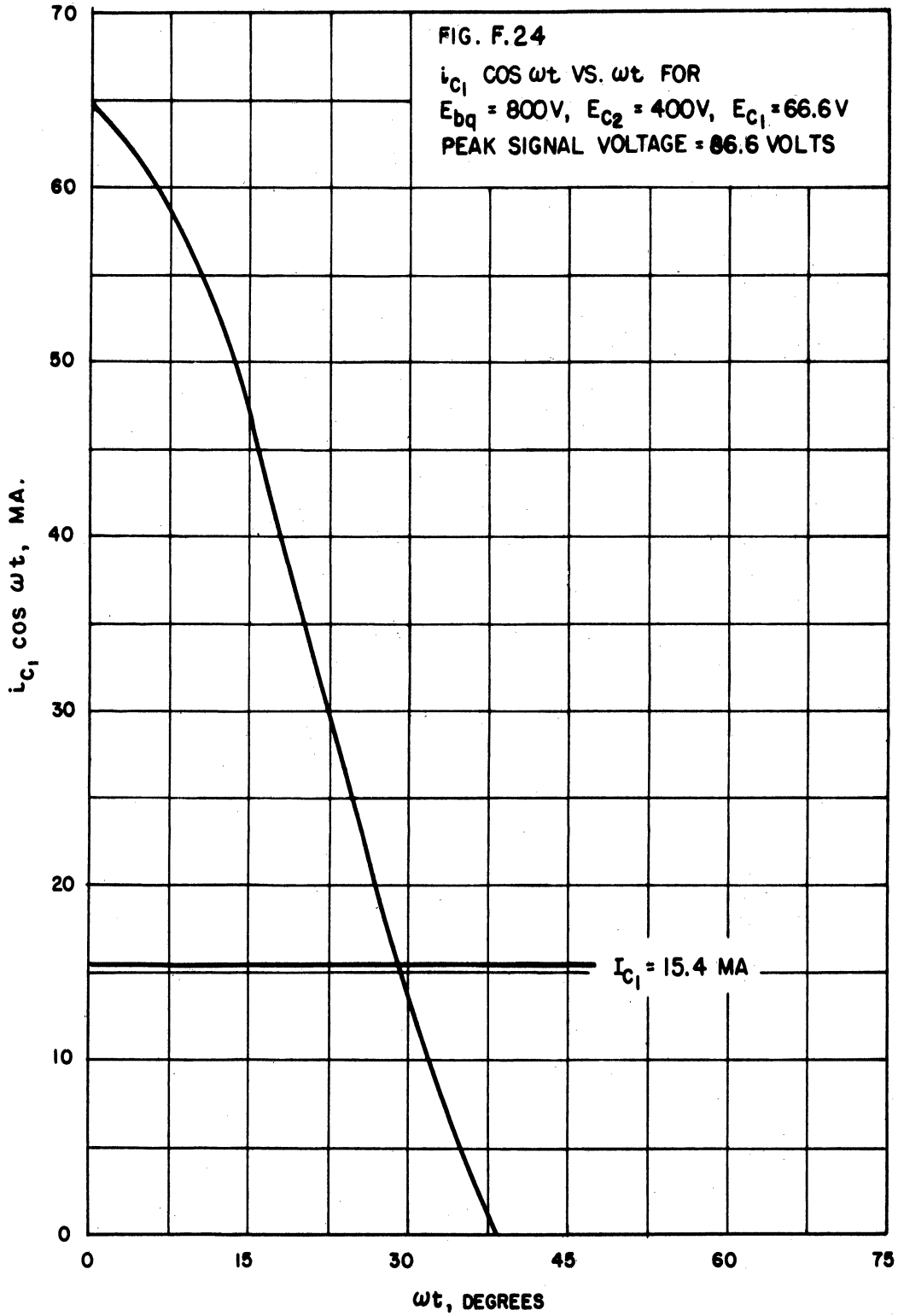


TABLE F.6

RESULTS AND COMPUTATIONS

$$E_{bq} = 800v, E_{c2} = 400v, E_{c1} = -80v, E_{sig} = 100 v \text{ peak}$$

$$I_b = 0.41 \text{ amps.}$$

$$I_1 = 0.68 \text{ amps.}$$

$$I_2 = 0.375 \text{ amps.}$$

$$I_c = 7.7 \text{ ma.}$$

$$I_{c1} = 14.6 \text{ ma.}$$

$$R_{geq} = 6.85 \text{ K } \Omega$$

$$\alpha_{odr} = 0.00365 \text{ nepers/section}$$

$$\frac{\alpha_{odr}}{\alpha_0} = 0.0367$$

$$E_{bb} = 650 \text{ volts}$$

$$\text{Power Output} = 407 \text{ watts}$$

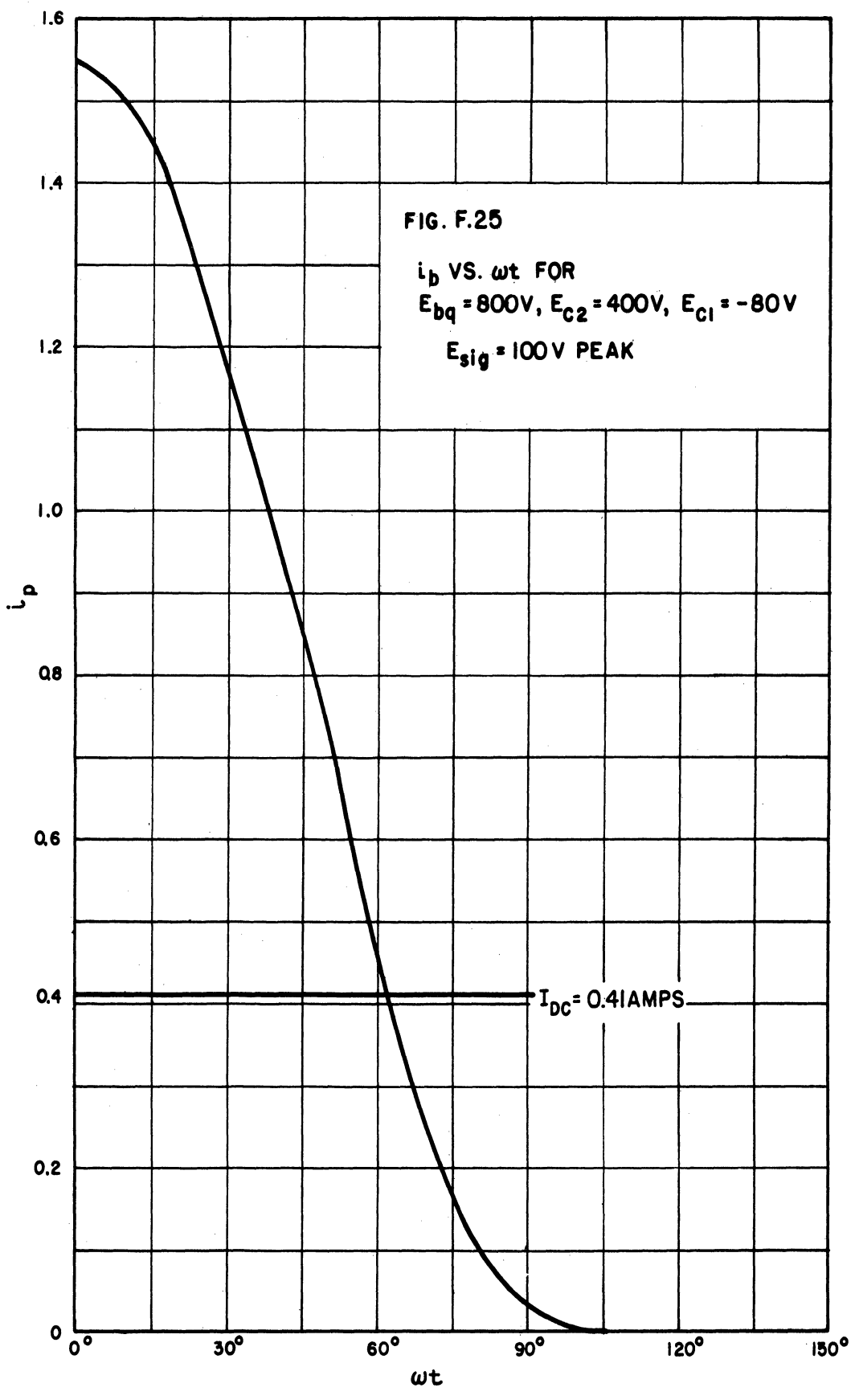
$$\text{Power Output} = 2400 \text{ watts}$$

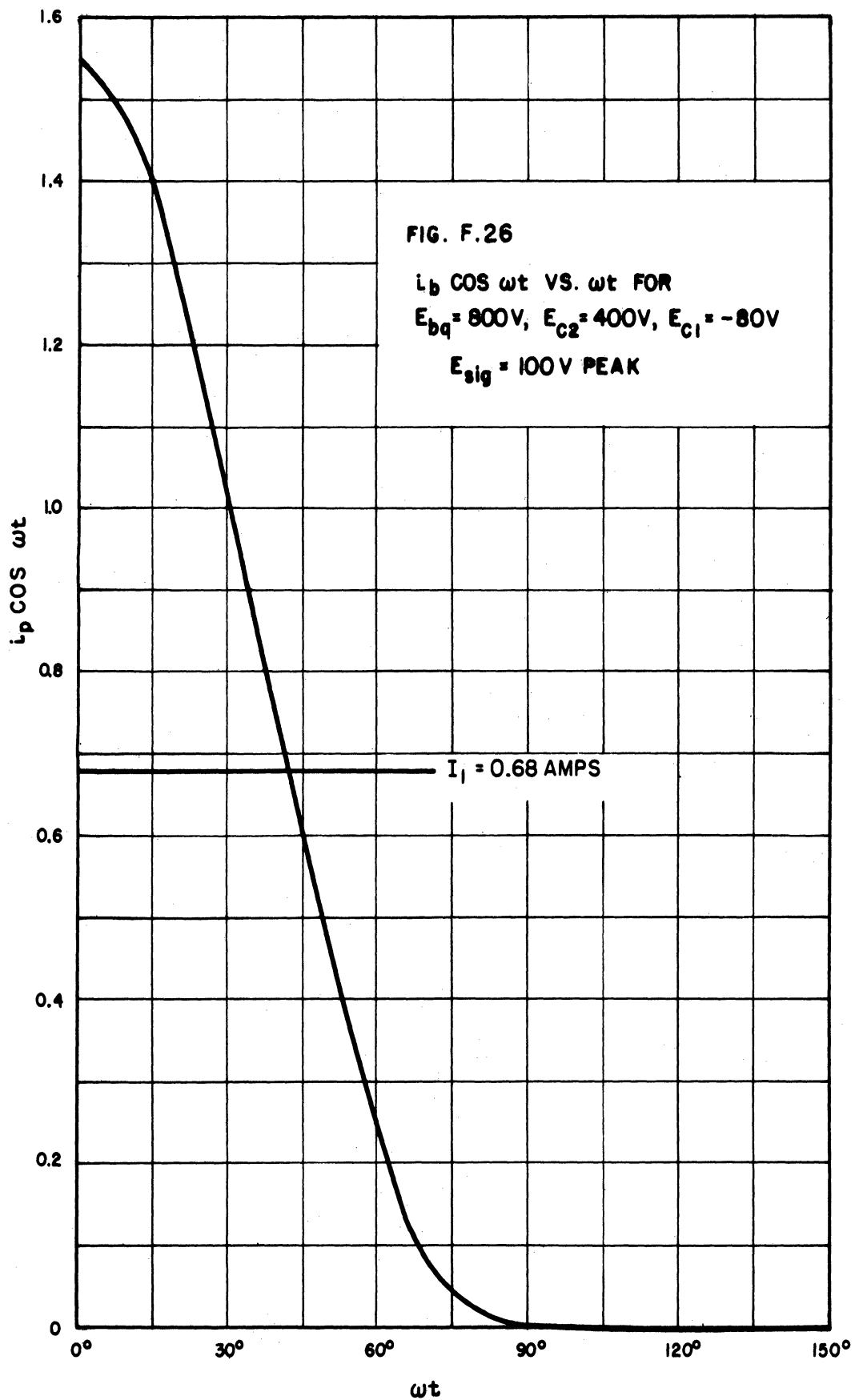
$$\eta = 17\%$$

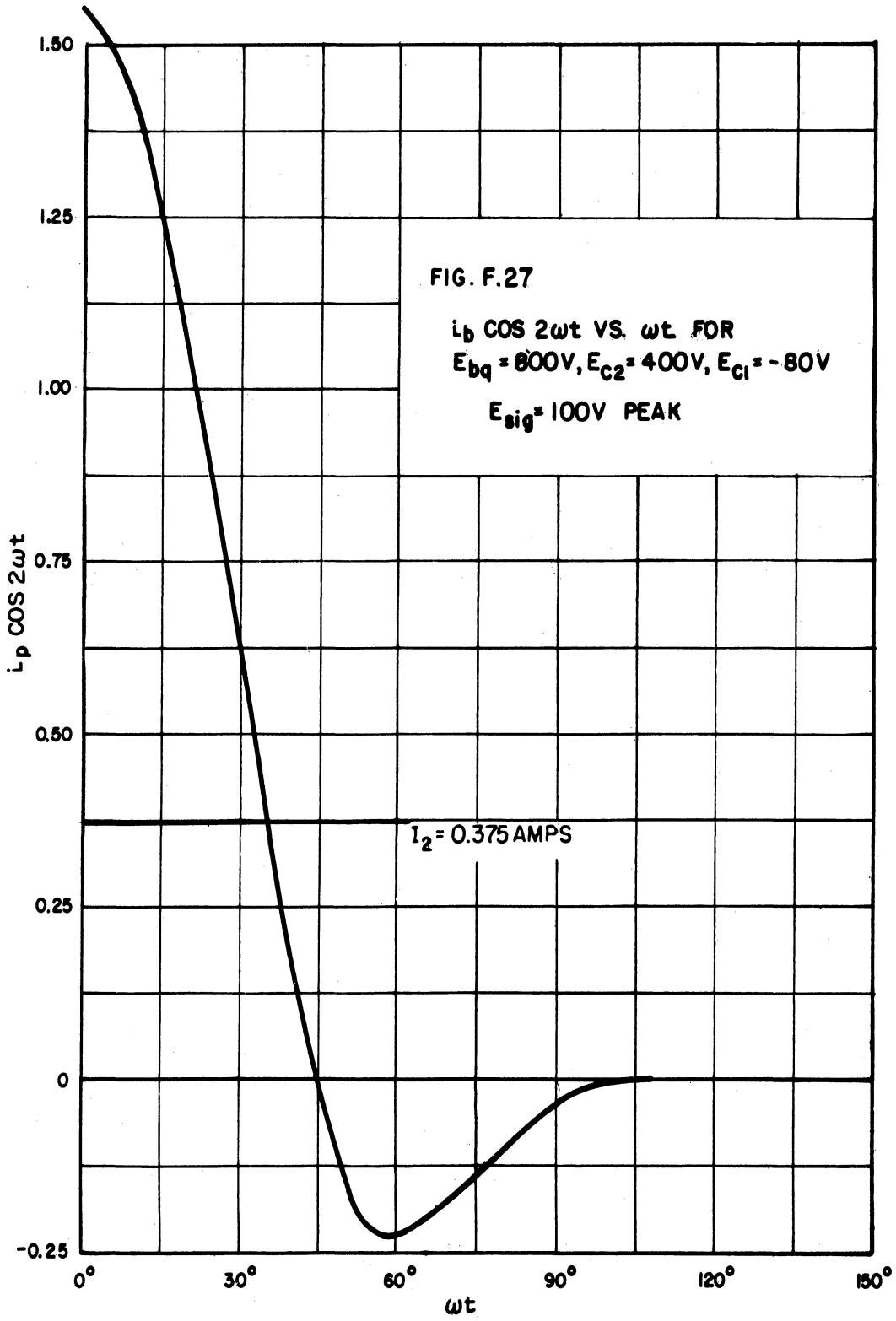
$$\text{Driving Power} = 100 \text{ watts}$$

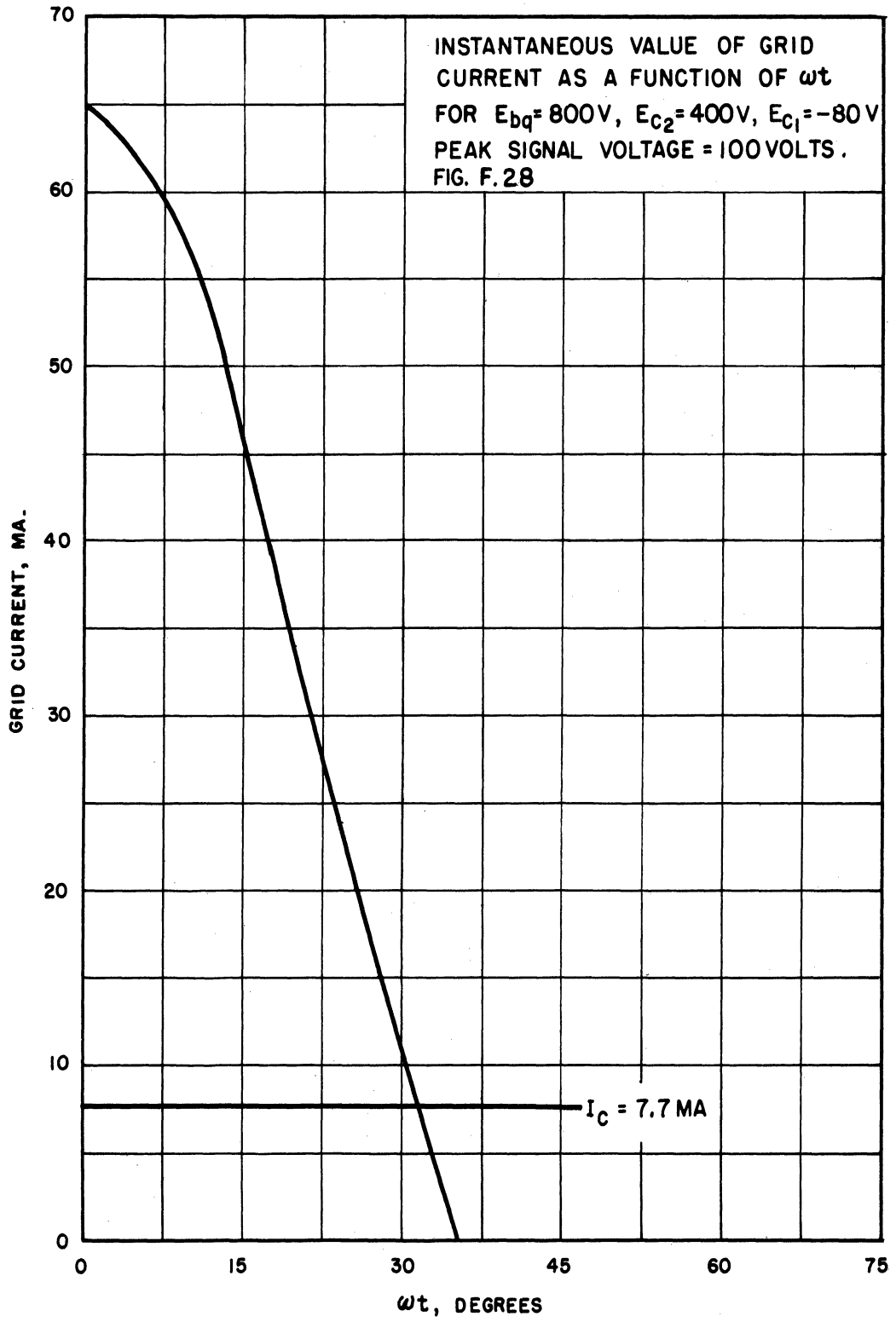
$$\text{Frequency Tolerance} = 0.42$$

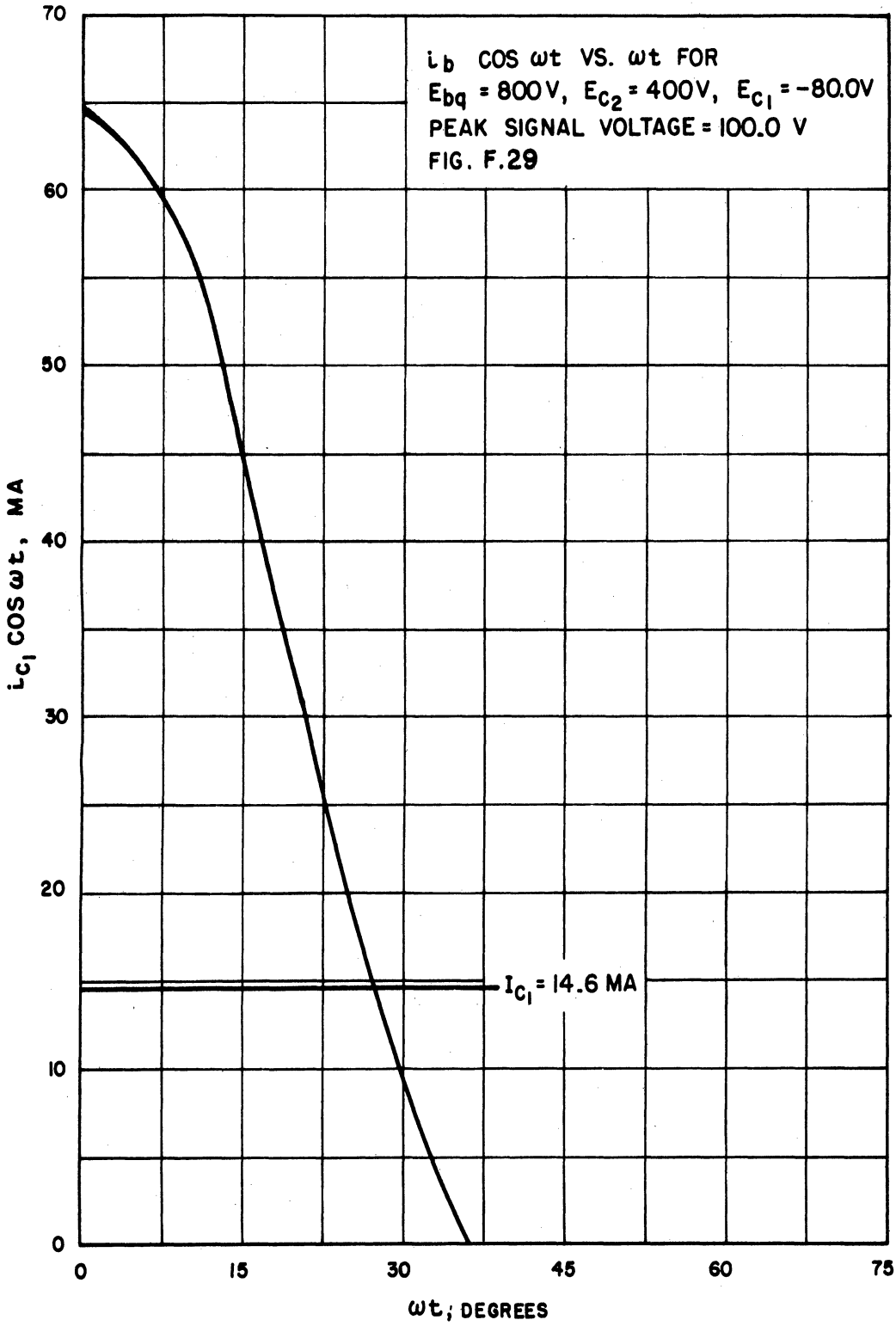
$$\text{Power Out } 2^{\text{nd}} \text{ Harmonic} = 128 \text{ watts}$$











BIBLIOGRAPHY

1. Ginzton, Hewlett, Jasberg, Noe, "Distributed Amplification", Proc. IRE, Vol. 36, pp. 956-969, August 1948.
2. Horton, Jasberg, Noe, "Distributed Amplifiers: Practical Considerations and Experimental Results", Proc. IRE, Vol. 38, pp. 748-753, July 1950.
3. D. O. Pederson, "The Analysis and Synthesis of Distributed Amplifiers with Ladder Networks", Technical Report No. 34 (N6onr251, Task 7) Stanford University (Electronics Research Laboratory), May 15, 1951.
4. A. D. Moore, "Synthesis of Distributed Amplifiers for Prescribed Amplitude Response", Technical Report No. 53 (N6onr Task 7), Stanford University (ERL) September 1, 1952.
5. D. O. Pederson, "The Distributed Pair", Technical Report No. 70 (N6onr251, Task 7) Stanford University (ERL) October 5, 1953.
6. H. Spett, "Design Notes on Distributed Amplifiers", Technical Memorandum No. M-1480, Signal Corps Engineering Laboratories, March 18, 1953.
7. H. B. Demuth, "An Investigation of the Iterative Synthesis of Distributed Amplifiers", Technical Report No. 77 (N6onr251, Task 7) Stanford University (ERL) August 5, 1954.
8. L. Kings and W. M. Furlow, Jr., "A Theoretical and Experimental Study of the Use of Triodes in a Distributed Amplifier Circuit", Technical Report issued by Melpar, Inc., Alexandria, Va.
9. D. V. Payne, "Distributed Amplifier Theory", Proc. IRE. Vol. 41, June 1953, pp. 759-762.
10. LePage and Seely, "General Network Analysis", McGraw-Hill 1952.
11. Johnson, "Transmission Lines and Networks", McGraw-Hill 1950.
12. M. J. O. Strutt and A. van der Ziel, "The Causes for the Admittances of Modern High-Frequency Amplifier Tubes for Short Waves", Proc. IRE, Vol. 26, pp. 1011-1032, August 1938.
13. Sarbacher and Edson, "Hyper and Ultra-High Frequency Engineering", pp. 431-436, Wiley, New York, 1943.
14. K. R. Sturley, "Radio Receiver Design", Part I, pp. 53, Wiley, New York, 1943.
15. K. R. Spangenberg, "Vacuum Tubes", pp. 493, McGraw-Hill, New York, 1948.
16. E. A. Guillemin, "Communication Networks", Vol. II, pp. 447, Wiley, New York, 1935.

DISTRIBUTION LIST

1 Copy Director, Electronic Research Laboratory
Stanford University
Stanford, California
Attn: Dean Fred Terman

1 Copy Commanding General
Army Electronic Proving Ground
Fort Huachuca, Arizona
Attn: Director, Electronic Warfare Department

1 Copy Chief, Research and Development Division
Office of the Chief Signal Officer
Department of the Army
Washington 25, D. C.
Attn: SIGEB

1 Copy Chief, Plans and Operations Division
Office of the Chief Signal Officer
Washington 25, D. C.
Attn: SIGEW

1 Copy Commanding Officer
Signal Corps Electronics Research Unit
9560th TSU
Mountain View, California

50 Copies Transportation Officer, SCEL
Evans Signal Laboratory
Building No. 42, Belmar, New Jersey

FOR - SCEL Accountable Officer
Inspect at Destination
File No. 22824-PH-54-91(1701)

1 Copy H. W. Welch, Jr.
Engineering Research Institute
University of Michigan
Ann Arbor, Michigan

1 Copy J. A. Boyd
Engineering Research Institute
University of Michigan
Ann Arbor, Michigan

1 Copy Document Room
Willow Run Research Center
University of Michigan
Willow Run, Michigan

10 Copies	Electronic Defense Group Project File University of Michigan Ann Arbor, Michigan
1 Copy	Engineering Research Institute Project File University of Michigan Ann Arbor, Michigan

UNIVERSITY OF MICHIGAN



3 9015 03695 5436